

JAERI - M
82-192

ANNUAL REPORT OF THE
OSAKA LABORATORY FOR RADIATION CHEMISTRY
JAPAN ATOMIC ENERGY RESEARCH INSTITUTE

(NO. 15)

April 1, 1981 - March 31, 1982

December 1982

Osaka Laboratory for Radiation Chemistry

日 本 原 子 力 研 究 所
Japan Atomic Energy Research Institute

JAERI-Mレポートは、日本原子力研究所が不定期に公刊している研究報告書です。
入手の問い合わせは、日本原子力研究所技術情報部情報資料課（〒319-11茨城県那珂郡東海村）あて、お申しこしてください。なお、このほかに財団法人原子力弘済会資料センター（〒319-11茨城県那珂郡東海村日本原子力研究所内）で複写による実費頒布をおこなっております。

JAERI-M reports are issued irregularly.

Inquiries about availability of the reports should be addressed to Information Section, Division of Technical Information, Japan Atomic Energy Research Institute, Tokai-mura, Naka-gun, Ibaraki-ken 319-11, Japan.

©Japan Atomic Energy Research Institute, 1982

編集兼発行 日本原子力研究所
印 刷 いばらき印刷(株)

Osaka Laboratory for Radiation Chemistry
Japan Atomic Energy Research Institute
25-1 Mii-minami machi, Neyagawa
Osaka, Japan

JAERI-M 82-192

ANNUAL REPORT OF THE
OSAKA LABORATORY FOR RADIATION CHEMISTRY
JAPAN ATOMIC ENERGY RESEARCH INSTITUTE
(No. 15)

April 1, 1981 - March 31, 1982

(Received November 19, 1982)

This report describes research activities of Osaka Laboratory for Radiation Chemistry, JAERI during one year period from April 1, 1981 through March 31, 1982. The latest report, for 1981, is JAERI-M 9856.

Detailed descriptions of the activities are presented in the following subjects: studies on reactions of carbon monoxide, hydrogen and methane; polymerization under the irradiation of high dose rate electron beams; modification of polymers, degradation, cross-linking, and grafting.

Previous reports in this series are:

Annual Report, JARRP, Vol. 1	1958/1959*
Annual Report, JARRP, Vol. 2	1960
Annual Report, JARRP, Vol. 3	1961
Annual Report, JARRP, Vol. 4	1962
Annual Report, JARRP, Vol. 5	1963
Annual Report, JARRP, Vol. 6	1964
Annual Report, JARRP, Vol. 7	1965
Annual Report, JARRP, Vol. 8	1966
Annual Report, No. 1, JAERI 5018	1967
Annual Report, No. 2, JAERI 5022	1968
Annual Report, No. 3, JAERI 5026	1969
Annual Report, No. 4, JAERI 5027	1970
Annual Report, No. 5, JAERI 5028	1971
Annual Report, No. 6, JAERI 5029	1972
Annual Report, No. 7, JAERI 5030	1973
Annual Report, No. 8, JAERI-M 6260	1974
Annual Report, No. 9, JAERI-M 6702	1975
Annual Report, No.10, JAERI-M 7355	1976
Annual Report, No.11, JAERI-M 7949	1977
Annual Report, No.12, JAERI-M 8569	1978
Annual Report, No.13, JAERI-M 9214	1979
Annual Report, No.14, JAERI-M 9856	1980

* Year of the activities

Keywords: Electron Beam Irradiation, γ -Irradiation, Carbon Monoxide-Hydrogen Reaction, Methane, Radiation-Induced Reaction, Polymerization, Emulsion Polymerization, Grafting, Polymer Modification, Cross-Linking, Vinyl Monomer, Dienes, Polystyrene, Polyvinyl Chloride Powder, Radiation Chemistry

昭和56年度日本原子力研究所 大阪支所年報

日本原子力研究所・高崎研究所・大阪支所

(1982年11月19日受理)

本報告は、大阪支所において昭和56年度に行なわれた研究活動を述べたものである。主な研究題目は、一酸化炭素、水素およびメタンの反応ならびにそれに関連した研究、高線量率電子線照射による重合反応の研究、ポリマーの改質および上記の研究と関連して重合反応、高分子分解、架橋ならびにグラフト重合に関する基礎的研究などである。

日本放射線高分子研究協会年報	Vol. 1		1958/1959
日本放射線高分子研究協会年報	Vol. 2		1960
日本放射線高分子研究協会年報	Vol. 3		1961
日本放射線高分子研究協会年報	Vol. 4		1962
日本放射線高分子研究協会年報	Vol. 5		1963
日本放射線高分子研究協会年報	Vol. 6		1964
日本放射線高分子研究協会年報	Vol. 7		1965
日本放射線高分子研究協会年報	Vol. 8		1966
日本原子力研究所大阪研における放射線化学の基礎研究No. 1	JAERI	5018	1967
日本原子力研究所大阪研における放射線化学の基礎研究No. 2	JAERI	5022	1968
日本原子力研究所大阪研における放射線化学の基礎研究No. 3	JAERI	5026	1969
日本原子力研究所大阪研における放射線化学の基礎研究No. 4	JAERI	5027	1970
日本原子力研究所大阪研における放射線化学の基礎研究No. 5	JAERI	5028	1971
日本原子力研究所大阪研における放射線化学の基礎研究No. 6	JAERI	5029	1972
日本原子力研究所大阪研における放射線化学の基礎研究No. 7	JAERI	5030	1973
Annual Report, Osaka Lab., JAERI, No. 8	JAERI-M	6260	1974
Annual Report, Osaka Lab., JAERI, No. 9	JAERI-M	6702	1975
Annual Report, Osaka Lab., JAERI, No. 10	JAERI-M	7355	1976
Annual Report, Osaka Lab., JAERI, No. 11	JAERI-M	7949	1977
Annual Report, Osaka Lab., JAERI, No. 12	JAERI-M	8569	1978
Annual Report, Osaka Lab., JAERI, No. 13	JAERI-M	9214	1979
Annual Report, Osaka Lab., JAERI, No. 14	JAERI-M	9856	1980

CONTENTS

I.	INTRODUCTION -----	1
II.	RECENT RESEARCH ACTIVITIES	
[1]	Radiation-Induced Reactions of Carbon Monoxide, Hydrogen, and Methane	
1.	The Gamma Ray-Induced Radiolysis of Methane at Elevated Pressures -----	4
2.	Radiation Chemical Reactions of Methane- Hydrogen Mixture at Large Dose -----	11
3.	Radiation Chemical Reactions of Methane- Deuterium Mixture at Large Dose -----	16
4.	Formation of Carbonaceous Solid by Irradiation of Methane over Molecular Sieve 5A and Silica Gel -----	29
5.	Radiation-Induced Reactions of Methane- Hydrogen Mixtures over Molecular Sieve 5A -----	36
6.	Radiation-Induced Reactions of Carbon Monoxide with Water Adsorbed on Silica Gel and Some Other Metal Oxides -----	42
7.	Photo-Emission from Carbon Monoxide Induced by 0.6 MeV Electron Irradiation -----	47
[2]	Radiation-Induced Polymerization	
1.	Cationic Oligomerization of Butadiene with 1-Bromo-2-Butene -----	55
2.	Oligomerization of Butadiene with Dihalogen Compounds -----	61
3.	Oligomerization of Butadiene with Acetic Anhydride -----	68
4.	Bulk Polymerization of Methyl Methacrylate -----	72

5.	Emulsion Polymerization of Styrene in a Batch System -----	74
6.	Polymerization of Acetylene in the Plastic Crystalline State by γ -Irradiation -----	77
[3]	Modification of Polymers	
1.	Preparation of Cation-Exchange Resin by Graft Copolymerization -----	83
2.	Grafting of Fluorine-Containing Monomer onto Poly(Vinyl Chloride) Composite Disc -----	88
III.	LIST OF PUBLICATIONS	
[1]	Published Papers -----	91
[2]	Oral Presentations -----	93
IV.	EXTERNAL RELATIONS -----	94
V.	LIST OF SCIENTISTS -----	95

目 次

I	序文	1
II	研究活動	
	〔1〕 CO-H ₂ 及び CH ₄ の放射線化学反応	
	1. 昇圧下のメタンのγ線による放射線化学反応	4
	2. 大線量照射によるメタン・水素混合気体の放射線化学反応	11
	3. 大線量照射によるメタン・重水素混合気体の放射線化学反応	16
	4. モレキュラーシーブ 5 A 及びシリカゲル上のメタンの照射によって生成する含炭素固体	29
	5. モレキュラーシーブ 5 A 上におけるメタン・水素混合気体の放射線化学反応	36
	6. シリカゲル及び二・三の金属酸化物上に吸着された水と一酸化炭素との放射線化学反応	42
	7. 0.6 MeV 電子線照射による CO の励起発光	47
	〔2〕 放射線重合	
	1. 1-ブロモ-2-ブテンによるブタジエンのカチオン・オリゴメリゼーション	55
	2. ジハロゲン化合物によるブタジエンのオリゴメリゼーション	61
	3. 無水酢酸によるブタジエンのオリゴメリゼーション	68
	4. メタクリル酸メチルの塊状重合	72
	5. バッチシステムでのスチレンの乳化重合	74
	6. γ線照射による柔軟性結晶状態におけるアセチレンの重合	77
	〔3〕 ポリマーの改質	
	1. グラフト共重合によるカチオン交換樹脂の合成	83
	2. ポリ塩化ビニル・ディスクへの含フッ素モノマーのグラフト重合	88
III	発表記録	
	〔1〕 論文など	91
	〔2〕 口頭発表	93
IV	外部との関連	94
V	研究者一覧表	95

I. INTRODUCTION

Osaka Laboratory was founded in 1958 as a laboratory of the Japanese Association for Radiation Research on Polymers (JARRP), which was organized and sponsored by some fifty companies interested in radiation chemistry of polymers. The JARRP was merged with Japan Atomic Energy Research Institute (JAERI) on June 1, 1967, and the laboratory has been operated as Osaka Laboratory for Radiation Chemistry, Takasaki Radiation Chemistry Establishment, JAERI. The research activities of Osaka Laboratory have been oriented towards the fundamental research on applied radiation chemistry.

The results of the research activities of the Laboratory were published from 1958 until 1966 in the Annual Reports of JARRP which consisted essentially of original papers. During the period between 1967 and 1973, the publication had been continued as JAERI Report which also consisted mainly of original papers. From 1974, the Annual Report has been published as JAERI-M Report which contains no original papers, but presents outlines of the current research activities in some detail. Readers who wish to have more information are advised to contact with individuals whose names appear under subjects.

The present annual report covers the research activities of the Laboratory between April 1, 1981 and March 31, 1982.

Most of the studies carried out in the Laboratory are continuation from the previous year, emphasis being laid on two fields; one is "Effect of radiation on the reaction of carbon monoxide, methane and hydrogen" and the other, "Radiation research on polymers".

In an attempt to improve the selectivity of the reaction to form ethane in the radiation chemical reaction of methane, studies have been carried out using flow system without circulation under electron beam irradiation in the presence of molecular sieves which have pores of uniform dimensions. The results indicated that the selectivity toward C₂ and C₃

hydrocarbon products was improved by the presence of molecular sieves which limit the growing hydrocarbon chain within the size determined by the pore diameter. Addition of hydrogen to methane in large quantity prevents poisoning of the catalyst surface without sacrificing its selectivity.

The γ -irradiation of methane in a pressurized vessel was carried out to clarify the effect of irradiation temperature, pressure, and dosage on the amounts of products. Ethane and hydrogen were found as the only radiolysis products of methane at -72°C .

Optical emission spectra from CO under electron beam irradiation was carried out in an attempt to elucidate the role of excited states in the radiation-induced reaction producing carbonaceous solid. The several bands due to excited CO and C_2 were observed and the emission intensities were studied under different reaction conditions.

The water gas shift reaction was found to occur with the formation of lower hydrocarbons when carbon monoxide was irradiated over silica gel or various metal oxides which has been equilibrated with water vapor. The amounts of the products depend on the amount of adsorbed water, temperature, and dose rate, and the experimental results are well correlated with those of the radiolysis of adsorbed water.

The studies in an attempt to synthesize reactive oligomers having halogen atoms at its both terminals by telomerization reaction induced by electron beams have been continued under the presence of several chain transfer agents. When 1-bromo-2-butene (1B2B) was used as a chain transfer agent, higher rate of oligomerization and lower molecular weight butadiene oligomer were obtained compared with the case with 1-chloro-2-butene (1C2B). Nevertheless, the number of terminal halogen per molecule was much less in 1B2B oligomer than 1C2B one. Oligomerizations of butadiene with dihalobutane homologues and acetic anhydride were also studied. In the studies on emulsion polymerization in a batch system using anionic, cationic, and nonionic emulsifier, polymer emulsion of average

diameter of ca. 40 nm was obtained only in the presence of anionic emulsifier.

In order to prepare polymers having electric conductivity by radiation-induced polymerization, a preliminary study was carried out comparatively on the structure of polyacetylenes which were obtained in the gas, liquid, and solid phase polymerization.

The relation between the reaction conditions and adsorption properties to metal ions was studied on several polyvinylchloride (PVC) and polyvinylidenechloride (PVD) grafted with 2-acrylamide-2-methylpropane sulfonic acid (AMPS) by in situ irradiation technique. The degree of grafting for PVC becomes larger with increasing content of acetone in the AMPS solution, but the maximum rate of adsorption to metal ion was obtained when the grafted polymer was prepared from the solution (water : acetone = 3 : 2). For PVD, both the degree of grafting and the rate of metal ion adsorption increased with increasing acetone content in the solution.

According to the results of a preliminary experiment in order to improve abrasion resistance on the surface of PVC plates, it was revealed that the vapor phase graft polymerization of fluorine containing monomer onto PVC was useful for this purpose.

Dr. Isamu Kuriyama, Head
Osaka Laboratory for Radiation Chemistry
Japan Atomic Energy Research Institute

II. RECENT RESEARCH ACTIVITIES

[1] Radiation-Induced Reactions of Carbon Monoxide, Hydrogen, and Methane1. The Gamma Ray-Induced Radiolysis of Methane at Elevated Pressures

In the last annual report¹⁾, we described that in the electron irradiation of methane, the amounts of the main products increased proportionally to the pressure in the pressure range from 500 to 1500 Torr. Temperature dependence of the amounts of the products was also reported in the temperature range between 50° and 750°C. This year, studies have been carried out to obtain the amounts of products formed by irradiation of methane as functions of pressure and temperature in wide range of these reaction conditions: $4.63 \times 10^3 \sim 6.43 \times 10^4$ Torr (6.4 to 87.5 kg/cm²) and -72° ~ 400°C. For this purpose, the irradiation was carried out using Co⁶⁰ γ -rays instead of electrons from an accelerator for easiness of penetration of radiation through the stainless steel wall of an autoclave containing pressurized methane and for more accurate control of the irradiation temperature at low temperature region below 50°C.

The γ -irradiation was carried out in an autoclave (78 ml in volume) with a Bourdon type pressure gauge. The autoclave was placed in an electric furnace or a Dewar vessel containing coolant of desired temperature during the irradiation. The temperature was controlled within $\pm 2^\circ\text{C}$ during the irradiation. Most experiments were carried out at 6.5 Mrad, below this dose, almost linear dose-conversion curve being obtained. The dose rate was 0.06 Mrad/h for the irradiation at the temperature above 0°C and was 0.04 Mrad/h for the irradiation below 0°C.

The products identified were hydrogen and saturated hydrocarbons and unsaturated hydrocarbons were not detected in

the present study.

The dose-conversion curves obtained at 50°C and 3.67×10^4 Torr are shown in Fig. 1 for hydrogen, ethane, propane, and n- and iso-butananes. The amounts of hydrogen and ethane increase with increasing dose, but the latter tends to level-off as the dose increases above 8 Mrad. A knick point appeared at 8 Mrad in the dose-conversion curve of propane. The results seem to contradict partly those obtained by electron irradiation in the flow system, where the amounts of these products increased linearly with increasing dose up to 60 Mrad. The amounts of n-butane and iso-butane increased with increasing dose. No data were obtained for the amounts of hydrogen at 18 and 59 Mrad.

The G values of the products obtained at 50°C and 6.5 Mrad are plotted as a function of pressure for ethane, propane and

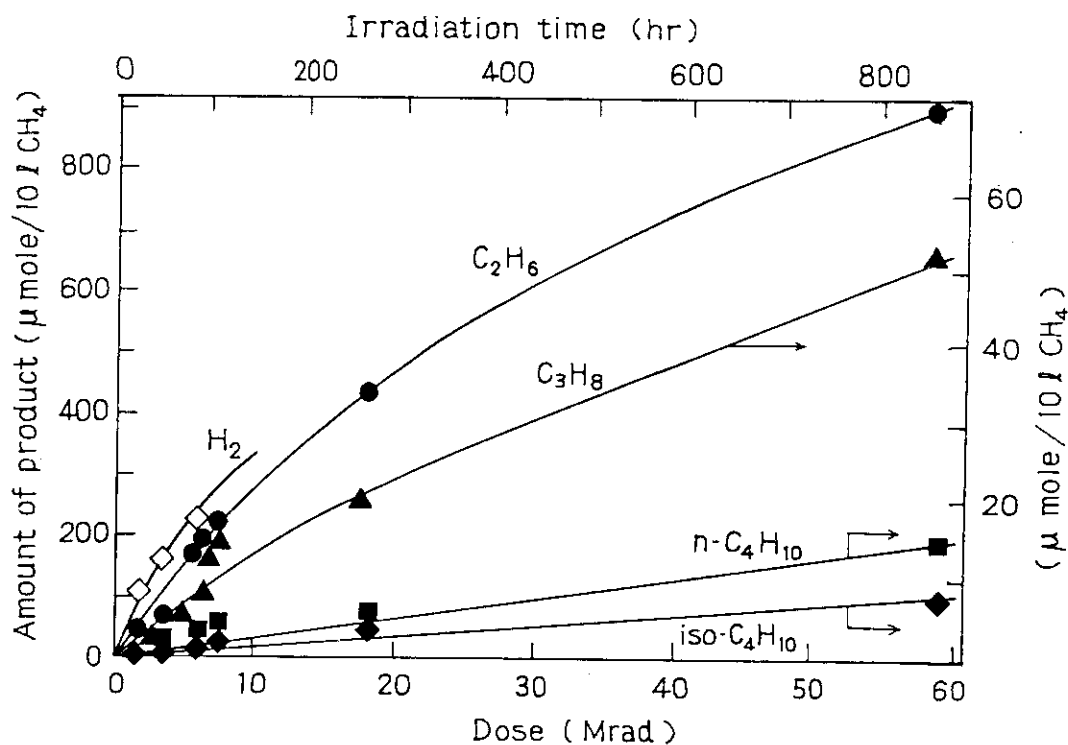


Fig. 1. Dose conversion curves: pressure, 36700 Torr; amount of methane, 0.155 mole; dose rate, $0.069 \text{ Mrad}\cdot\text{h}^{-1}$; temperature, 50°C.

butanes in Fig. 2 and for higher hydrocarbons in Fig. 3. It is noted that $G(\text{C}_2\text{H}_6)$ is independent of pressure, while G values of higher hydrocarbons increase with increasing pressure. The $G(\text{C}_2\text{H}_6)$ found at the present study is higher by a factor of 1.5 than the values obtained by electron irradiation at atmospheric pressure²⁾ where most G values of ethane formation are reported to be ca. 2.2 by different authors, but no data obtained at elevated pressures are available in literatures to compare with the present result.

The G values are plotted as a function of temperature in Fig. 4 for hydrogen, ethane, propane, *n*- and iso-butanes, and for hydrocarbons of different carbon numbers in Fig. 5. It is

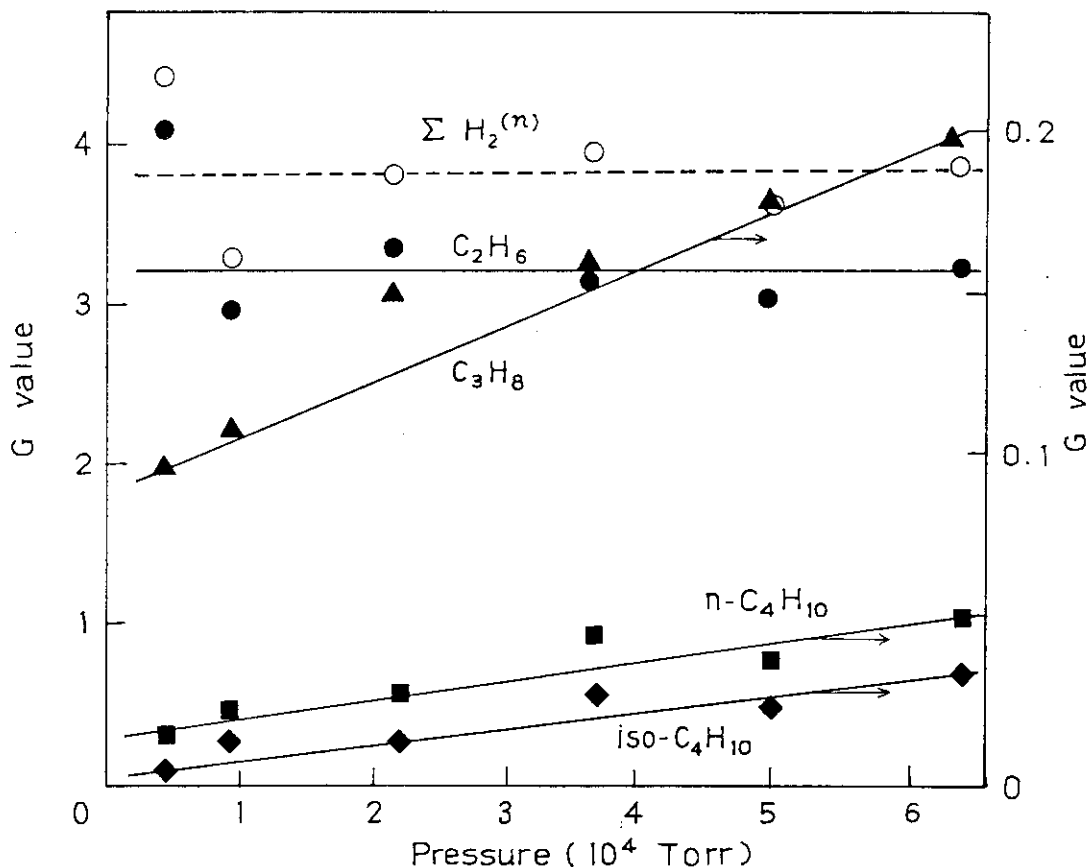


Fig. 2. G -values of $\text{C}_2 \sim \text{C}_4$ hydrocarbon products as a function of pressure: dose, 6.5 Mrad; temperature, 50°C . $\Sigma \text{H}_2^{(n)}$ denotes the sum of H_2 produced as a counterpart of hydrocarbon having n carbon atoms.

noted that the $G(\text{C}_2\text{H}_6)$ is equal to $G(\text{H}_2)$ and no other hydrocarbons were produced at -72°C , satisfying the following stoichiometric relation:



The result may support the earlier proposals^{2,3)} that ethane is formed by the combination reaction of two methyl radicals (2), or neutralization of ionic intermediate (4).

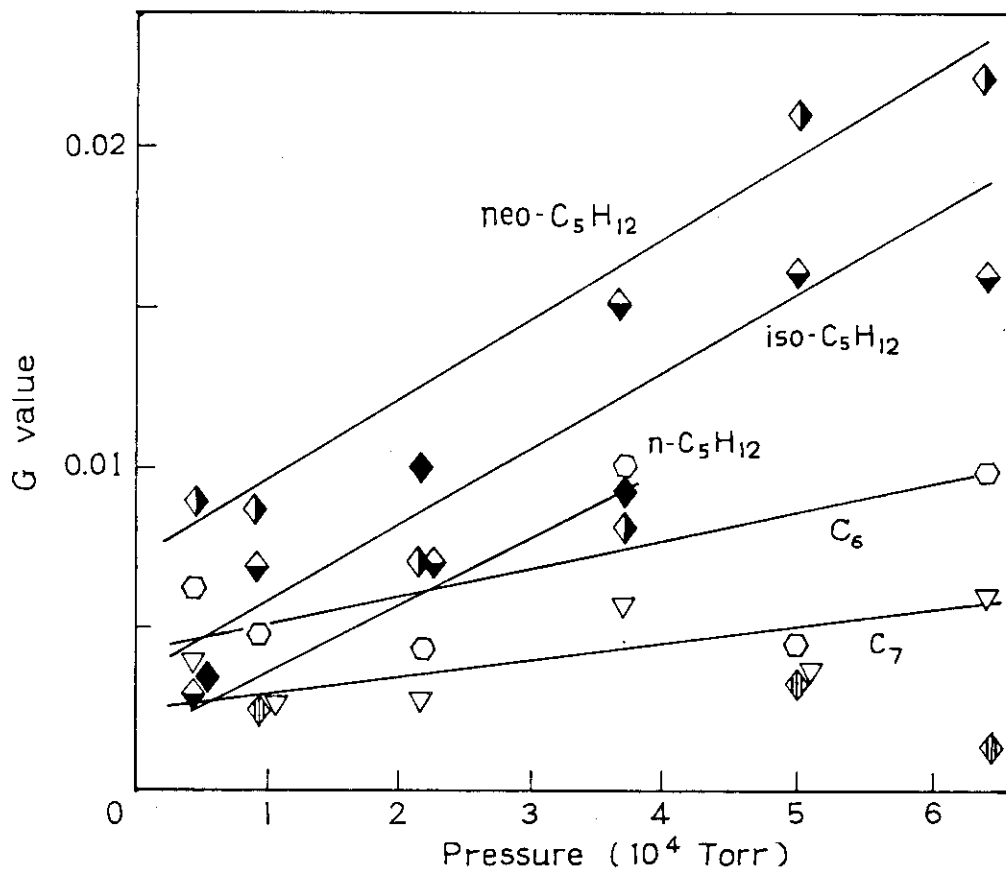
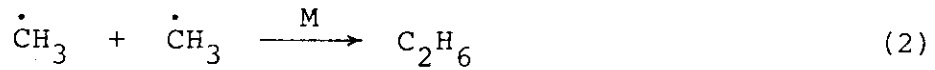
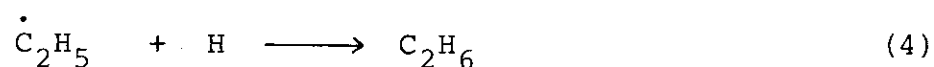
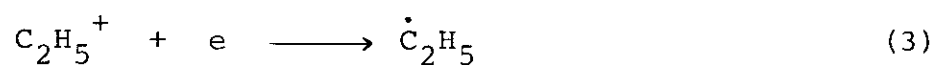


Fig. 3. G-values of $\text{C}_5 \sim \text{C}_7$ hydrocarbon products as a function of pressure: the reaction conditions are the same as those indicated in Fig. 2.



where M is a third body. With increasing temperature, the G values of hydrogen and hydrocarbons increased. The G value of hydrogen, $G(\text{H}_2)^{(n)}$, produced as a counterpart of hydrocarbon having n carbon atoms can be related with the G value of the hydrocarbon according to the stoichiometric relation (5):

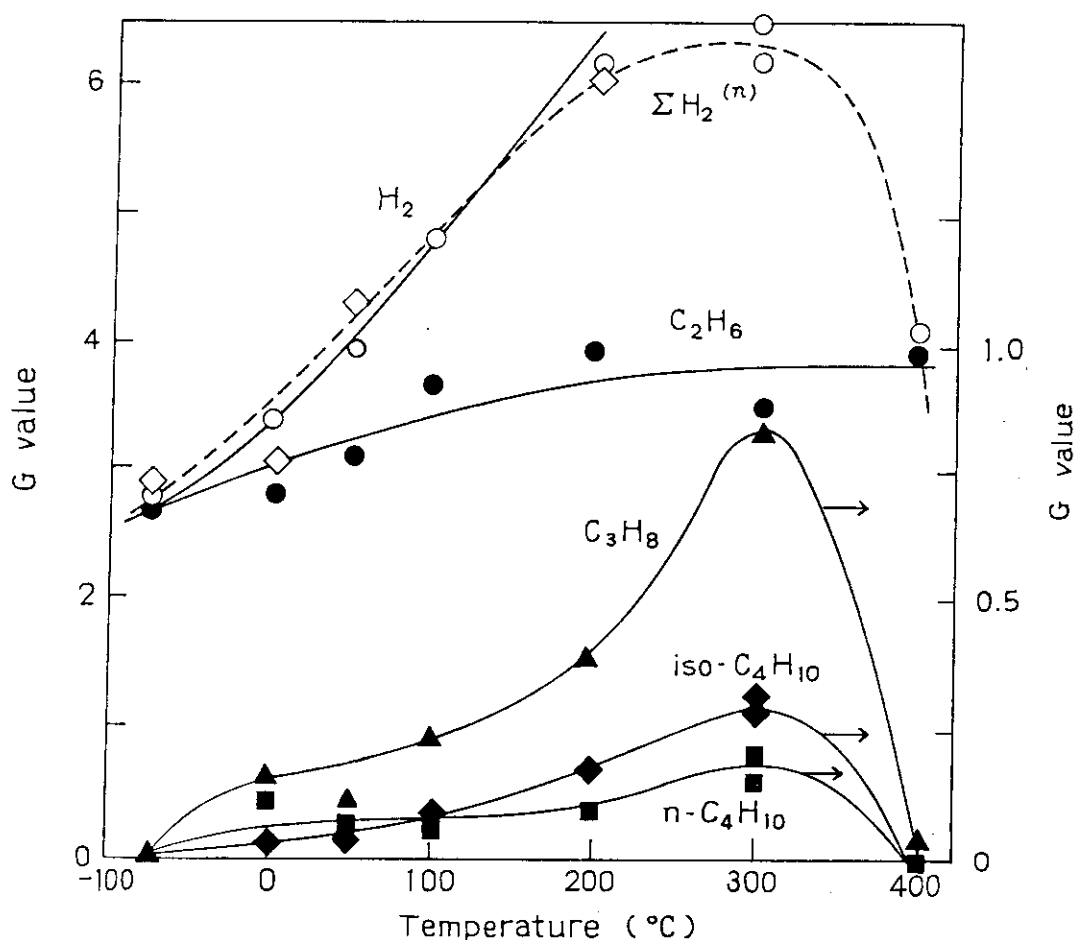
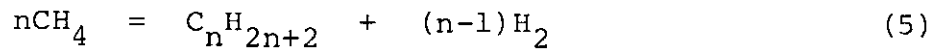


Fig. 4. G-values of hydrogen and C₂ ~ C₄ hydrocarbons as a function of temperature: dose, 6.5 Mrad; the other reaction conditions are the same as those indicated in Fig. 1.



In Fig. 4, the sum of $G(\text{H}_2)^{(n)}$ values calculated for $n = 2$ to 8 is also given by a broken line which fits well with the observed $G(\text{H}_2)$ in the temperature range between -72 and 200°C . This result indicates that some successive reactions to extend hydrocarbon chain of the products with activation energy occur with increasing temperature competing with the reaction producing C_2H_6 (2):

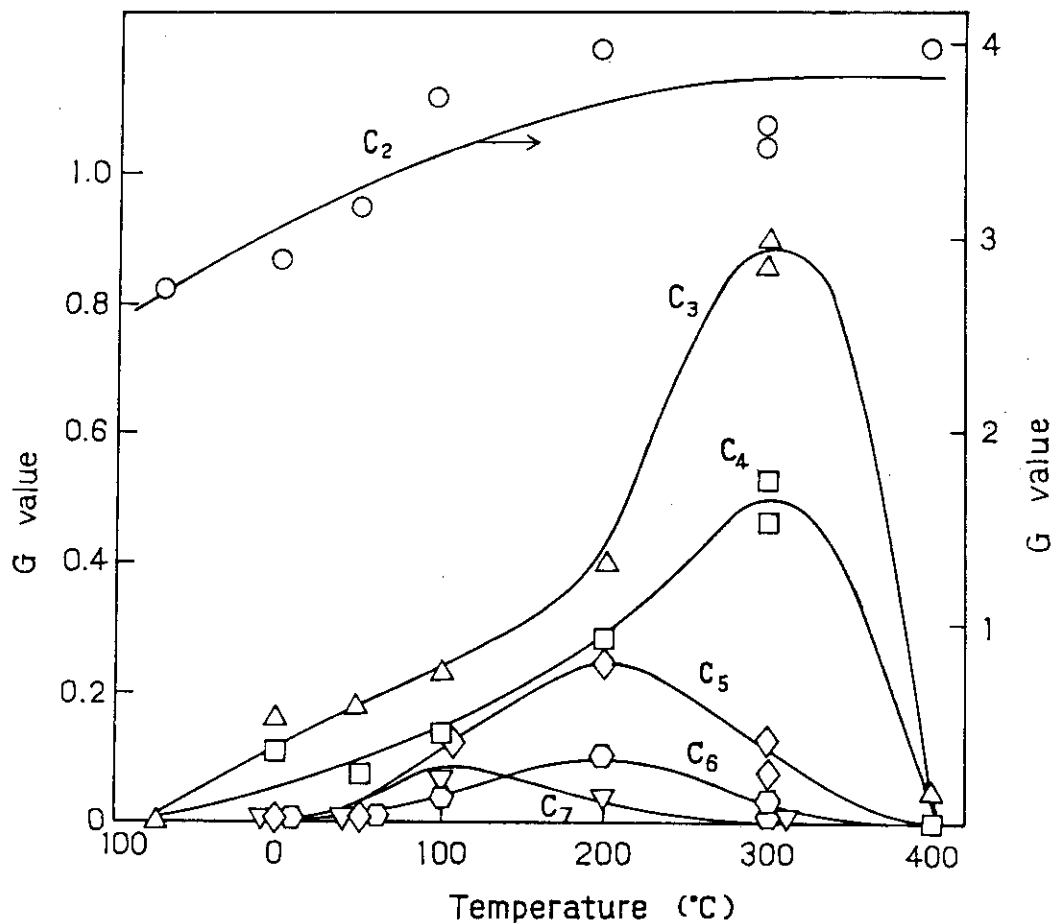
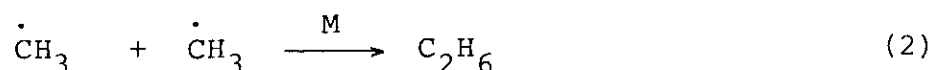
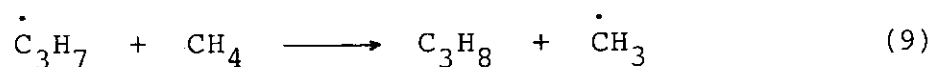
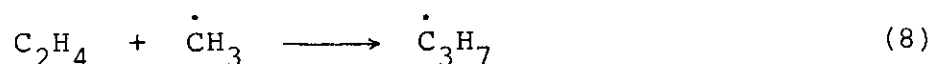


Fig. 5. G-values of hydrocarbon products as a function of temperature: dose, 6.5 Mrad; the other reaction conditions are the same as those indicated in Fig. 1.



These reactions may be accounted for by the leveling-off of the $G(\text{C}_2\text{H}_6)$ with increasing temperature above 200°C. The decrease of the G values of the higher hydrocarbons above 300°C is probably due to the thermal decomposition of the products. This may be supported by the fact that temperature at which the $G(\text{product})$ becomes maximum is lower, as the number of carbons in the product molecule increases (Fig. 5).

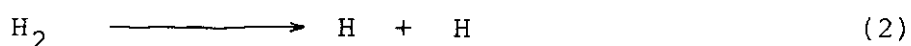
The present study indicates that in the pressure range between 4.63×10^3 to 6.43×10^4 Torr, G values of $\text{C}_3 \sim \text{C}_7$ hydrocarbons increased with increasing pressure in contrast to the results obtained in the pressure range between 500 and 1500 Torr where the G values of the products were independent of pressure. The fact that the G value of ethane is equal to that of hydrogen at -72°C indicates the selective formation of ethane and hydrogen from methane without any by-products.

(S. Sugimoto and M. Hatada)

- 1) M. Hatada, H. Arai, and S. Nagai, JAERI-M 9856, 67 (1981).
- 2) H. Arai, S. Nagai, and M. Hatada, Radiat. Phys. Chem., 17, 151 (1981).
- 3) K. Okazaki, S. Sato, and S. Ohno, Bull. Chem. Soc. Japan, 49, 174 (1981).

2. Radiation Chemical Reactions of Methane-Hydrogen Mixture at Large Dose

In the last annual report¹⁾, it is shown that liquid hydrocarbon and hydrogen are the main components when extremely large dose of radiation is given to methane. Since combination reaction (1) of alkyl radicals are considered to be a main reaction scheme to the liquid hydrocarbons, addition of hydrogen to methane in large quantity may decrease the amount of the liquid hydrocarbon, because hydrogen atoms produced from hydrogen molecules by radiation (2) will react with alkyl radicals by reactions (3) and (4) to interrupt the hydrocarbon chain growth (1):



This study has been carried out in an attempt to know whether the presence of hydrogen may increase the fraction of low molecular weight hydrocarbons in the radiolysis products of methane with large dose irradiation.

The methods of irradiation and analysis of the products were the same as those described previously¹⁾. A 7.1 l stainless steel irradiation vessel with aluminum window (0.1 mm thick) was used and the irradiation was carried out in a static condition without gas circulation using electron beams (0.6 MeV, 1 mA) from an accelerator of rectified transformer type. The dosages given to the gas were $3.6 \sim 3.9 \times 10^3$ and 4×10^4 Mrad. During irradiation, the irradiation vessel was cooled by air stream and the temperature of the gas as determined by the pressure increase during irradiation was $60^\circ \sim 80^\circ\text{C}$. After irradiation, the gas was analyzed simultaneously by three

gaschromatographs on Porapak Q, Porapak N and molecular sieve columns, respectively. Then, the gas contained in the irradiation vessel kept at 40°C was pumped off through a liquid nitrogen trap to collect condensable fractions from which C₂-C₃ fractions were later removed by vaporization at atmospheric pressure. The amount of condensable fraction was determined volumetrically. The irradiation window was removed to collect the residual fraction by scrapping off from the wall of the vessel and the non-volatile fraction was weighed.

Experimental results are shown in Table 1 along with the experimental conditions employed. In Table 2, the amounts of products (ca. $3.6 \sim 3.9 \times 10^3$ Mrad) normalized to those from 1 g methane are compared for methane-hydrogen mixture at 749 Torr (partial pressure of methane is 381 Torr) (S-16) and pure methane at 501 Torr (S-13). The normalized amounts of products for methane-hydrogen mixture relative to those for pure methane are larger for ethane and propane, and the value becomes lower as the number of carbon atoms in the product molecule increases, and non-volatile liquid was not found in the mixture. The amount of ethylene produced was also reduced by an order of magnitude by the presence of hydrogen. This result indicates that the presence of hydrogen does serve to reduce the molecular weight of the products as expected. The similar conclusion can be drawn when one compares the result obtained for the mixture (S-16) and that for pure methane at the same pressure, 760 Torr (S-7).

Similar comparison at larger dose (ca. 4×10^4 Mrad) is made in Table 3 for the mixtures (S-17 and S-18, both at ca. 1 atm) and pure methane at 1 atm (S-6). Similar tendency that the relative amounts of the products for the methane-hydrogen mixture to those for the pure methane decrease with increasing carbon number of the products is shown in the last column of the table except for the amount of the non-volatile liquid, which is even higher for the methane-hydrogen mixture. The amount of hydrogen in the irradiated gas is almost the same independent of the initial content of hydrogen in the gas to be irradiated, indicating that the steady state concentration of

Table 1. The Amounts of Products from Methane and Methane-Hydrogen Mixture by Electron Irradiation

Run No.	S-6	S-7	S-13	S-16	S-17	S-18
Pressure (Torr)	760	760	501	749	760	776
Amount of CH ₄ (g)	4.80 (0.30)	4.80 (0.30)	3.06(0.191)	2.37(0.148)	2.45(0.153)	2.37(0.148)
Amount of H ₂ (g)	0.	0.	0.	0.29(0.145)	0.27(0.135)	0.29(0.145)
(Values in parentheses in mole)						
Dose (Mrad)	4.3×10^4	3.6×10^3	3.6×10^3	3.9×10^3	4.3×10^4	4.3×10^4
Dose absorbed by hydrocarbons (eV)	4.3×10^{24}	1.1×10^{24}	6.9×10^{23}	6.4×10^{23}	2.6×10^{24}	2.6×10^{24}
Components of irradiated gas (g)						
H ₂	0.450	0.194	0.111	0.440	0.416	0.446
CH ₄	0.832	2.773	1.735	1.504	0.442	0.505
C ₂ H ₄	0.002	0.002	0.003	0.0003	0.00005	0.0001
C ₂ H ₆	0.495	0.700	0.424	0.329	0.206	0.233
C ₃ H ₆	0.004	0.0003	0.008	0.000	0.000	0.000
C ₃ H ₈	0.150	0.176	0.137	0.063	0.041	0.047
i-C ₄ H ₁₀	0.034	0.031	0.034	0.012	0.006	0.007
n-C ₄ H ₁₀	0.062	0.059	0.045	0.021	0.017	0.019
neo-C ₅ H ₁₂	0.008	0.010	0.012	0.0037	0.002	0.002
i-C ₅ H ₁₂	0.042	0.028	0.038	0.011	0.006	0.008
Condensable liquid	0.44	0.100	0.085	0.00005	0.0005	0.001
Non-volatile liquid	1.39	0.386	0.116	0.0	0.531	0.427
Total compounds	3.96	4.48	2.78	2.38	1.67	1.70
% Recovery	82.	93.4	91.0	89.8	61.3	64.

Table 2. Effect of Hydrogen Added to Methane on the Product Distribution at Small Dose ($3.6 \sim 3.9 \times 10^3$ Mrad)

Run No.	S-16	S-13	S-7	
Pressure (Torr)	749	501	760	
The amount of CH ₄ (g)	2.37	3.06	4.80	The amounts of products from the mixture relative to those from pure methane.
H ₂ (g)	0.29	0.00	0.00	
The amounts of products (in mg) normalized to 1 g CH ₄				
C ₂ H ₄	0.13	0.98	0.42	S-16/S-13 S-16/S-7
C ₂ H ₆	138.8	138.6	145.8	0.13 0.03
C ₃ H ₈	26.6	44.8	36.7	1.00 0.95
i-C ₄ H ₁₀	5.1	11.1	6.5	0.59 0.72
n-C ₄ H ₁₀	8.9	14.7	12.3	0.46 0.78
neo-C ₅ H ₁₂	1.6	3.9	2.1	0.61 0.72
i-C ₅ H ₁₂	4.6	12.4	5.8	0.41 0.76
Condensable liquid	0.02	27.8	20.8	0.37 0.79
Non-volatile liquid	0.	37.9	80.4	0.0007 0.001
				0. 0.

Table 3. Effect of Hydrogen Added to Methane on the Product
Distribution at Large Dose (4×10^4 Mrad)

Run No.	S-17	S-18	Ave.	S-6	S-17,18/S-6
The amount of CH ₄ (g)	2.45	2.37	2.41	4.80	
H ₂ (g)	0.27	0.29	0.28	0.0	
The amount of products (in mg) normalized to 1 g CH ₄					
C ₂ H ₄	0.01	0.02	0.015	0.41	0.037
C ₂ H ₆	42.9	48.5	45.7	103.1	0.44
C ₃ H ₈	8.5	9.8	9.	31.3	0.29
i-C ₄ H ₁₀	1.3	1.5	1.4	7.1	0.20
n-C ₄ H ₁₀	3.5	4.0	3.8	12.9	0.29
neo-C ₅ H ₁₂	0.4	0.4	0.4	1.7	0.24
i-C ₅ H ₁₂	1.3	1.7	1.5	8.8	0.17
Condensable liquid	0.1	0.2	0.15	91.7	0.002
Non-volatile liquid	110.6	89.0	99.8	289.6	0.34

hydrogen was reached by 1.5×10^4 Mrad.

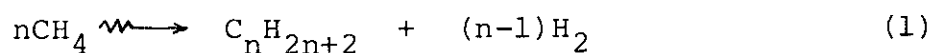
The result of the present study indicates that the presence of hydrogen in methane in equal amount increases the lower fractions of hydrocarbon products with very low yields of olefins as expected, but ambiguity remains in that the amount of non-volatile fraction found in the methane-hydrogen mixture irradiated with large dose (4×10^4 Mrad) was larger than that found in the corresponding pure methane.

(M. Hatada, S. Sugimoto, and S. Nagai)

- 1) M. Hatada, H. Arai, and S. Nagai, JAERI-M 9856, 39 (1981).

3. Radiation Chemical Reactions of Methane-Deuterium Mixture at Large Dose

In the last annual report¹⁾, it was reported that hydrogen, methane, and liquid hydrocarbons were the main components of the irradiated methane at 10^4 Mrad. Irradiation of methane produces hydrogen and hydrocarbons by reaction (1), but simultaneously, methane is reproduced from the hydrocarbons by irradiation in the presence of hydrogen.



By the analysis of isotopic abundance of methane in the methane-deuterium mixture after irradiation, it is possible to estimate the amount of original methane survived after irradiation.

In the preceding section of this volume, it is also reported that the presence of hydrogen in methane in equal amount increases the concentration of lower hydrocarbons produced by electron beam irradiation with an exception at extremely large dose (4×10^4 Mrad) where larger concentration of non-volatile liquid hydrocarbon products was found in the radiolysis of the mixture than in the pure methane. It is interesting to know whether hydrogen initially present in the

system is involved in the radiation chemical reactions of methane or it plays merely a role of diluent in the reaction. When deuterium is used instead of hydrogen in the methane mixture, deuterium containing hydrocarbon products will be found in the former case and not in the latter. The present study has been carried out in the expectation that the isotopic distribution in the products may help to give an insight to the above problem.

The methods of irradiation and analysis were exactly the same as those described in the foregoing section except that deuterium was used instead of hydrogen and the isotopic distribution of the products was carried out by the technique described below. A combination of a gaschromatograph (Yanaco G 800 modified for TCD operation and equipped with 3 m Porapak Q columns) and a quadrupole mass filter (NEVA NAG-530 type) was used for the determination of isotopic distribution of hydrogen, methane, ethane, and propane. Argon was used for analysis of hydrogen and helium was used for hydrocarbon products as carrier gas.

The condensable and non-volatile liquid hydrocarbon products were collected as described previously¹⁾, and subjected to infrared spectroscopy on a Hitachi model 210 infrared spectrophotometer.

Methane and deuterium were supplied by Takachiho Chemicals and Showa Denko Co., respectively, and were used as received.

The mass spectrum of a component of each fraction is shown in Fig. 1 A through D, and the standard mass spectrum obtained for the corresponding authentic sample having no deuterium in Fig. 1 a through d. Qualitative comparison of a pair of spectra, e.g., A and a, etc., shows that the deuterated equivalents containing up to 2, 4, 4, and 4 deuterium atoms for hydrogen, methane, ethane, and propane, respectively, were produced from the $\text{CH}_4\text{-D}_2$ mixture by the irradiation. Hereafter, the isotopic species will be expressed as either in the form of CH_4 and CD_3H , or methane- d_0 and methane- d_3 , respectively, for example.

In order to determine the amounts of isotopic species from

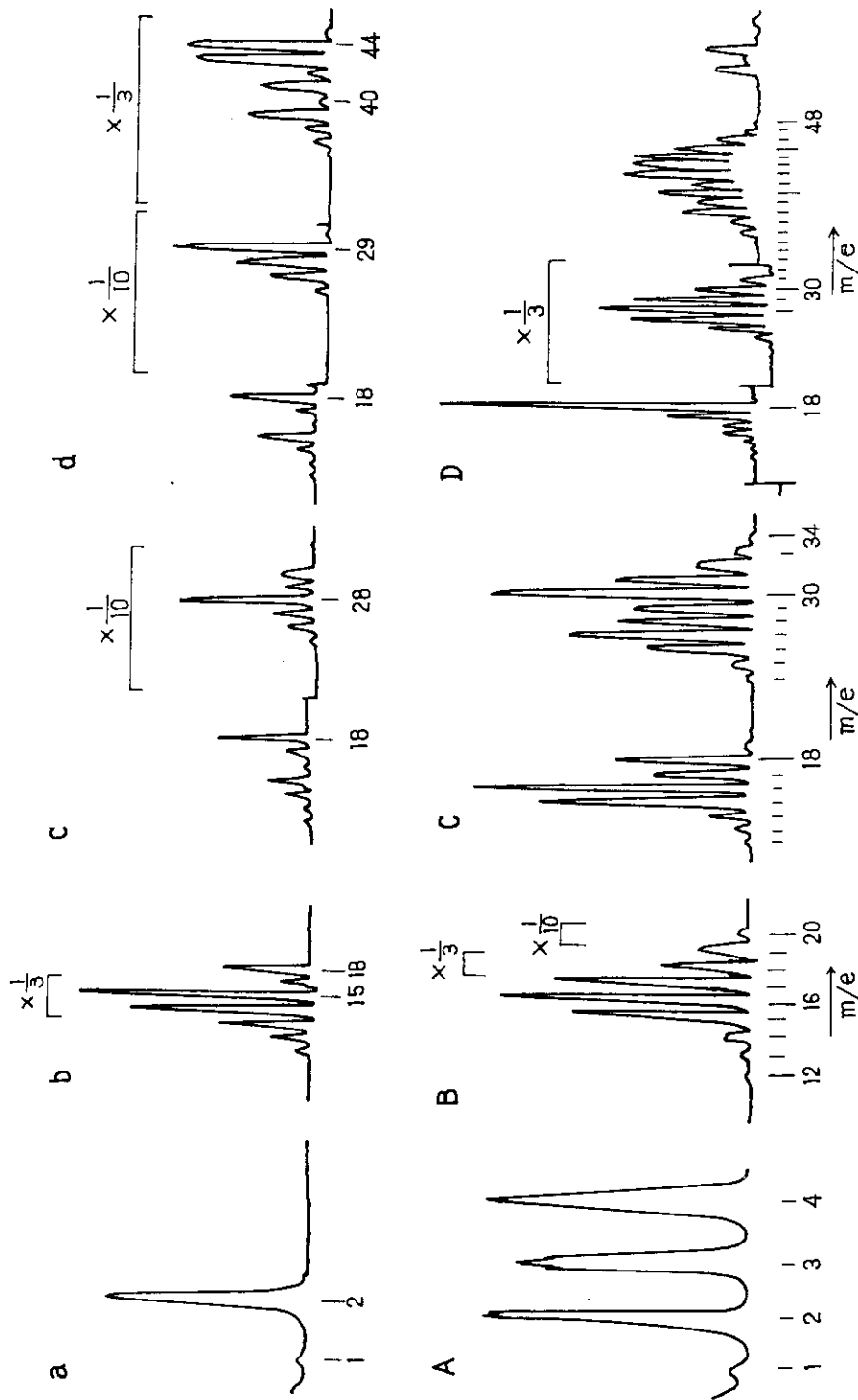


Fig. 1. Mass spectra of standard samples of hydrogen (a), methane (b), ethane (c), and propane (d), and those obtained from CH₄-D₂ mixture (denoted by capital letters).

the mass spectrum, the standard mass spectrum of each species or the cracking pattern of each isotopic species must be obtained experimentally for the mass spectrometer in use, or for approximate calculation, the mass spectra of authentic samples obtained under similar conditions should be known in advance at least. None of these were difficult to know in the present study except for methane and its four deuterated²⁾. Therefore, the cracking patterns of deuterated hydrocarbons were calculated under the assumptions that the bond dissociation of the deuterated molecules by electron impact occurs in the same way as those of the corresponding non-deuterated molecule, and a statistical elimination of H vs D occurs for partially deuterated molecules ignoring the isotopic effect in bond dissociation processes. The relative abundance, RA, of $C_iH_aD_{r-a}$ ion formed from $C_iH_mD_n$ molecule can be calculated from the following formula:

$$RA = f_r \frac{m^C \cdot a \cdot n^C \cdot r-a}{m+n} C_r$$

where f_r is a relative abundance of C_iH_r ion formed from molecule having no deuterium atoms, C_iH_{m+n} . The calculated cracking patterns for deuterated and partially deuterated hydrocarbons are listed in Table 1 a through c together with the cracking patterns obtained experimentally for non-deuterated compounds. In Table 1 a, the experimental cracking patterns reported for methane and its deuterated substitutes are also included for comparison. The agreements between the calculated and observed values are not completely well due to the ignored isotopic effects and instrumental difference, but the calculated cracking patterns still seem to be useful for approximate calculations. Isotopic distribution of hydrogen can be calculated directly under the above assumptions. The calculated isotopic abundance of hydrogen, methane, ethane, and propane are listed in Table 2.

The infrared spectra of non-volatile liquid products obtained for CH_4-H_2 and CH_4-D_2 mixtures are shown in Fig. 2. Exactly the same spectrum was recorded for the volatile liquid

Table 1-a. Cracking Patterns of Methane and Deuterated Methanes

m/e	CH ₄	CH ₃ D	CH ₂ D ₂	CHD ₃	CD ₄
20					100 (100) [100]
19				100 (100)	
18			100 (100)	18.4 (39.4)	73.4 (70.4) [87.2]
17		100 (100)	36.8 (54.9)	55.1 (42.6)	
16	100 (100)	55.1 (62.0)	38.7 (24.5)	5.7 (3.2)	11.4 (3.6) [13.6]
15	73.5 (73.4)	24.6 (13.6)	7.6 (3.3)	5.7 (1.8)	
14	11.4 (6.2)	6.1 (2.1)	4.5 (1.5)	3.9 (1.3)	5.2 (6.7) [7.25]
13	5.2 (2.2)	3.9 (1.1)	2.6 (0.6)	1.3 (0.4)	
12	1.6 (0.7)	1.6 (0.4)	1.6 (0.4)	1.6 (0.6)	1.6 (0.4) [3.2]

Values in parentheses and brackets were taken from ref. 2 obtained by high resolution mass spectrometry, and by ordinary mass spectrometry.

Table 1-b. Cracking patterns of Ethane and Deuterated Ethanes

m/e	C_2H_6	C_2H_5D	$C_2H_4D_2$	$C_2H_3D_3$	C_2D_6
34					100
33				100	28.8
32			100	43.2	86.8
31		100	57.5	131.2	234.7
30	100	71.9	204.8	270.2	200.6
29	86.3	307.7	259.3	143.4	73.8
28	440	208.1	108.5	71.6	57.0
27	123.3	88.5	67.8	54.8	43.2
26	80.9	54.0	32.4	16.2	5.4

Table 1-c. Cracking Patterns of Propane and Deuterated Propanes

m/e	C_3H_8	C_3H_7D	$C_3H_6D_2$	$C_3H_5D_3$	$C_3H_4D_4$
48				100	100
47				100	43.7
46			100	54.6	47.0
45	3.35(i*)	100	65.6	38.2	12.0
44	100	76.5	30.0	16.5	23.5
43	87.4	22.3	23.2	27.3	22.0
42	15.2	33.1	27.4	17.1	11.6
41	46.8	21.8	15.8	19.3	25.8
40	8.4	25.1	32.3	32.2	27.4
39	55.7	38.8	26.7	18.5	12.9
38	15.8	13.2	11.1	9.5	8.6
37	10.5	9.2	7.9	6.6	5.3
36	1.1	1.1	1.1	1.1	1.1

* impurity

Table 2. Isotopic Abundance of the Products (mole %) from
 $\text{CH}_4\text{-D}_2$ Mixture by Electron Beam Irradiation

Hydrogen	Methane			Ethane			Propane		
H ₂	33.0	CH ₄	74.7	C ₂ H ₆	29.6	C ₃ H ₈	39.4		
HD	32.0	CH ₃ D	17.8	C ₂ H ₅ D	40.2	C ₃ H ₇ D	32.2		
D ₂	35.0	CH ₂ D ₂	5.6	C ₂ H ₄ D ₂	21.8	C ₃ H ₆ D ₂	18.7		
		CHD ₃	1.6	C ₂ H ₃ D ₃	7.2	C ₃ H ₅ D ₃	7.4		
		CD ₄	0.3	C ₂ H ₂ D ₄	1.3	C ₃ H ₄ D ₄	2.3		

fraction obtained for $\text{CH}_4\text{-D}_2$ mixture by irradiation. The spectrum of the liquid products obtained for $\text{CH}_4\text{-D}_2$ mixture shows clearly the splitting of the absorption due to C-H stretching vibrations resulted by the isotopic replacement of C-H bond with C-D bond. The number of C-H bonds relative to that of C-D bonds was estimated to be 5.1 from the integrated absorption intensities of the two peaks.

The above results on isotopic analyses of hydrogen and hydrocarbon products together with those of ordinary gas-chromatographic analyses on chemical species allow us to display product distribution including isotopic identify. The results are shown in Table 3.

The amounts of hydrogen and deuterium added over main

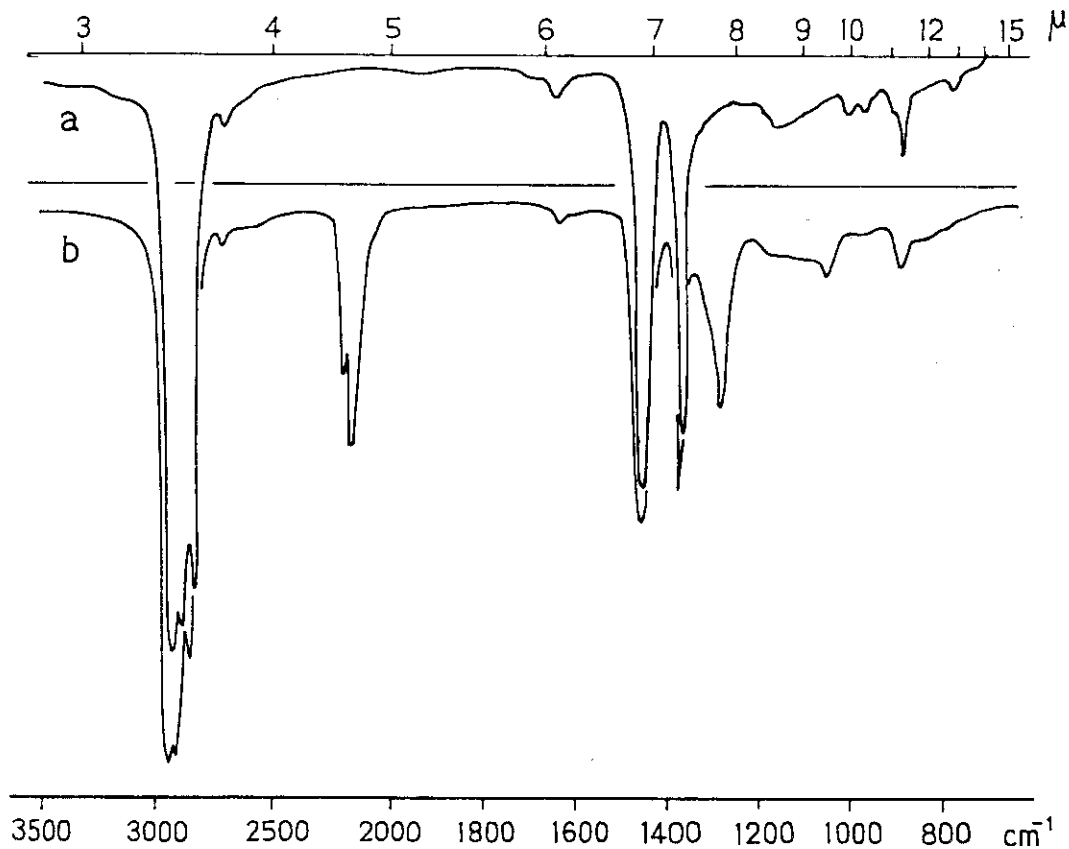


Fig. 2. Infrared spectra of non-volatile liquid hydrocarbon products obtained from $\text{CH}_4\text{-H}_2$ (a) and $\text{CH}_4\text{-D}_2$ (b) mixtures by electron beam irradiation.

Table 3. The Amounts of Products from CH₄-D₂ Mixture
by Electron Beam Irradiation

Composition of starting mixture

CH ₄	367 Torr at 23°C	0.141 mole	2.256 g
D ₂	380	0.146	0.584

Irradiation

0.6 MeV, 1 mA, 21600 sec.

Temperature during irradiation 91°C

Products		m mole		mg	
Hydrogen	H ₂	72.9	222.4	146	672
	HD	71.4		214	
	D ₂	78.1		312	
Methane	CH ₄	55.0	75.3	960	
	CH ₃ D	14.3		243	1312
	CH ₂ D ₂	4.5		81	
	CHD ₃	1.3		24	
	CD ₄	0.2		4	
Ethane	C ₂ H ₆	5.5	18.44	164	576
	C ₂ H ₅ D	7.4		231	
	C ₂ H ₄ D ₂	4.0		129	
	C ₂ H ₃ D ₃	1.3		44	
	C ₂ H ₂ D ₄	0.24		8.2	
Propane			3.1		136
i-Butane			0.45		26
n-Butane			1.0		59
neo-Pentane			0.1		8
i-Pentane			0.4		26
n-Pentane			0.04		3
Liquid hydrocarbon	(CH)		12.06		169
	(CD)		2.36		38
					3025

products are 0.589 and 0.276 mole, respectively, giving the H/D ratio of 2.1. Since the amounts of hydrogen and deuterium contained in the original mixture were 0.564 and 0.292, respectively, the amounts of H and D in the original mixture are conserved well in the products and the H/D ratio of the original mixture agrees well with the one calculated for the products, indicating the accuracy of the experiment.

When m mole of CH_4 in the mixture containing n mole of CH_4 and n mole of D_2 is reacted to form ethane and hydrogen independently each other, the stoichiometric relation can be given by eq. (1).

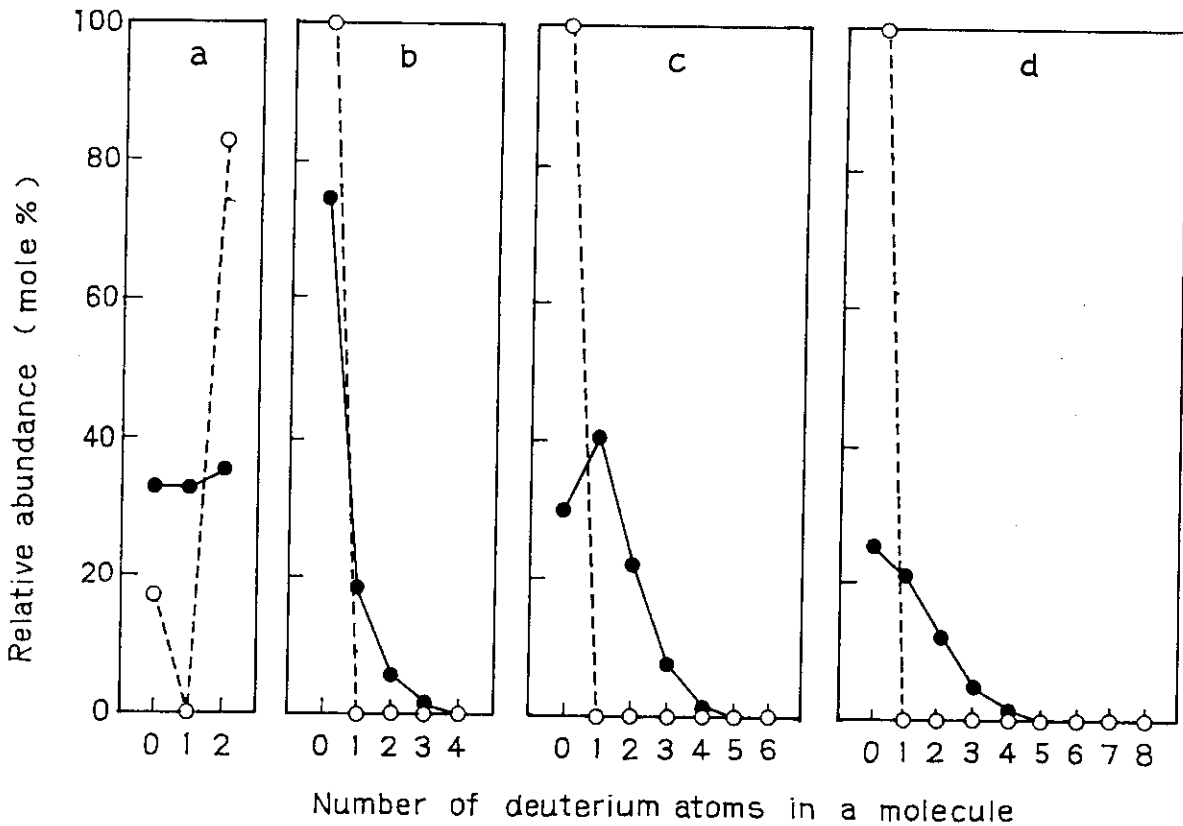
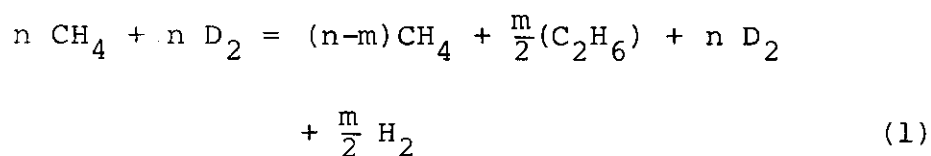
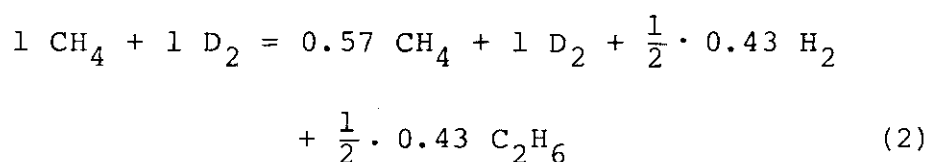


Fig. 3. Relative abundance of product as a function of number of deuterium atoms in a molecule: hydrogen (a), methane (b), ethane (c), and propane (d); ---○--- calculated under the assumption that no exchange of H and D atoms between molecules occurs; —●— found.



In this equation, only ethane is considered as a product for simplicity. Since 43% of methane is consumed by 4×10^4 Mrad irradiation, eq. (1) can be rewritten using $n = 1$ and $m = 0.43$:



The relative isotopic abundances of hydrogen, methane, ethane, and propane expected from the above relation are compared with those found in the experiment (S-19) in Fig. 3. It is apparent

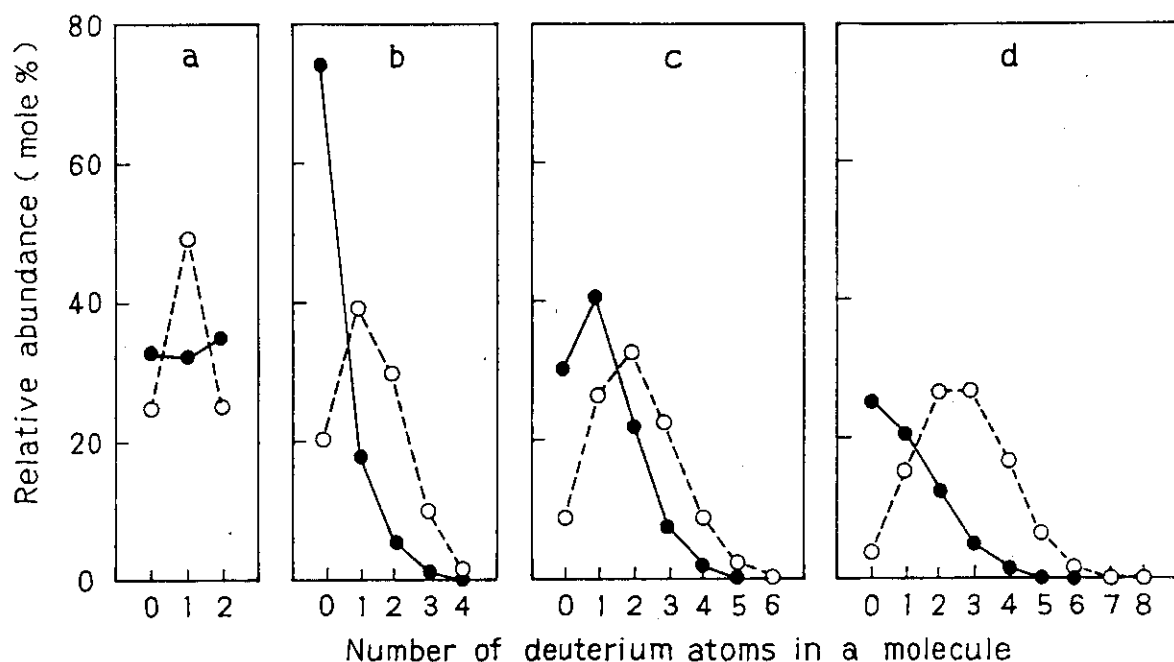


Fig. 4. Relative abundance of products as a function of number of D atoms in a molecule: hydrogen (a), methane (b), ethane (c), and propane (d); ---○--- calculated; —●— found.

that the calculated isotopic abundance on the basis of eq. (2) can not explain the experimental result, showing that the isotopic exchange does occur during irradiation and that the hydrogen initially present in the system is not merely a diluent.

The assumption of the other extreme is that the complete isotopic equilibrium exists between hydrogen, methane, ethane, propane, and liquid hydrocarbon, the latter three of which are further assumed to have the same isotopic abundance. Since original H/D ratio is 2, the isotopic abundance of a compound having k hydrogen atoms can be calculated as binomial expansion terms:

$$(a + 1)^k ; a = 2 \quad (3)$$

The calculated and experimental values are compared in Fig. 4.

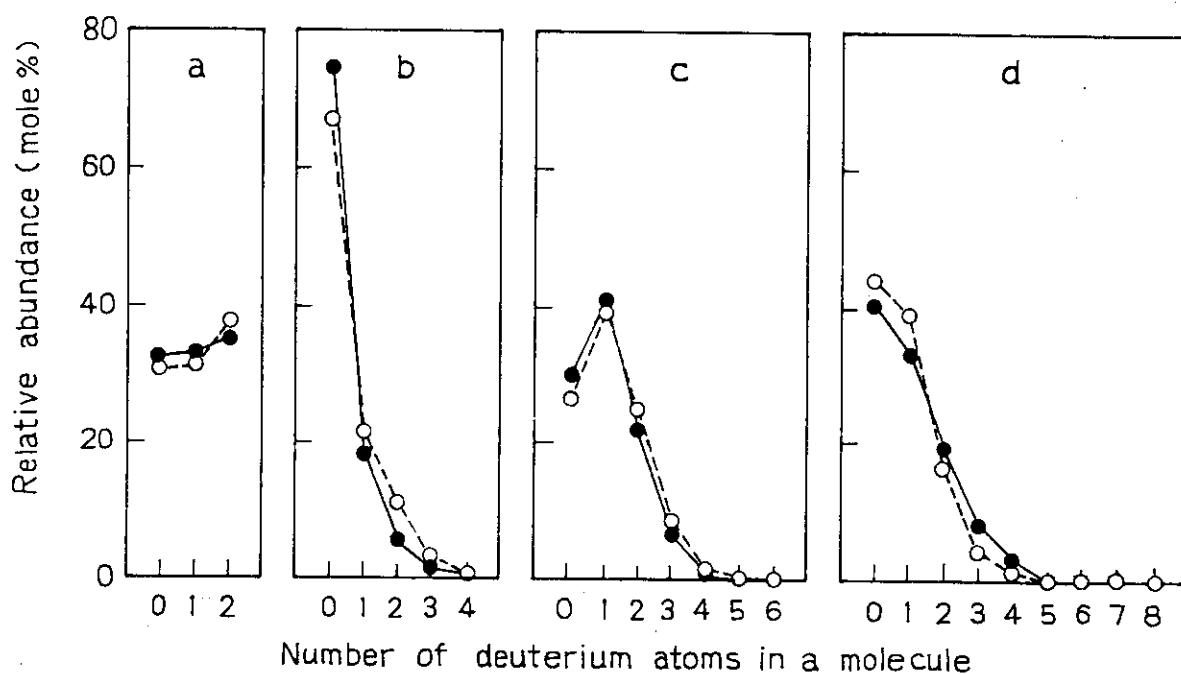


Fig. 5. Relative abundance of products as a function of number of D atoms in a molecule: hydrogen (a), methane (b), ethane (c), and propane (d); ---○--- calculated; —●— observed.

This model also fails to explain the experimental results. The best fitted calculated results shown in Fig. 5 were obtained for hydrogen under the assumption that about 3/10 of D_2 remains unchanged as D_2 and 7/10 of D_2 is reacted for complete randomization in $H/D = 2$; for methane, about 1/2 of methane is left unchanged (in the form of CH_4) and the hydrogen atoms in the rest of methane randomize with deuterium in the ratio of $H/D = 3$; for ethane, all hydrogens in ethane randomize in the ratio of $H/D = 4$; and for propane, in the ratio of $H/D = 9$. Further detailed investigation should be made on whether there is any contradiction in these assumptions. What indicates the H/D ratio giving the best fit isotopic abundance in the products is not known at present, but the result certainly shows that the hydrogens originally exist in the mixture do not only play a role of diluent, but also react with methane to be incorporated in the product molecules, so do the hydrogens produced from methane during the irradiation. All of the methane molecules present in the system after 4×10^4 Mrad irradiation are not unreacted methane molecules but ca. 50% of methane molecules present in the system were produced by the results of repeated cycles of consumption of methane and regeneration by the radiolysis of hydrocarbon products under the presence of hydrogen.

(M. Hatada, S. Sugimoto, and S. Nagai)

- 1) M. Hatada, H. Arai, and S. Nagai, JAERI-M 9856, 39 (1981).
 - 2) L. L. Hills, M. L. Vestal, and J. H. Futrell, J. Chem. Phys., 54, 3834 (1971).
4. Formation of Carbonaceous Solid by Irradiation of Methane over Molecular Sieve 5A and Silica Gel

In the last annual report¹⁾, it was reported that the yields of hydrogen and C_2 - C_3 hydrocarbons produced from methane over molecular sieve (MS) 4A and MS 5A by electron beam irradiation decreased gradually with irradiation time and

approached to the values obtained by the homogeneous radiolysis of methane. After irradiation, the MS's changed in color to dark brown, due to the deposition of the carbonaceous solid on the surface which was thought to poison the activity for the radiation chemical reaction of methane. The present study was carried out in an attempt to evaluate the amount of the carbonaceous solid deposited on the MS's and to confirm the poisoning of the methane reaction due to the formation of the solid. For this purpose, a series of experiments of desorption and irradiation under either flowing Ar or H₂ was carried out on the MS 5A which had been irradiated in the methane flow. The concentrations of the products in the effluent gas were monitored by the gaschromatographs¹⁾. For comparison, similar experiments were carried out with silica gel.

The results of product analysis with MS 5A are shown in Fig. 1. After methane was irradiated in the presence of MS 5A in the reactor at 300°C for 183 min (a), the methane feed and irradiation were stopped and Ar gas was passed over the MS 5A while the temperature was being kept at 300°C (b). After the concentrations of the desorbable products, mainly C₂H₄ and C₂H₆, in addition to the methane remained in the path, decreased below the detection limit, the Ar feed was stopped and H₂ gas was introduced to the reactor kept at 300°C (c). Methane was again detected by the H₂ flowing due to either the desorption induced by the H₂ flushing, the chemical reaction of the carbonaceous solid with H₂, or both. When irradiation was again started under the H₂ flow over the MS 5A at 300°C (d), the low molecular weight hydrocarbons were found in the emerged gas in the concentrations comparable to those observed during irradiation of methane over a fresh MS 5A (a). Methane and C₂H₆ were still observed when the feed gas was changed from H₂ to Ar while irradiation being continued (e), but their concentrations in the Ar flowing are much lower than those in the H₂ flowing (d). When H₂ gas was again introduced instead of Ar (f), the concentrations of hydrocarbons in the emerged gas again increased to the level which had been observed in the previous stage (d) under the same irradiation conditions.

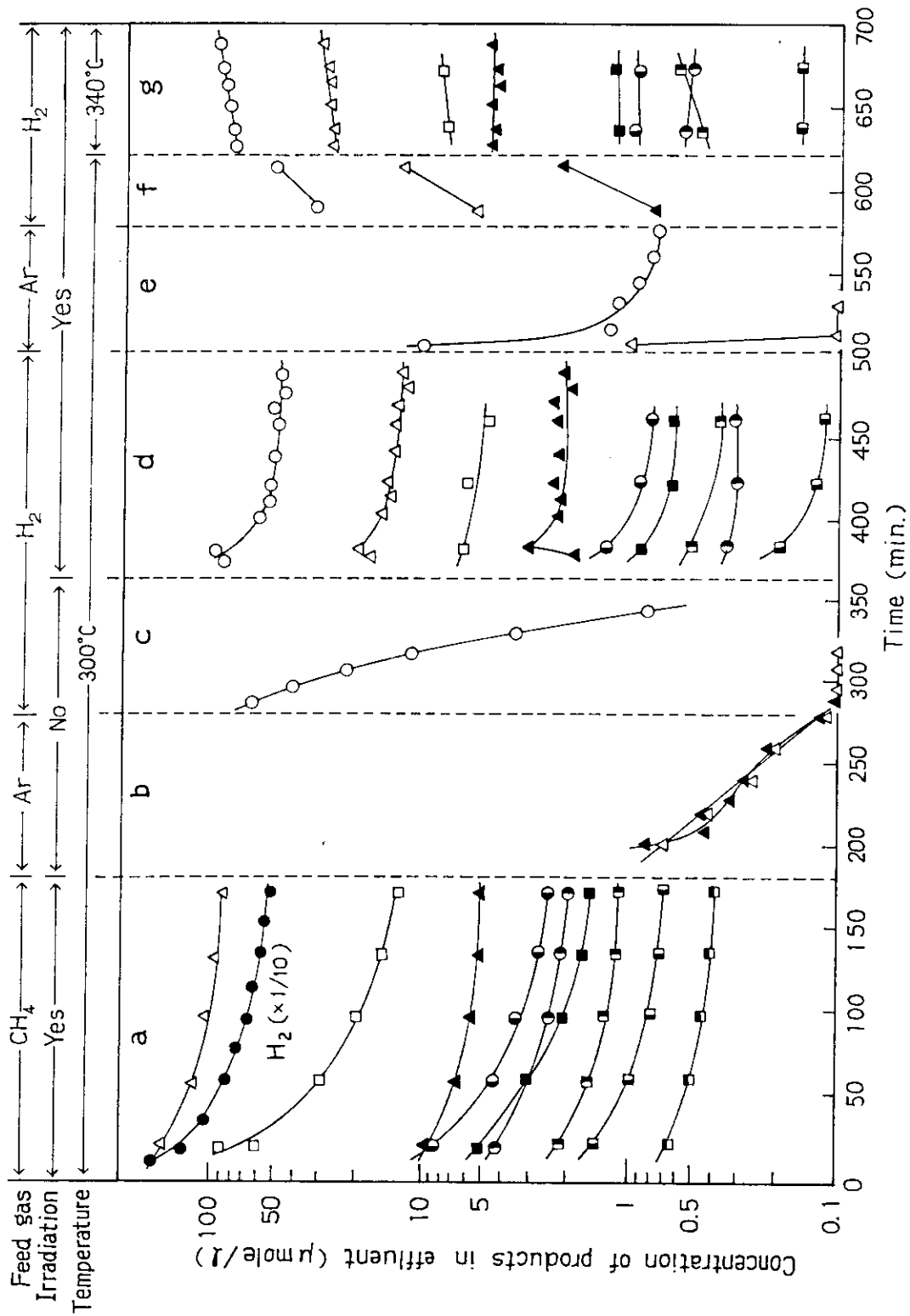


Fig. 1. Concentrations of products during and after irradiation of methane over molecular sieve 5A: (○) CH₄, (▲) C₂H₄, (△) C₂H₆, (■) C₃H₆, (□) C₃H₈, (●) n-C₄H₁₀, (⊙) i-C₄H₁₀, (■) n-C₅H₁₂, (⊙) i-C₅H₁₂, (⊙) neo-C₅H₁₂.

Table 1. Product Yields by Irradiation of Methane in the Presence of MS 5A*

Product	a. Irrad. of CH ₄	b. Desorption by Ar	c. Desorption by H ₂	d. Irrad. in H ₂	e. Irrad. in Ar	f. Irrad. in H ₂	g. Irrad. in H ₂	Σ b ^o g
H ₂	12821	—	—	—	—	—	—	—
CH ₄	—	—	127	718	11.2	144	582	1582
C ₂ H ₄	104	3.3	0.2	28.2	—	4.8	31.5	68
C ₂ H ₆	1836	2.8	0.2	177	0.9	29.8	95.1	306
C ₃ H ₆	44.5	1.4	—	8.4	—	—	7.6	17
C ₃ H ₈	415	0.3	—	62.1	—	—	55.4	118
i-C ₄ H ₁₀	43.8	—	—	3.8	—	—	3.2	7.0
n-C ₄ H ₁₀	68.7	—	—	11.3	—	—	6.1	17.3
neo-C ₅ H ₁₂	7.8	—	—	—	—	—	—	—
i-C ₅ H ₁₂	23.7	—	—	5.4	—	—	1.1	6.5
n-C ₅ H ₁₂	14.8	—	—	—	—	—	—	—
Σ hydrocarbon	2559	7.8	127	1014	12	178	782	2122
Σ C	5940	17	128	1427	13	213	1067	2865

* Product yields are given in μmoles. For reaction conditions, see Fig. 1.

irradiation of methane over MS 5A produces the carbonaceous solid in a considerable amount as well as hydrogen and low molecular weight hydrocarbons. Comparison of the numbers of carbons of the total hydrocarbons observed during and after irradiation (see the bottom row in Table 1) indicates that the yield of the carbonaceous solid amounts to at least about half the yield of the total hydrocarbons produced during irradiation. After the reaction (g) in Fig. 1, methane was again irradiated over the MS 5A at 300°C. The concentrations of H₂ and hydrocarbons agreed with those that have been observed in the first stage (a) in Fig. 1. Therefore, it can be concluded that the carbonaceous solid deposited on MS 5A during irradiation of methane indeed acts as a poison of the radiation chemical reaction of methane.

The results obtained with silica gel are shown in Fig. 2. Irradiation of methane over silica gel (a) produces hydrogen and hydrocarbons in the concentrations much higher than those over MS 5A, and the concentrations show little or no decrease with time. After this reaction, silica gel changed in color, due to the deposition of carbonaceous solid as well as MS 5A. The Ar and H₂ flowing over the silica gel (b and c) induce desorption of C₁-C₃ hydrocarbons in low concentrations. Irradiation of the silica gel under H₂ flow (d) produces hydrocarbons consisting dominantly of methane. It is noted that the initial concentrations of hydrocarbons produced are much lower than those in the first stage (a) in contrast to the result obtained with MS 5A and decrease rapidly with irradiation time. This result indicates that silica gel exhibits greater activity under electron beam irradiation for hydrogenolysis of the carbonaceous solid produced from methane than MS 5A. Increase of the irradiation temperature to 340°C (e) results in a slight increase in the initial concentrations of hydrocarbons.

Table 2 shows the product yields estimated from the data in Fig. 2. The material balance of hydrogen during irradiation of methane equals to approximately 1.2, indicating that the reaction of methane over silica gel leaves less carbonaceous solid on the surface than that over MS 5A. By taking into

Table 2. Product Yields by Irradiation of Methane in the Presence of Silica Gel*

Product	a. Irrad. of CH ₄	b. Desorption by Ar	c. Desorption by H ₂	d. Irrad. in H ₂	e. Irrad. in H ₂	Σ b o e
H ₂	43369	—	—	—	—	—
CH ₄	—	—	6.7	922	5.8	935
C ₂ H ₄	394	—	—	2.3	—	2.3
C ₂ H ₆	8906	0.6	—	108	6.3	115
C ₃ H ₆	548	0.1	—	0.9	—	1.0
C ₃ H ₈	2858	0.3	—	42.7	0.9	44
i-C ₄ H ₁₀	3220	—	—	24.2	—	24
n-C ₄ H ₁₀	989	—	—	12.3	—	12
neo-C ₅ H ₁₂	191	—	—	—	—	—
i-C ₅ H ₁₂	1026	—	—	6.8	—	6.8
n-C ₅ H ₁₂	298	—	—	—	—	—
Σ Hydrocarbon	18430	1.0	6.7	1119	13	1140
Σ C	53229	2.4	6.7	1453	21	1483

* Product yields are given in μmoles. For reaction conditions, see Fig. 2.

account the fact that the carbonaceous solid deposited on silica gel surface is rapidly decomposed to low molecular weight hydrocarbons by irradiation under flowing H_2 , it seems reasonable to assume that during the irradiation of methane, the carbonaceous solid reacts with H_2 , which is the most abundant radiolysis product of methane, to form hydrocarbons having more than two carbons in good yields.

(S. Nagai, Y. Shimidzu, and M. Hatada)

- 1) S. Nagai, Y. Shimidzu, and M. Hatada, JAERI-M 9856, 72 (1981).

5. Radiation-Induced Reactions of Methane-Hydrogen Mixtures over Molecular Sieve 5A

As described in the preceding paper¹⁾, irradiation of methane over molecular sieve (MS) 5A produces a considerable amount of carbonaceous solid on the surface which causes serious loss in activity of MS 5A for the formation of low molecular weight hydrocarbons. The carbonaceous solid deposited on the surface of MS 5A, however, was found to be decomposed to hydrocarbons if irradiated under H_2 flow. This finding suggests that the temporal loss in the activity of MS 5A during irradiation of methane would be suppressed if H_2 is added to the reactant methane at the concentrations sufficient to decompose the carbonaceous solid or to inhibit the formation of the solid. In the present study, product analysis was carried out on the radiation-induced reaction of methane containing hydrogen up to 75 mol%, attention being paid to the yields of C_2 - C_3 hydrocarbons which have been found to be selectively produced over MS 5A²⁾.

Methane-hydrogen mixtures with the hydrogen contents of 25, 50 and 75 mol% were irradiated at 300°C in the presence of MS 5A which had been outgassed at ~450°C for several hrs. Irradiation and product analysis were carried out in the same manner as described already²⁾. For comparison, studies were

Table 2. Initial and Final Product Yields in the Radiolysis
of CH₄-H₂ Mixtures over MS 5A at 300°C^a

Yield (μmole/10% NTP)	CH ₄		H ₂		Initial		Final	
	Flow rate (mℓ/min)	100	75	25	Initial	Final	Initial	Final
H ₂			5973					
C ₂ H ₄		125	59	98	76	77	63	63
C ₂ H ₆		1733	754	1149	825	851	529	556
C ₃ H ₆		90	9	63	54	35	43	29
C ₃ H ₈		885	100	599	576	361	315	325
i-C ₄ H ₁₀		63	19	48	33	26	20	18
n-C ₄ H ₁₀		134	18	79	73	40	40	34
neo-C ₅ H ₁₂		9	4	7	4	3	2	2
i-C ₅ H ₁₂		31	9	26	20	16	14	13
n-C ₅ H ₁₅		25	5	15	11	8	6	6

^a Initial and final product yields are those determined 22 and 175 min on stream, respectively.

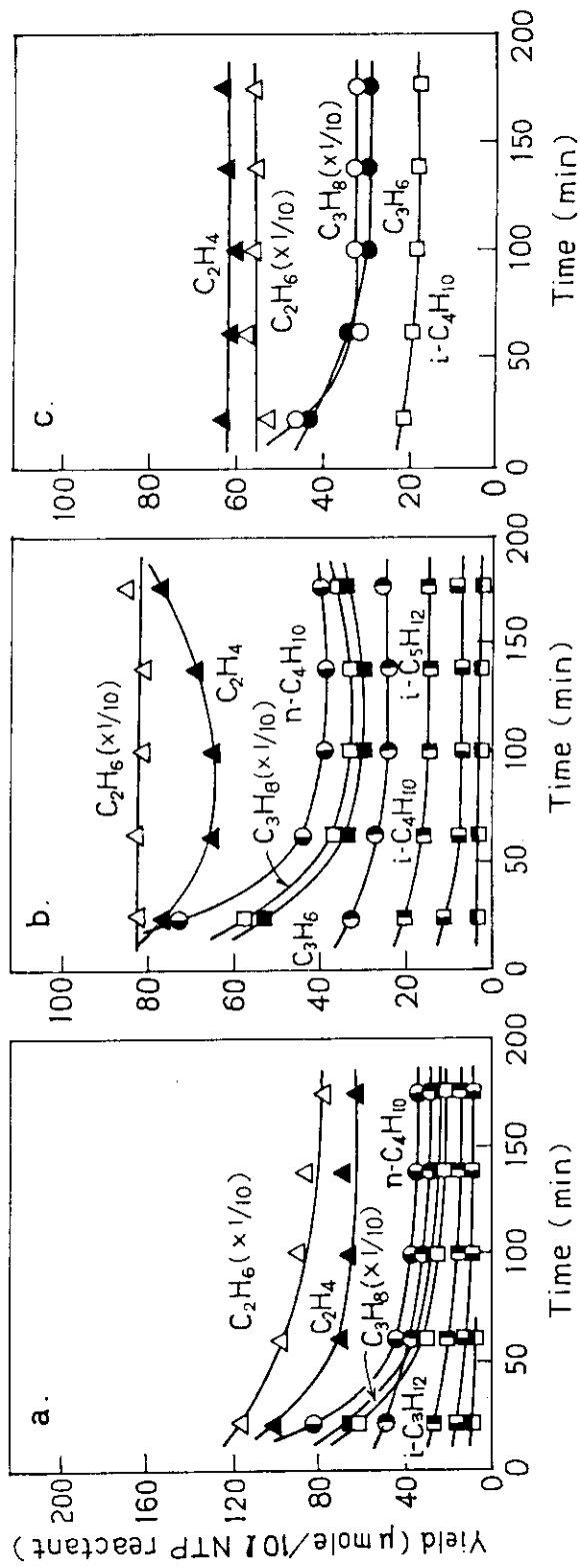


Fig. 1. Yields of the products by irradiation of methane-hydrogen mixtures over molecular sieve 5A at 300°C, as a function of time after initiating irradiation: (a) 3 : 1 $\text{CH}_4\text{-H}_2$; (b) 1 : 1 $\text{CH}_4\text{-H}_2$; (c) 1 : 3 $\text{CH}_4\text{-H}_2$.

also carried out on the homogeneous radiolysis of the methane-hydrogen mixtures.

Table 1 summarizes the product yields, in $\mu\text{moles per } 10 \text{ g}$ reactant and in G values, determined for the homogeneous radiolysis of methane-hydrogen mixtures. With increasing H_2 content in the mixtures, the yields of the most hydrocarbons decreased nearly proportionately as expected. The yields of ethylene and propylene, however, decreased markedly with the increase in the H_2 content, possibly due to the hydrogenation of the olefins. The distribution of hydrocarbons from the methane-hydrogen mixtures almost agreed with that from pure methane. This result contrasts to that obtained when methane-hydrogen mixtures were irradiated to a high dose ($4 \times 10^4 \text{ Mrad}$)³⁾, which indicates that hydrogen added to the reactant methane serves to increase the yields of low molecular weight hydrocarbons, especially ethane and propane. The discrepancy may arise from the large difference in the irradiation doses employed in both studies.

Figure 1 a-c shows the hydrocarbon yields by irradiation of methane-hydrogen mixtures over MS 5A, as a function of time after initiating irradiation. It is noted that the decrease in the yields of C_2 hydrocarbons with time is almost completely suppressed in the mixtures containing hydrogen more than 50 mol% although the yields of C_3 hydrocarbons show a slight decrease with time even in the mixture containing 75 mol% H_2 .

The initial and final yields of C_2 hydrocarbons, which were determined 22 and 175 min on stream, respectively, are plotted as a function of H_2 content in the reactant mixtures in Fig. 2, and those of hydrocarbons up to C_5 are summarized in Table 2. As can be seen from Fig. 2, the initial yields slightly deviate from the broken line which denotes the yields expected in H_2 acts as a simple diluent. The final yields are lower than the initial yields for the mixtures containing 0 and 25 mol% H_2 , but becomes in accord with each other for the mixtures containing 50 and 75 mole% H_2 , indicating that addition of H_2 more than 50 mol% is necessary to suppress the undesirable loss in activity of MS 5A for the formation of C_2 hydrocarbons under electron beam irradiation. Further addition of H_2 is

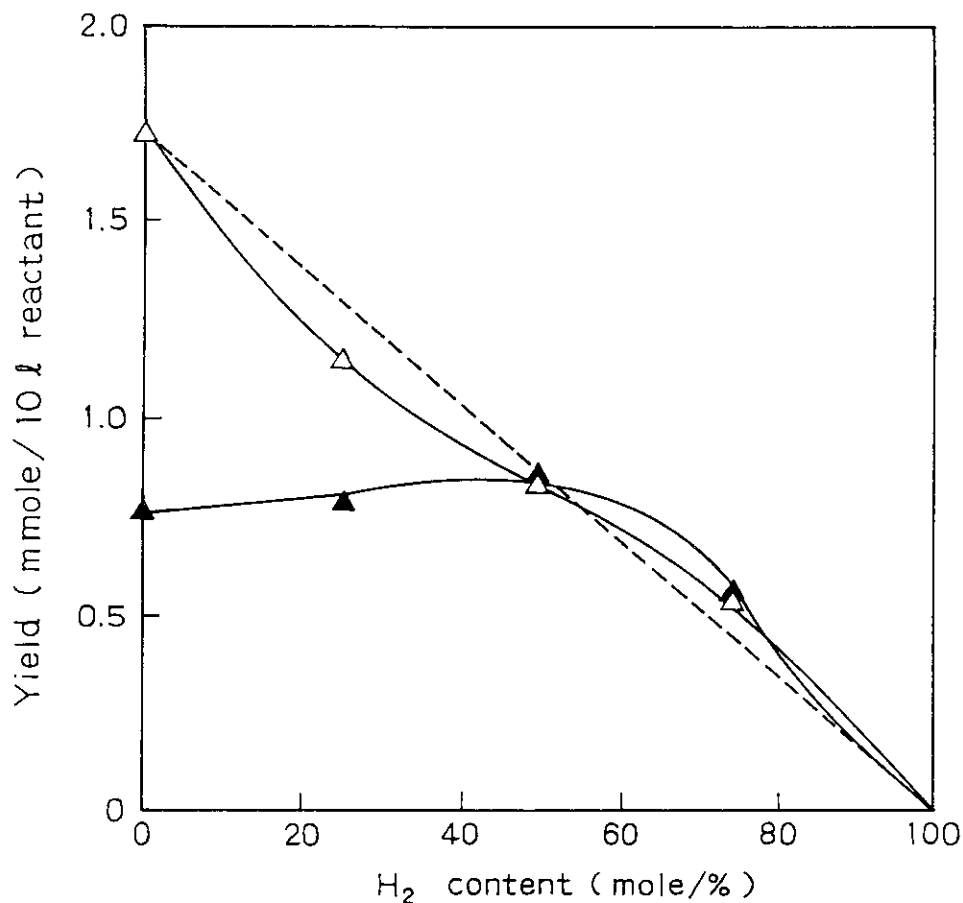


Fig. 2. Initial and final yields of ethane produced by irradiation of methane-hydrogen mixtures over molecular sieve 5A at 300°C, as a function of H₂ content. The initial (Δ) and final (▲) yields were determined 22 and 175 min on stream, respectively.

needed for suppressing the activity loss for the formation of C₃ hydrocarbons as seen from Table 2.

Addition of Ar or N₂ instead of H₂ to the reactant methane proved ineffective at all for suppressing the activity loss for hydrocarbon formation. Carbonaceous solid from methane was found to deposit on the surface of MS 5A even from methane containing 98 mol% Ar. Since the carbonaceous solid produced from methane is hardly decomposed by irradiation under Ar flow as reported already²⁾, it appears that Ar contained in methane

has no ability to inhibit the formation of the carbonaceous solid under irradiation, too.

(Y. Shimizu, S. Nagai, and M. Hatada)

- 1) Y. Shimizu, S. Nagai, and M. Hatada, This report.
- 2) S. Nagai, Y. Shimizu, and M. Hatada, JAERI-M 9856, 72 (1981).
- 3) M. Hatada, S. Sugimoto, and S. Nagai, This report.

6. Radiation-Induced Reactions of Carbon Monoxide with Water Adsorbed on Silica Gel and Some Other Metal Oxides

Preliminary studies on the radiation-induced reactions of carbon monoxide (CO) and water adsorbed on silica gel indicate that silica gel exhibits catalytic activity for the reaction under electron beam irradiation to produce H₂, CO₂ and low molecular weight hydrocarbons¹⁾. The present study was carried out in order to establish the previous finding and to see if some other metal oxides such as alumina and ZnO would also exhibit activity for the water gas shift (WGS) reaction as well as silica gel.

Metal oxides used in the present study are silica gel (mallinkrodt), alumina (Nakarai), MgO (Nakarai), ZnO (Nakarai) and TiO₂ (Merck). All these oxides were used as received. The water contents as determined by a thermogravimetric analysis (TGA) using Shinku Riko TGD-3000 Differential Thermal Micro Balance were 18.2% for silica gel, 7.6% for alumina and 7.5% for MgO. The water contents of ZnO and TiO₂ were too low (< 0.2%) to be determined. Irradiation and product analysis were carried out in the same manner as reported previously¹⁾.

Figure 1 shows the concentrations of H₂ and CO₂ produced by irradiation of alumina under flowing of Ar decreased gradually with time. As will be described later, irradiation of alumina under Ar flow produces O₂ as well as H₂ in the concentration ratio of O₂/H₂ = 1 : 2. When Ar gas was replaced with CO while irradiation was being continued, the H₂ concen-

tration suddenly increased by several times in the initial stage and then decreased gradually with time as well as the concentration of CO_2 . These results are the same as reported already for silica gel¹⁾. However, by contrast to the reaction over silica gel, increase of the irradiation dose rate (beam current) which is accompanied with temperature rise hardly results in the increase on the concentration of H_2 as seen from Fig. 1.

The results obtained with MgO (Fig. 2) show that the concentration of H_2 increases slightly on replacing Ar with CO and does markedly when the irradiation temperature reaches around 300°C by increasing the dose rate.

The increase of the H_2 concentration on replacing Ar flow with CO indicates that water adsorbed on alumina and MgO reacts

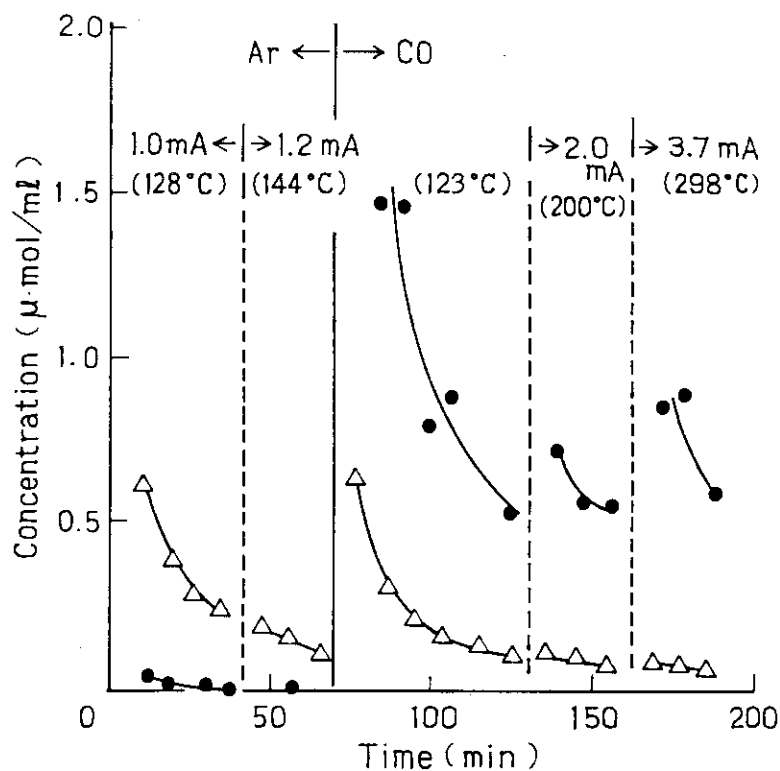


Fig. 1. Concentrations of H_2 and CO_2 produced by irradiation of alumina in Ar and/or CO flow at the flow rate of 50 ml/min: (Δ) H_2 ; (\bullet) CO_2 .

with CO to produce H₂ under electron beam irradiation as well as water adsorbed on silica gel.

Thermogravimetric curves for silica gel, alumina and MgO are compared in Fig. 3, which indicate that the water content of silica gel is larger than the water contents of the latter two which are almost the same each other. It is noted that the dominant desorption of adsorbed water from MgO occurs at around 300°C which is the temperature at which the H₂ concentration increased markedly during irradiation of MgO under CO flowing. This implies that the desorption of water from the surface plays an important role in the radiation chemical reaction of adsorbed water with CO.

Experiments with ZnO and TiO₂, on the other hand, provided no evidence for occurrence of the reaction between adsorbed

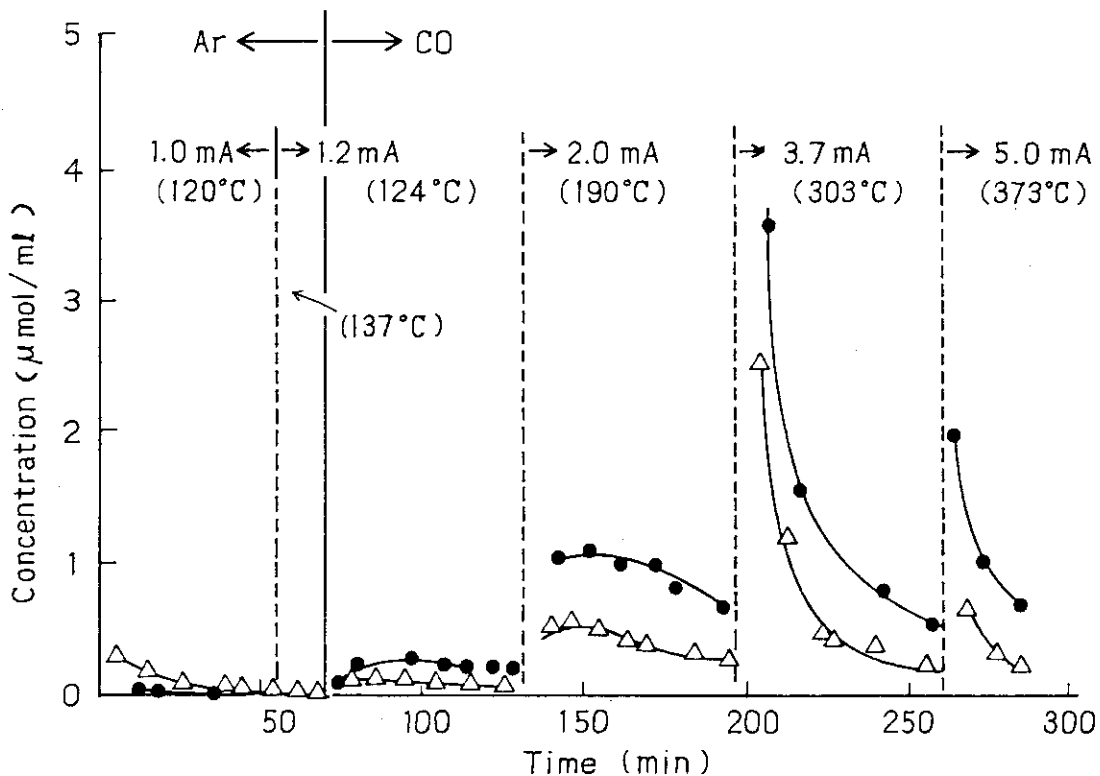


Fig. 2. Concentrations of H₂ and CO₂ produced by irradiation of MgO in Ar and/or CO flow at the flow rate of 50 ml/min: (Δ) H₂; (●) CO₂.

water and CO. That is, the concentration of H_2 produced by irradiation of either ZnO or TiO_2 under Ar flowing showed no increase on replacing the Ar flow with CO flow.

In an attempt to compare quantitatively the H_2 yields produced by the radiolysis of adsorbed water and the WGS reaction, a series of experiments was carried out on silica gel at three different dose rates at a constant temperature, $200^\circ C$. In each run of these experiments, a fresh 2 gr. lot of silica gel was irradiated under either Ar or CO flowing. Table 1 shows the H_2 yields produced by irradiation for 90 min after initiating irradiation. The H_2 yields produced under CO flowing are greater by more than one order of magnitude than those under Ar flowing and increase with the dose rate. By contrast, the H_2 yields under Ar flowing are independent of the dose rate, possibly because the dose rate influences similarly the rate of the reverse reaction of water decomposition.

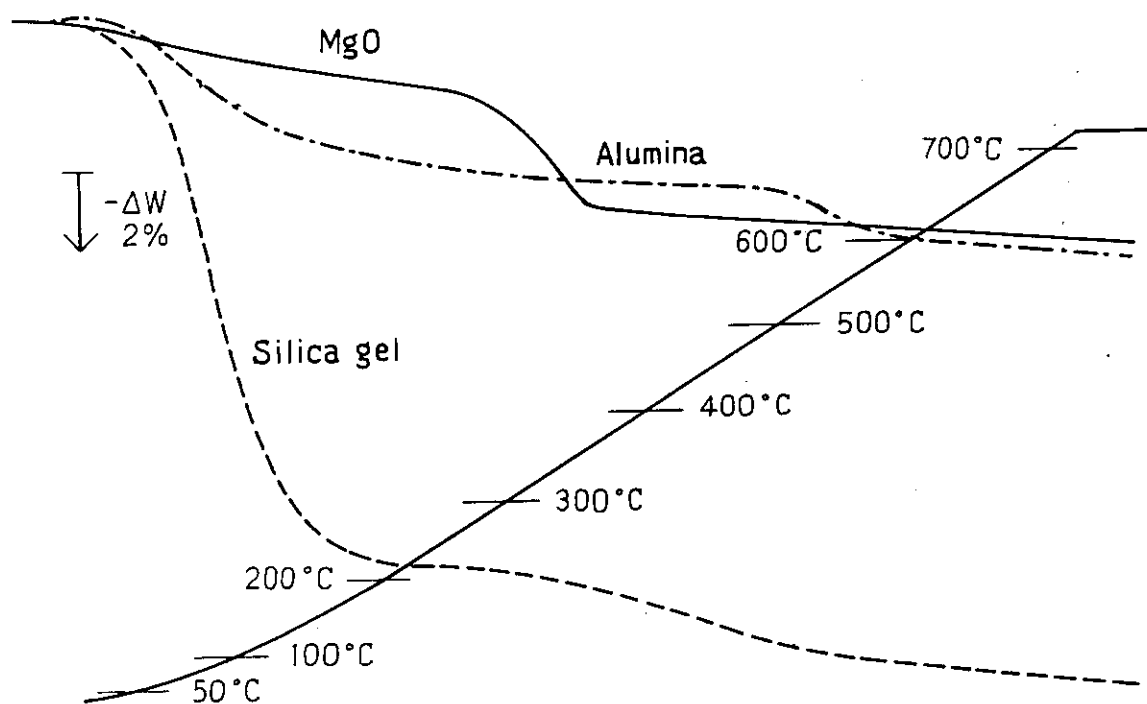


Fig. 3. Thermogravimetric curves of hydrated silica gel, alumina and MgO .

Table 1. The Amount of H₂ Produced from Hydrated Silica Gel*

Beam current (mA)	Under CO flow	Under Ar flow
0.5	1980	115
1	2719	142
2	3269	114

* in μmol produced by irradiation for 90 min at 200°C

It was found in these experiments that the H₂ concentration produced under CO flowing reaches a maximum at around 10 min after initiating irradiation and then decreases with time whereas the concentration under Ar flowing decreases monotonously with time. This result suggests that the WGS reaction proceeds through a mechanism involving some rather stable intermediates.

As mentioned already, irradiation of alumina and silica gel produced O₂ as well as H₂. Both concentrations of O₂ and H₂ decrease gradually with irradiation time, the ratio of the concentrations being always 1 : 2, indicating that the O₂ and H₂ detected are produced by the radiolysis of adsorbed water. Irradiation of silica gel, alumina and MgO under CO flowing, however, produces no trace of O₂ at any reaction conditions studied here. Therefore, OH radicals and O atoms which are produced by the radiolysis of adsorbed water react with CO to produce CO₂ under CO flowing, which suppresses the reverse reaction of water radiolysis, giving rise to the formation of H₂ in concentrations much greater than those by water radiolysis.

In an attempt to get information concerning the intermediates of the WGS reaction, ESR studies were carried out on the radicals produced by γ -irradiation of CO and water adsorbed on silica gel. γ -Irradiation of silica gel at -196°C produces ESR spectrum due to OH radicals and defects of silica gel. The ESR

spectrum due to OH radicals shows narrowing in line width on raising the temperature but persists up to -100°C . The spectrum observed from CO adsorbed on silica gel shows the formation of $\text{H}\dot{\text{C}}\text{O}$ radicals and CO_2^- in addition to OH radicals. On raising the temperature to -150°C , the OH radicals disappeared completely leaving the spectrum due to $\text{H}\dot{\text{C}}\text{O}$ radicals and CO_2^- . This result indicates that OH radicals produced from adsorbed water react with CO.

(S. Nagai and Y. Shimizu)

1) S. Nagai and Y. Shimizu, JAERI-M 9856, 28 (1981).

7. Photo-Emission from Carbon Monoxide Induced by 0.6 MeV Electron Irradiation

In previous papers¹⁾, it was described that irradiation of methane containing a small amount of carbon monoxide produces organic acids by a series of ionic reactions initiated by CH_3^+ ion, but later experiment revealed that the amounts of the acids formed in CO abundant mixture are larger than those expected from the proposed mechanism. In order to explain the amounts of acids as a function of CO content covering the whole region of CO content, excited or ionic species derived from CO has to be assumed as a possible precursor for the acids.

This report describes studies on optical emission spectra of CO under electron irradiation which have been carried out in an attempt to obtain the knowledge on excited species formed in CO by electron irradiation.

Experimental methods and techniques were described in the previous annual report²⁾. Carbon monoxide was obtained from Seitetsu Kagaku Co. (V.H.P. grade, 99.95% up) and used as received. Carbon dioxide and oxygen were obtained from Takachiko Kagaku Co. (V.H.P. grade, 99.9% up) and also used without further purification. Irradiation was carried using electron beams from a Van de Graaff accelerator (0.6 MeV, 15 μA). Estimated dose rate was 2×10^4 rad/s. After irradiation, the

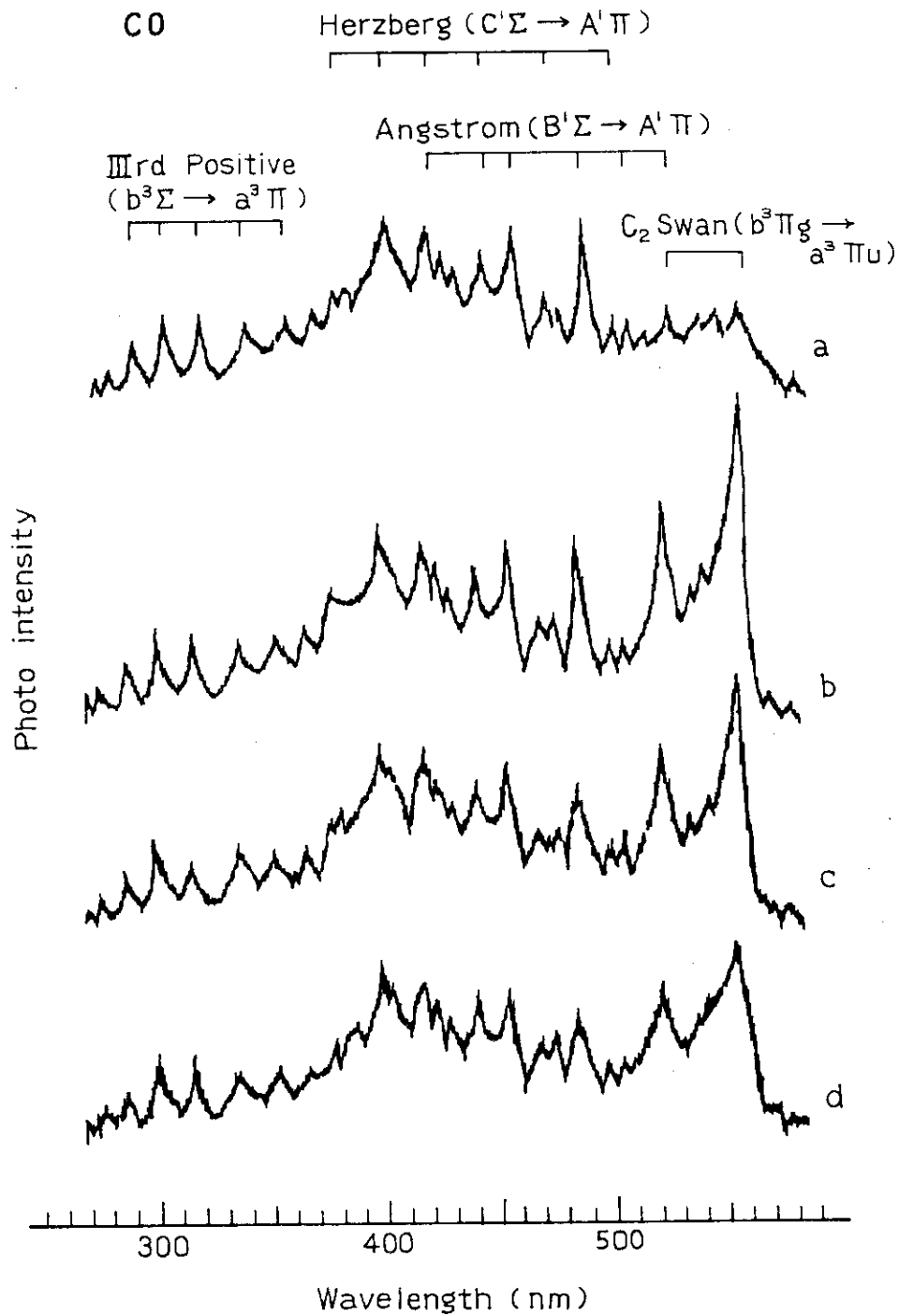


Fig. 1. Emission spectra of CO during electron beam irradiation: time after irradiation initiated, (a) 1 min., (b) 3 min., (c) 10 min., and (d) 15 min.; pressure, 760 Torr.

aluminum window of the irradiation vessel was removed and brown powder was scraped off for infrared spectrophotometry by KBr disk method. A part of the powder was subjected to pyrolytic gaschromatography using a CDS-pyrolyzer (Model 100).

Figure 1 shows emission spectra of CO during irradiation taken at different time intervals from the initiation of the irradiation. Identifications of the bands are also given in the figure^{3,4}). It is evident from the figure that the emission due to C_2^* ($b^3\Pi_g \rightarrow a^3\Pi_u$; 0,0 and 1,2) increased with irradiation time, reached maximum, and then decreased gradually. The intensities of other bands changed a little and decreased slowly with irradiation time.

The time dependence of the intensity of C_2^* emission is more clearly shown in Fig. 2, where the intensities of C_2^* emission were recorded continuously with irradiation time while

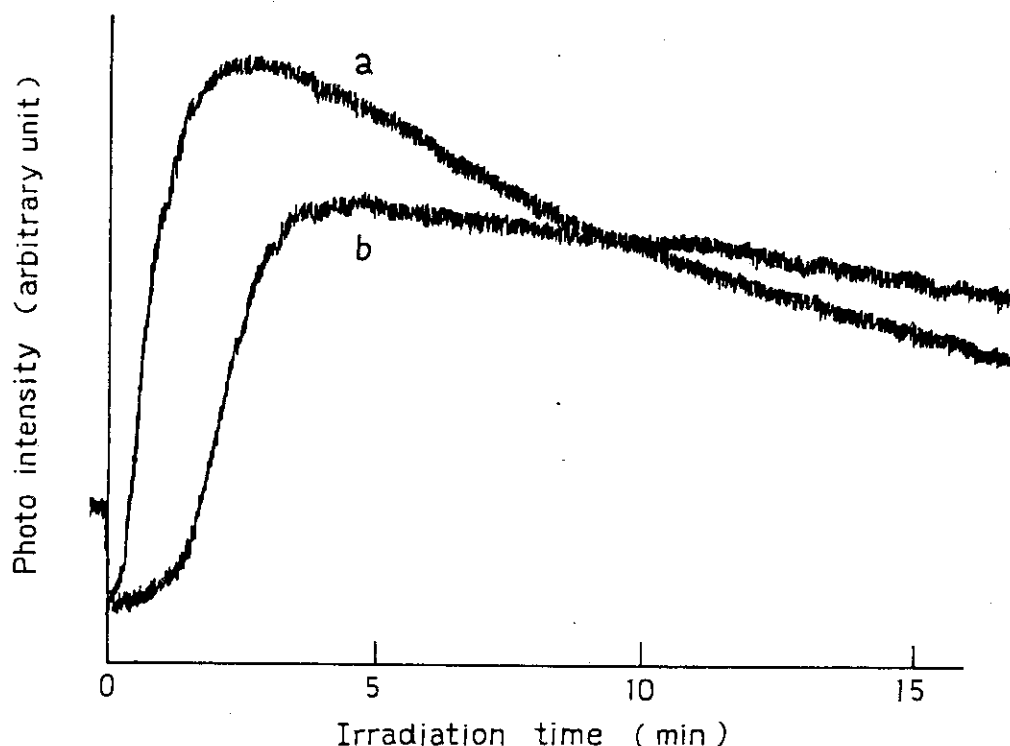
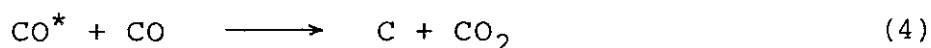


Fig. 2. Emission intensity from C_2^* as a function of time: (a) agitated by an electric fan during irradiation; (b) no agitation.

the wavelength was being fixed at 555 nm. Curve b was obtained without agitation of the gas in the irradiation vessel as was done in the most irradiation experiments, while curve a was taken under rigorous agitation of the gas by a small electric fan installed in the irradiation vessel. This result indicates that the spatial non-uniformity of the reactants or intermediate products may be a cause of the difference in the time dependent spectral intensity. When the irradiation started after an hour period of discontinuity, the emission intensity is stronger than that observed before the irradiation was interrupted. This recovery of the emission intensity becomes less prominent with increasing cycles of irradiation and interruption. These findings together with the relative slow rise followed by gradual decay of the C_2^* emission intensity indicate the presence of some precursor leading to C_2^* build-up and accumulation of the quencher formed during irradiation.

Several simple compounds are considered to quench the C_2^* emission. A small amount of oxygen and carbon dioxide, which are supposed to be quenchers to C_2^* emission, was added in the system, and found that the former quenched the emission completely by the addition of 5 Torr, and the latter did by the addition of 50 Torr (Fig. 3). Since G values of oxygen and carbon dioxide formations from CO are too small⁵⁾ (0.0 and 2.25, respectively) to give enough amount of the products to quench the C_2^* emission at early period of irradiation, these are not considered as a cause of quenching of C_2^* emission.

Only product considered as a possible candidate having long life time to quench C_2^* emission is C_3O_2 which is produced by a series of reactions^{6,7,8)}.



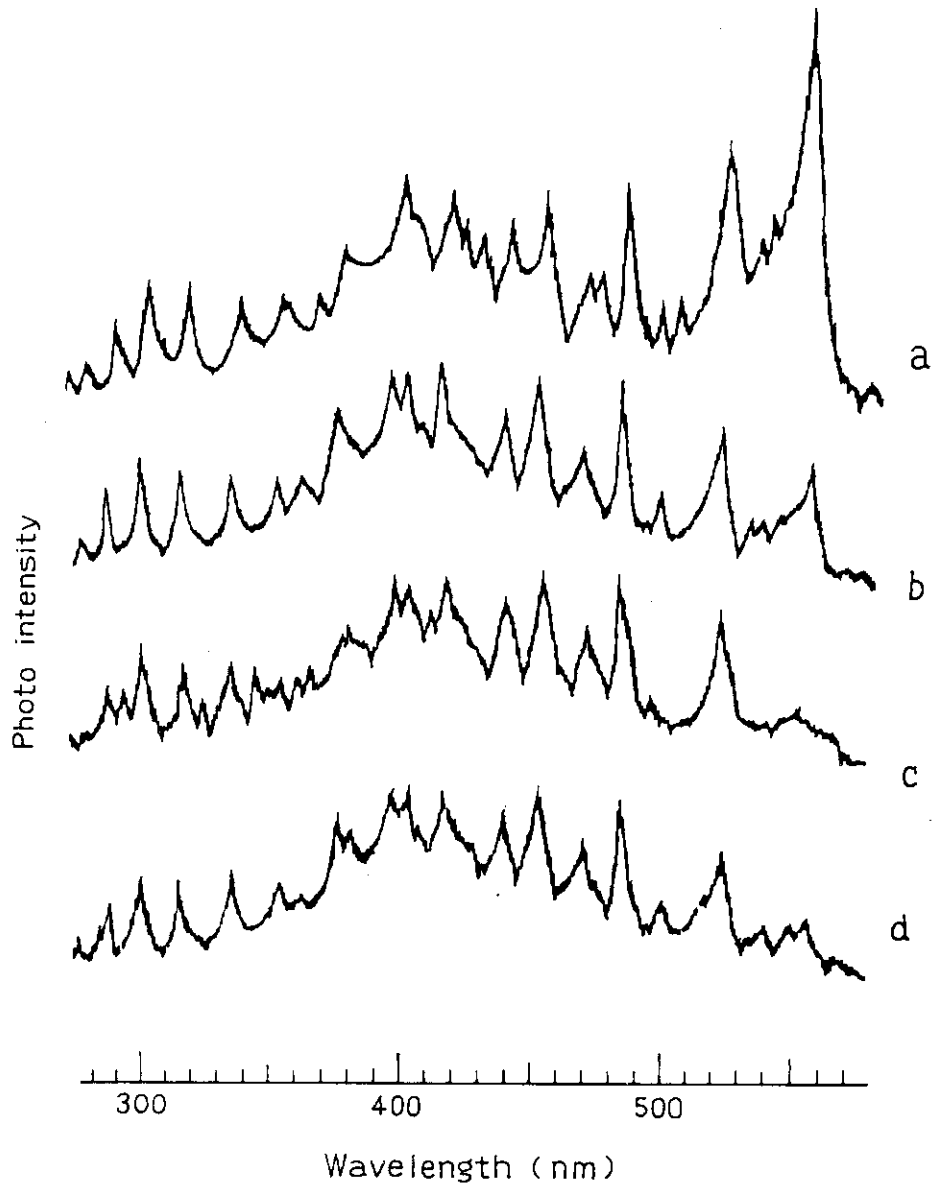


Fig. 3. Emission spectra of CO containing additives:
(a) none, (b) CO₂ (5 Torr), (c) CO₂ (50 Torr),
and (d) O₂ (5 Torr); pressure, 760 Torr;
electron beam current, 15 μ A.

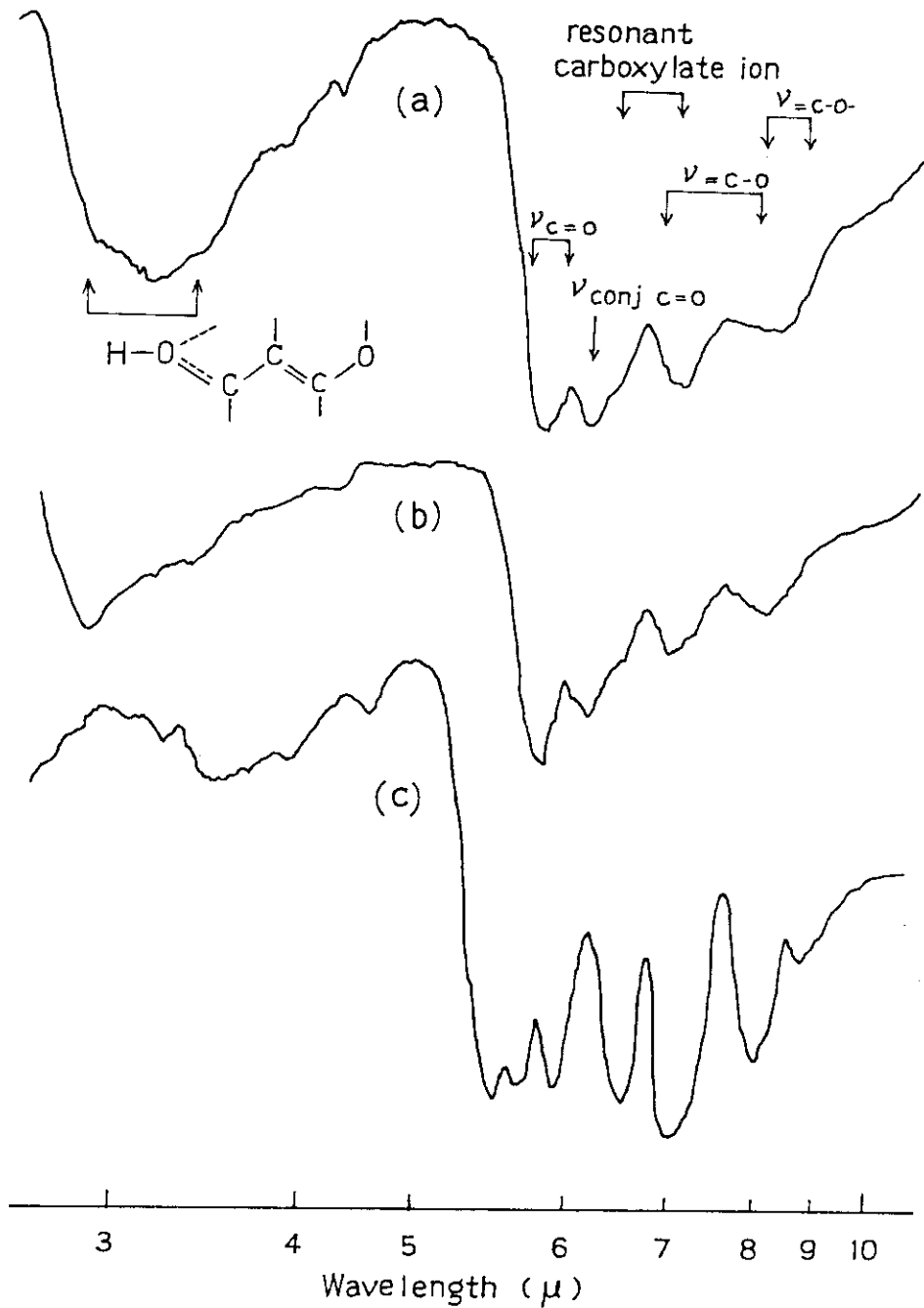
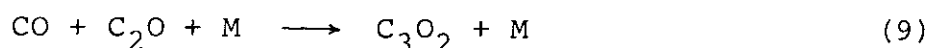
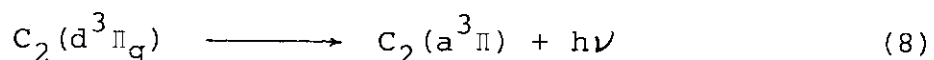
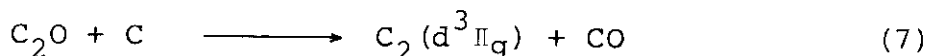
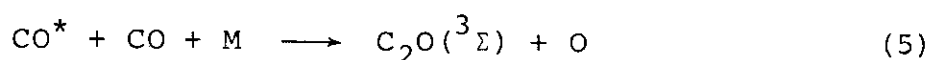
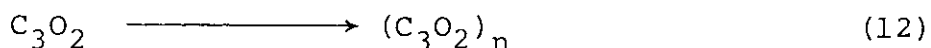
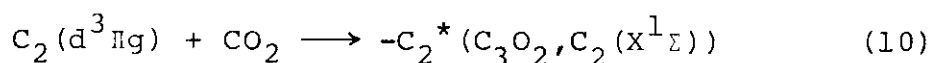


Fig. 4. Infrared spectrum of powder collected from the bottom of the irradiation vessel after irradiation (a); the spectra reported for the solid product obtained from CO by irradiation (b)⁹; and for carbon suboxide polymer (c)¹⁰.



A slow rise of C_2^* emission intensity after initiation of irradiation can be explained by build-up of C and C_2O which are formed by reactions (1), (3), (4), (5) and (6) and then react to form $\text{C}_2({}^d{}^3\Pi_g)$ by reaction (7). Since carbon suboxide (C_3O_2) is known to polymerize to form polymer (reaction (12)), disappearance of C_3O_2 in the gas phase may explain partial recovery of C_2^* emission after an hour period of discontinuation of irradiation. Gradual decrease of C_2^* emission intensity recovered by repeated cycles of irradiation and interruption may be explained by gradual accumulation of CO_2 in the gas phase, which quenches C_2^* emission (reaction (10)).



After several hours of irradiation, brown precipitate was found in the wall especially at the bottom of the irradiation vessel. Infrared spectrum of this precipitate gives almost identical one while is assigned to carbon suboxide polymer^{9,10,11} (Fig. 4). This result may support the above mechanism including C_3O_2 and its polymer.

(K. Matsuda and M. Hatada)

- 1) H. Arai, S. Nagai, and M. Hatada, JAERI-M 9214, 56 (1980); Radiat. Phys. Chem., 17, 211 (1981).
- 2) K. Matsuda, JAERI-M 9856, 114 (1981).
- 3) Y. Nakai, K. Matsuda, T. Takagaki, and T. Harami, JAERI 5030, 16 (1975).
- 4) Pearse and Gaydon, "The Identification of Molecular Spectra", 4th Ed., Chapman and Hall (1976); J. R. McDonnald, A. P. Baronavski, and V. M. Donnelly, Chem. Phys., 33, 161 (1978).
- 5) A. R. Anderson, "Fundamental Processes in Radiation Chemistry", P. Auslous, Ed., Interscience, N. Y., p.281 (1968).
- 6) P. Gosse, N. Sadeghi, and J. C. Pebay-Peyroula, Chem. Phys. Lett., 13, 557 (1972).
- 7) C. Devillers and D. A. Ramsay, Can. J. Phys., 49, 2839 (1971).
- 8) V. M. Donnelly, W. M. Pitts, and J. R. McDonald, Chem. Phys., 49, 289 (1980).
- 9) S. Nagai, H. Arai, and M. Hatada, JAERI-M 9214, 26 (1980).
- 10) R. N. Smith, D. A. Young, E. N. Smith, and C. C. Carter, Inorg. Chem., 2, 829 (1963); T. Kappe and E. Ziegler, Angew. Chem., 86, 529 (1974).
- 11) J. Wojtczak, K. Weiman, and J. M. Konarski, Monatshefte für Chem., 99, 501 (1968).

[2] Radiation-Induced Polymerization1. Cationic Oligomerization of Butadiene with
1-Bromo-2-Butene

Synthesis of oligomers having reactive atoms or groups such as halogen, double bond, etc. at their molecular ends is now one of important problems in polymer chemistry. Polymerization in the presence of chain transfer agent, namely telomerization, is one of the most general methods to introduce functional group(s) at the end of oligomer molecules. In this study, the radiation-induced oligomerization of butadiene (B) with 1-bromo-2-butene (1B2B) has been carried out and then the results were described in comparison with those¹⁾ obtained for the catalytic oligomerization with halogenated compounds including 1-chloro-2-butene (1C2B) which were described in the previous issues of this report.

Oligomerization was carried out in 50 mole% n-hexane solution changing the composition ratio of B to 1B2B. Solvent and telogen [T] were used after drying with calcium hydride. Irradiation was carried out with 1.5 MeV electron beams at 50 μ A (0.22 Mrad/s) at -10°C . Further details of the experimental procedures were the same as described before¹⁾.

In Fig. 1 (a), the relative rate of polymerization, i.e., R_p divided by [B] was plotted against the ratio of [T]/[B]. Although the number of data is quite limited, it appears that the value of $R_p/[B]$ greatly increases with increasing [T] up to [T]/[B] = 0.8 and then decreases at higher [T]/[B] ratio. At the maximum, the $R_p/[B]$ value is ca. 15 times as large as that in the absence of 1B2B. Such a maximum in relative R_p with increasing [T]/[B] ratio was generally observed in our previous oligomerization works with chlorinated compounds¹⁾.

In Fig. 1 (a) was also included the results obtained with 1C2B, in which oligomerization was carried out at n-hexane concentration of 20 ~ 25 mole%. Although the concentrations of telogen and monomer are relatively higher in 1B2B system, the

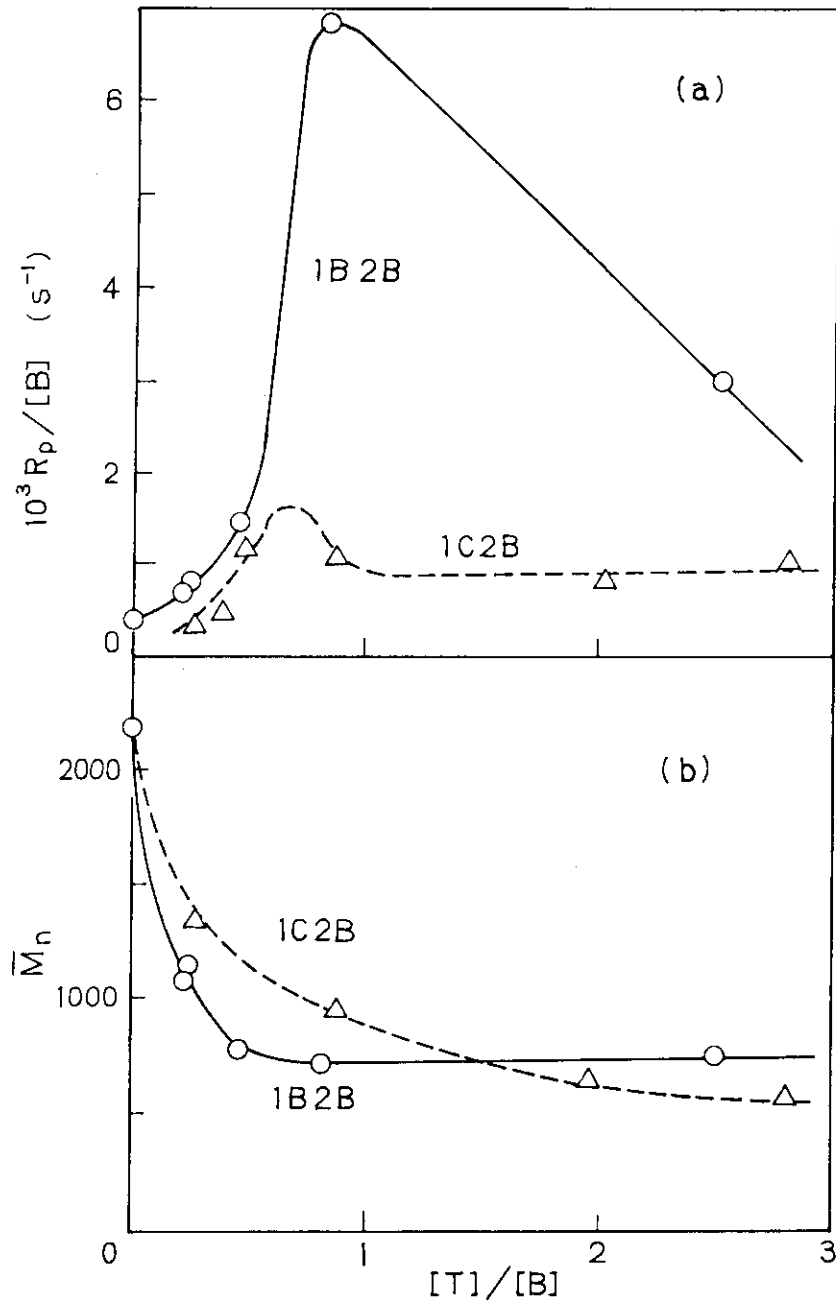


Fig. 1. The relative rate of oligomerization, $R_p/[B]$ (a) and \bar{M}_n (b) as a function of $[T]/[B]$. Telogens are 1-chloro-2-butene (1C2B) and 1-bromo-2-butene (1B2B). Irradiation, 0.22 Mrad/s; -10°C .

relative R_p in 1C2B system is substantially lower than in 1B2B system.

The \bar{M}_n value of the oligomer was determined by GPC applying an elution volume-MW relationship for polystyrene, which agreed with that of polybutadiene in oligomer region within an error of 10%²⁾. In Fig. 1 (b), the changes in \bar{M}_n are shown. The \bar{M}_n decreases more strongly in 1B2B system than in 1C2B suggesting a higher rate of chain transfer with 1B2B. The constant \bar{M}_n at high $[T]/[B]$ ratio in 1B2B system seems to be a general trend in free cationic oligomerization¹⁾. This is probably caused by the association of butadiene molecules in the medium, where all the associated monomers are polymerized before meeting the chain transfer agent.

The average number of terminal halogens in a molecule, N_X was evaluated from the \bar{M}_n and the relative area of $-\text{CH}_2\text{X}$ absorptions in $^1\text{H-NMR}$ spectrum. Here both allyl and alkyl type halomethyl groups were considered as end group since it was supposed that $-\text{CH}_2-\text{CH}_2\text{X}$ group was formed by a hydrogen shift reaction of $=\text{CH}-\text{CH}_2\text{X}$ group¹⁾. As shown in Fig. 2 (a), the N_X value in 1B2B oligomer is $0 \sim 0.5$ in contrast to $1.1 \sim 1.5$ in 1C2B. This is strange since the results in Fig. 1 (b) mean that the chain transfer reaction takes place much more frequently in 1B2B system than 1C2B.

The fractions of remained double bond in the oligomer are shown in Fig. 2 (b). In 1B2B system, the fraction decreases steeply with increasing $[T]/[B]$ ratio due to a cyclization reaction while in 1C2B system the decrease of double bond takes place very moderately.

It is expected that, on irradiation, 1B2B gives a higher ion yield and tends to detach a halogen anion more easily by an attack of positive ion than 1C2B. The higher ion yield in 1B2B explains the higher value of $R_p/[B]$ though both telogens give the same cationic species, $\text{CH}_3-\text{CH}=\text{CH}-\text{CH}_2^+$, on radiation.

There are three probable explanations for the low N_X value in the oligomerization with 1B2B. First is that in 1B2B system rate of chain transfer is not much different from that of termination. If this is true, the \bar{M}_n decrease in Fig. 1 is

attributed to both chain transfer to 1B2B and termination with impurity water in the system. However, it was found on Karl-Fischer titration that water content in 1B2B was not much different from that in 1C2B when these had been dried with calcium hydride. Furthermore, a simple calculation based on a reasonable assumption of the initiating cation yield proved that chain transfer reaction took place at least 3 ~ 4 times greatly in the 1B2B system.

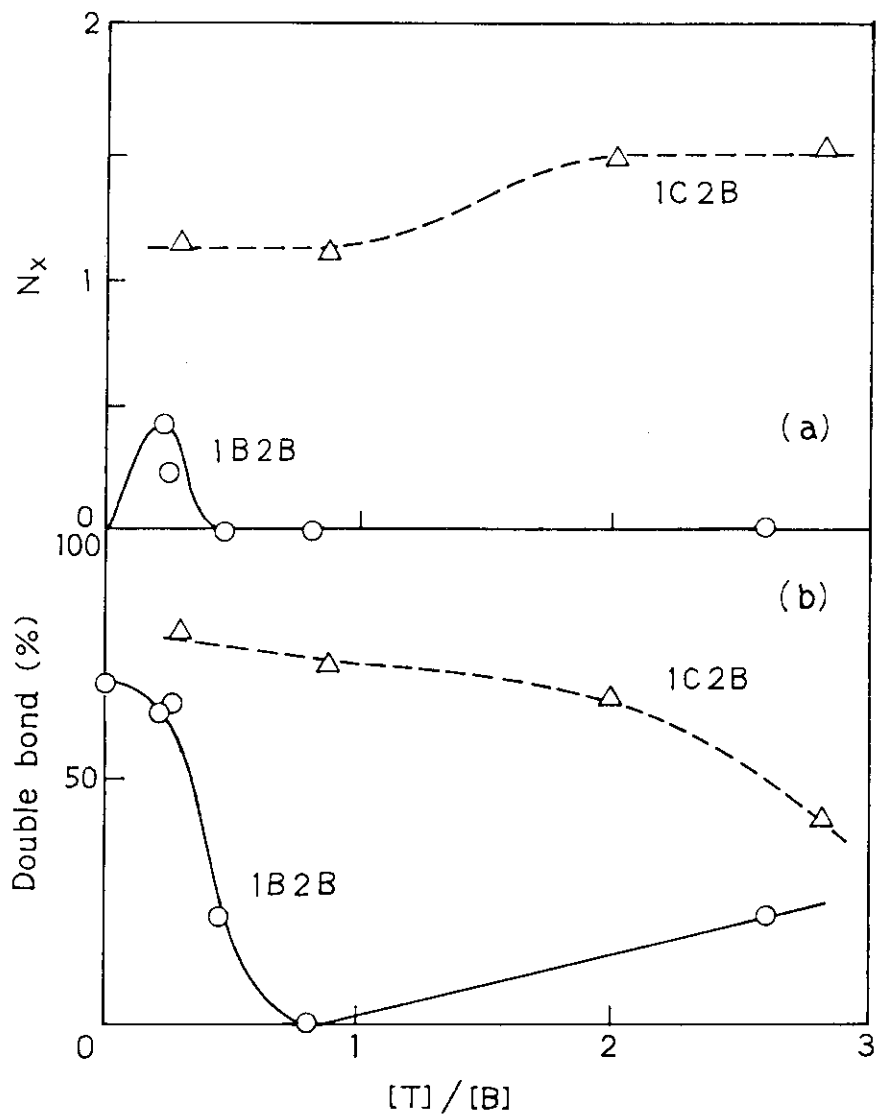


Fig. 2. Average number of halogen terminals per molecule, N_x (a) and amount of the remaining double bond (b) in the oligomers.

The second explanation involves a detachment of bromine atom from once formed C-Br end of oligomers by the influence of radiation. To verify this, a commercial liquid polybutadiene with bromine terminal (Polysar) was irradiated in n-hexane solution in the presence and the absence of 1B2B. As shown in Fig. 3 (a) and (b), in the absence of 1B2B all of the terminal bromine atom disappeared by 50 second radiation accompanying with a large loss of double bond as well. However, with an addition of 10 mole% of 1B2B to n-hexane, no disappearance of bromine terminal was observed with a reduced loss of double bond, which indicated a protective effect of 1B2B from radiation damaging of the solute. At the equimolar concentration of 1B2B and n-hexane, relative amount of end group was increased by irradiation probably because of bromine addition to pendant vinyl groups of oligobutadiene.

The third possibility is that in the presence of 1B2B, two kinds of chain transfer reaction take place; one is an ordinary

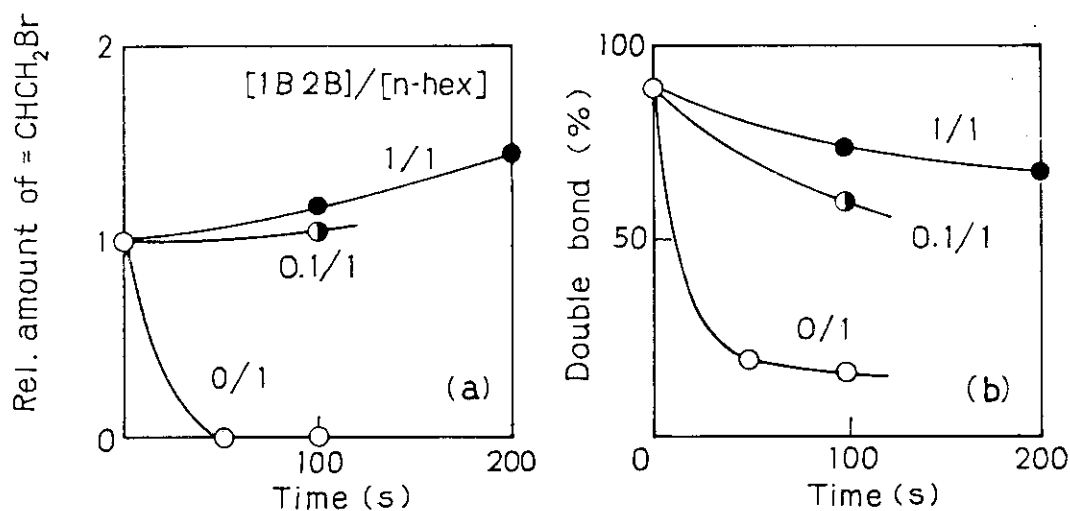


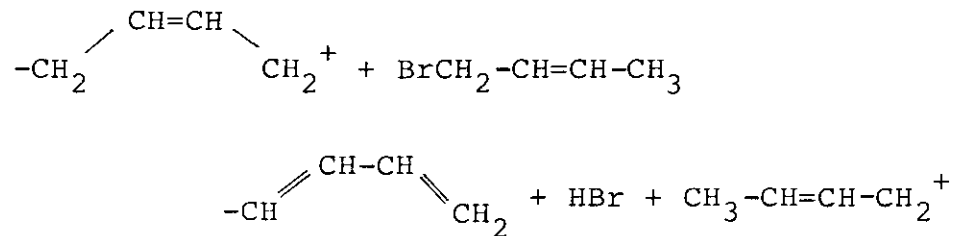
Fig. 3. Effect of radiation on polybutadiene with bromine-terminal: change of terminal Br group (a) and remaining double bond (b) as a function of irradiation time. The values in the figures mean mole ratio of 1B2B to n-hexane. [PB-Br]/[n-hexane] = 10 wt%. Irradiation, 0.22 Mrad/s, -10°C.

Table 1. Oligomerization of Butadiene with Bromo-compounds in n-Hexane
 Solution by Electron Beam Irradiation at 0.22 Mrad/s

Telogen	[T]/[B]/[S] (mole ratio)	Temp. (°C)	Irrad. time (s)	Conver- sion (%)	\bar{M}_n	N _{Br}	Double bond (%)
None	0/1.00/1.00	-10	100	4.1	2200	0	69
1-Bromo-2-butene	0.90/1.10/2.00	-10	75	42.7	690*	0	0
"	0.98/1.05/1.97	15	50	9.2	1260	0.47	44
3-Bromo-1-butene	1.00/0.05/2.05	15	50	6.3	1240	0.51	63

* Partly gel

one is accompanied by a bromine addition to the oligomer end and the other is the one without bromine addition. If 1B2B molecule undergoes a dissociative proton capture after abstracting a proton from the terminal monomer unit of a propagating cation, a cation to continue the oligomerization reaction is regenerated as shown:



In Table 1, results of oligomerization with 1B2B and 3-bromo-1-butene at 15°C were compared with the results at -10°C. It is found that all the reaction rates, oligomerization, chain transfer and cyclization, are relatively reduced and that bromine atom is present at 15°C.

Experiments for studying the possibility of the above given mechanism are now in progress.

(K. Hayashi and S. Okamura)

- 1) K. Hayashi and S. Okamura, JAERI-M 9856, 91 (1981).
- 2) K. Hayashi, T. Kijima, and S. Okamura, unpublished result.

2. Oligomerization of Butadiene with Dihalogen Compounds

In the cationic telomerization of butadiene with mono-halogenated compounds by electron beam irradiation, we obtained oligomers having a single halogen atom at the end of each molecule by using 1-chloro-2-butene as a telogen¹⁾. In this article, results are described on some preliminary works which were carried out to obtain oligomers having two halogen atoms at both ends of each molecule.

In Table 1, \bar{M}_n and average number of halogen terminal per

Table 1. Oligomerization of Butadiene with Dihalogen Compounds in
n-Hexane Solution by Electron Beam Irradiation at
0.22 Mrad/s for 100 seconds

Telogen	[T]/[B]/[S] (mole ratio)	Conver- sion(%)	\bar{M}_n	N _X	Double bond(%)
None	0 / 1.0 / 1.0	4.1	2200	0	69
1,3-Dichlorobutane	0.98/1.04/0.98	9.7	1400	0	*
2,3-Dichlorobutane	1.04/0.93/1.03	11.5	1650	0	*
1,4-Dichloro-2-butene	0.95/1.10/0.95	7.6	2080	0	*
1,4-Dichlorobutane	1.15/0.97/0.88	8.0	930	1.36	89
1,3-Dibromobutane	0.93/0.94/1.13	13.5	1190	0.83	31
1,4-Dibromobutane	1.00/1.00/1.00	21.6	1370**	0.91	41

* not measured; ** partly gel

molecule, N_X are given for approximately equimolar solutions of butadiene (B), telogen (T) and solvent (S: n-hexane) along with the results in the absence of telogen as a reference²⁾. In these six compounds, mostly dihalobutanes, the presence of terminal halogen was detected in the case of 1,4-dichlorobutane, 1,3- and 1,4-dibromobutane by ¹H-NMR absorption of -CH₂X group.

In Table 2, results with two dihalo-p-xylenes are shown. Methylene dibromide was used as a solvent to dissolve these telogens. In the absence of the telogen, however, the presence of -CH₂Br terminal and substantial decrease of \bar{M}_n compared with

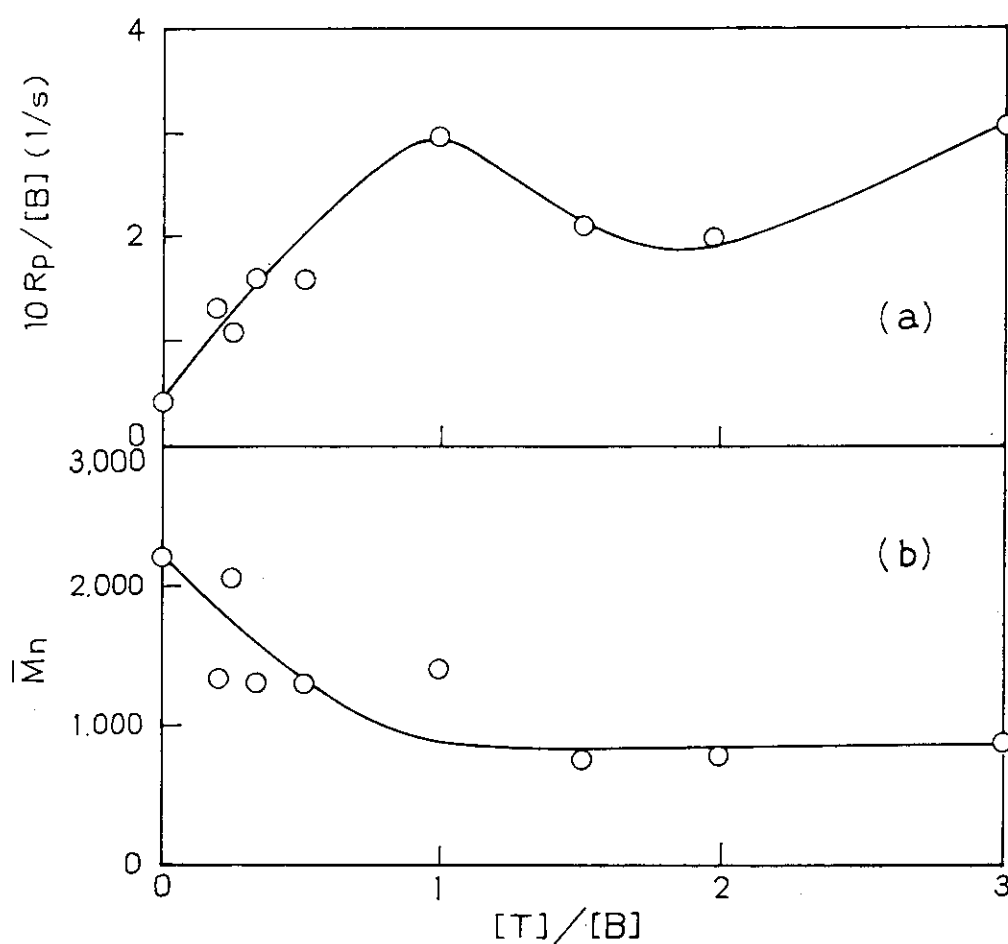


Fig. 1. $R_p/[B]$ (a) and \bar{M}_n (b) as a function of $[T]/[B]$ in the oligomerization of butadiene in n-hexane solution by 14DBB: electron beam irradiation, 0.22 Mrad/s; -10°C; [n-hexane] = 50 ± 1 mole%.

Table 2. Oligomerization of Butadiene in Methylene Dibromide
 Solution by Electron Beam Irradiation at
 0.22 Mrad/s for 50 seconds at 15°C

Telogen	[T]/[B]/[S] (mole ratio)	Conver- sion(%)	\bar{M}_n	N _{Br}	Double bond(%)
None	0 / 2.96/10.78	7.4	1280	0.83	73
Dichloro-p-xylene	0.40/2.96/10.33	20.3	-*	0.7**	35**
Dibromo-p-xylene	0.19/2.97/10.38	14.8	-*	-*	-*

* mostly gel; ** measurement for a soluble part

Table 3. Oligomerization of Butadiene in n-Hexane Solution by
Electron Beam Irradiation at 0.22 Mrad/s for
100 seconds at -10°C

Telogen	[T]/[B]/[S] (mole ratio)	Conver- sion (%)	\bar{M}_n	N_{Cl}	Double bond (%)
1,4-Dichlorobutane	3.20/2.98/3.06	8.0	930	1.36	52
	2.21/2.11/4.44	9.2	800	0.43	66
	4.52/2.49/2.27	3.1	830	0.57	52

that in n-hexane solution²⁾ at the same butadiene concentration indicate that chain transfer reaction to the solvent is taking place. The products obtained in the presence of these dihalo-p-xylenes were mostly gel. For the soluble part of the product in dichloro-p-xylene system, NMR measurement was carried out. Although the oligomer yield increased by the presence of telogens, the obtained value of N_x was not much different from the value for the product obtained in the absence of the telogens and the amount of double bond residue was substantially low compared with those in Table 1. This means that the telogen which is supposed to give high ion yield and high

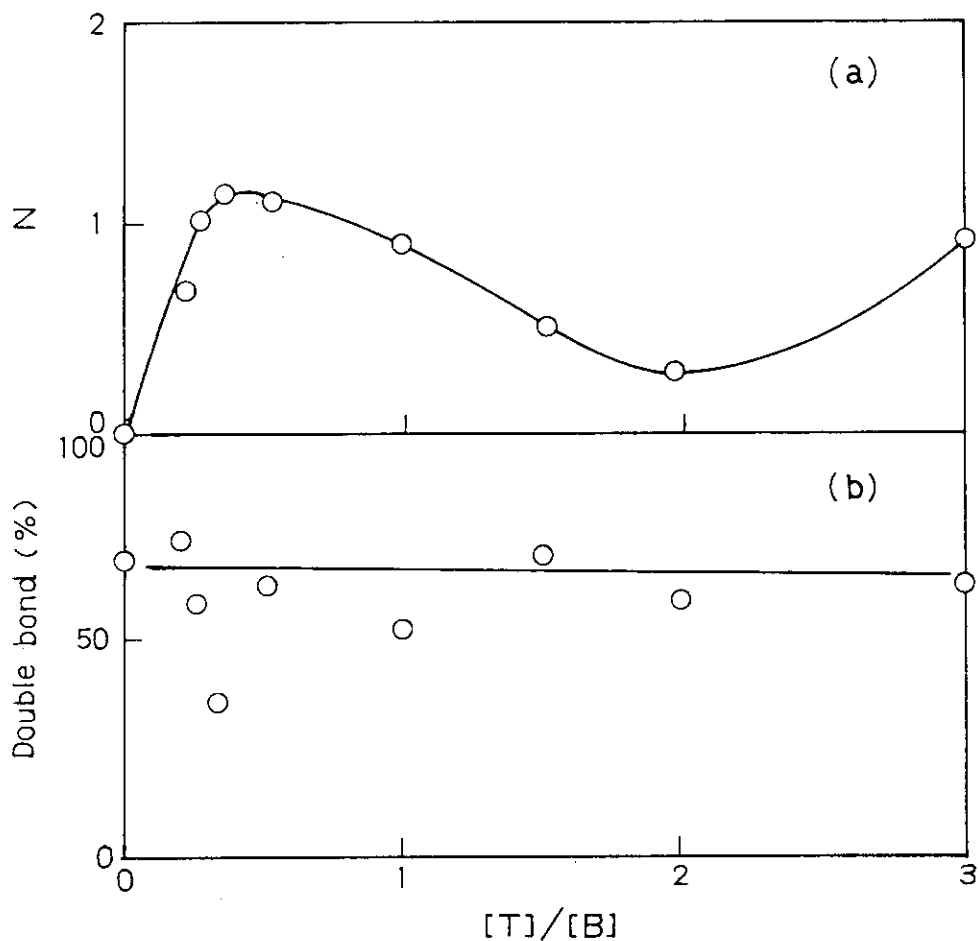


Fig. 2. Number of bromine terminals per molecule, N_{Br} (a) and fraction of remaining double bond (b) in the oligomer as a function of $[T]/[B]$.

efficiency of chain transfer greatly enhances side reactions such as cyclization and crosslinking in addition to telomerization reaction, in agreement with our previous results¹⁾.

Two additional runs were added to the result with 1,4-dichlorobutane in Table 1. As shown in Table 3, N_{Cl} values are relatively low though \bar{M}_n does not change so much in these three runs.

Taking into account of the higher reactivity of bromine compound than chlorine one in chain transfer reaction, a detailed study was carried out in 1,4-dibromobutane (14DBB) system. A variation of $R_p/[B]$ value, a relative rate of polymerization with composition ratio of telogen (T) and butadiene (B) is shown in Fig. 1 (a). The relative rate increases with increasing 14DBB concentration due to the increase of initiating cation yield and at the excess of the telogen, the relative rate changes complicatedly. The change of \bar{M}_n of the oligomer is given in Fig. 1 (b). In spite of scattered data, the \bar{M}_n value stays almost constant at high $[T]/[B]$ ratio greater than unity, which agrees with the results of the series of oligomerization studies by radiation^{1,3)}.

Number of $-CH_2Br$ terminal per molecule, N_{Br} is given in Fig. 2 (a). It shows a complicated variation with $[T]/[B]$; it is approximately 1 in $[T]/[B]$ region of 0.3 ~ 1.0, then once decreases down to 0.3 and increases again to unity at $[T]/[B] = 3$. These values are higher than those with 1-bromo-2-butene (1B2B)³⁾ but still far from the expected value of 2. The fraction of remained double bond in the oligomer shown in Fig. 2 (b) is almost constant, in contrast to the case with 1B2B³⁾.

When these results are compared with those by 1B2B described in the preceding section³⁾, it is clear that 14DBB shows a very mild reactivity in enhancement of R_p , in reducing \bar{M}_n and in consuming double bond in the oligomer by cyclization. These are probably consequences of lower cation yield in 14DBB than in 1B2B and lower reactivity of the cation formed by radiolysis of 14DBB and chain transfer to 14DBB than the cation formed in 1B2B system.

The low N_x value can be tentatively explained with an assumption that BrC_4H_8^+ which is supposed to appear on radiolysis of 1,4-DBB and chain transfer is not stable enough and undergoes detachment of a bromine atom to form a more stable cation to reinitiate the oligomerization.

(K. Hayashi and S. Okamura)

- 1) K. Hayashi and S. Okamura, JAERI-M 9856, 91 (1981).
- 2) K. Hayashi, K. Kagawa, and S. Okamura, J. Polym. Sci. Polym. Chem. Ed., 19, 1977 (1981).
- 3) K. Hayashi and S. Okamura, the preceding paper.

3. Oligomerization of Butadiene with Acetic Anhydride

It was reported that oligomerization of styrene took place with acetic anhydride (AA) by cationic catalyst yielding oligomer with acetyl and acetate groups at each molecular end¹⁾. In this article, result on a cationic oligomerization of butadiene with AA by high dose rate electron beam irradiation is described.

Oligomerization was carried out in 45 ~ 50 mole% n-hexane solution varying the concentration ratio of telogen (T) to butadiene (B). In Fig. 1 (a), $R_p/[B]$, the relative rate of oligomerization is plotted against $[T]/[B]$. The extent of increase in the relative rate with the addition of AA was ca. 30% at the maximum, which was quite low compared with the cases of halogenated hydrocarbons as a telogen²⁻⁴⁾. This is probably because radiation yield of initiating cation in the system does not increase so much by the AA addition and inhibitor content is relatively high in this system. On the contrary, \bar{M}_n of the oligomer is greatly reduced with small amount of AA added as shown in Fig. 1 (b). The extent of \bar{M}_n decrease with $[T]/[B]$ at the initial stage is very large even compared with the 1B2B case³⁾. No high yield of 1 : 1 adduct which was a main product in catalytic oligomerization¹⁾ was found in the present system. The MWD of products at low conversion were relatively narrow;

\bar{M}_w/\bar{M}_n values were 1.4 ~ 1.8.

Determination of the number of acetyl and acetate group per molecule was made on the basis of the \bar{M}_n value calculated from the results of GPC and $^1\text{H-NMR}$ absorptions of $\text{Ac-CH}_2\text{-CH}_2\text{-}$ (2.45 ppm), $\text{Ac-CH}_2\text{-CH=}$ (3.10 ppm) and $\text{AcO-CH}_2\text{-CH=}$ (4.50 ppm), where Ac means an acetyl group, $\text{CH}_3\text{CO-}$.

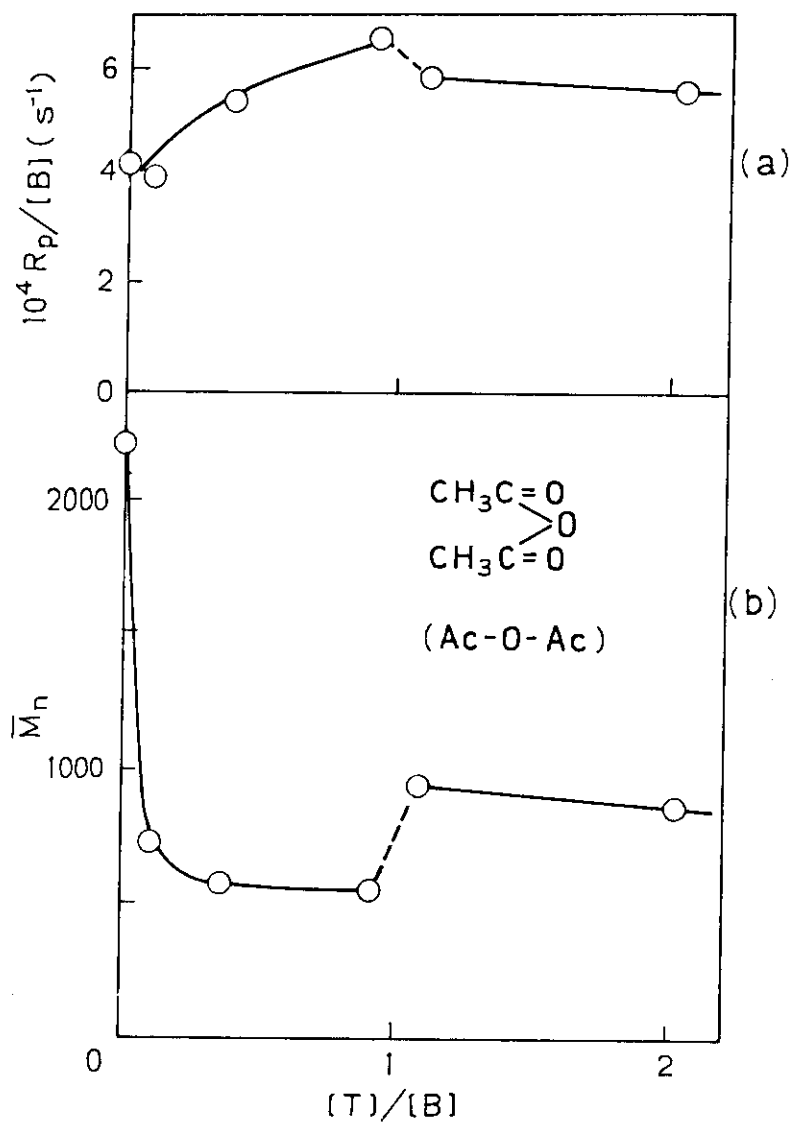


Fig. 1. $R_p/[B]$ (a) and \bar{M}_n (b) as a function of $[T]/[B]$ in the oligomerization of butadiene in n-hexane solution (45 ~ 50 mole%) with acetic anhydride: electron beam irradiation, 0.22 Mrad/s, -10°C.

It is strange that in no sample $\text{AcO-CH}_2\text{-CH}_2\text{-}$ absorption (ca. 4.0 ppm) was observed though such an alkyl type terminal is always formed as well as allylic terminal in the oligomerization of butadiene by radiation²⁻⁴).

In Fig. 2 (a), numbers of the two terminal groups are shown. It is contrasting that the number of acetyl group is approximately unity even at low AA concentration but that of acetate group is always less than half. In Fig. 2 (b), fraction

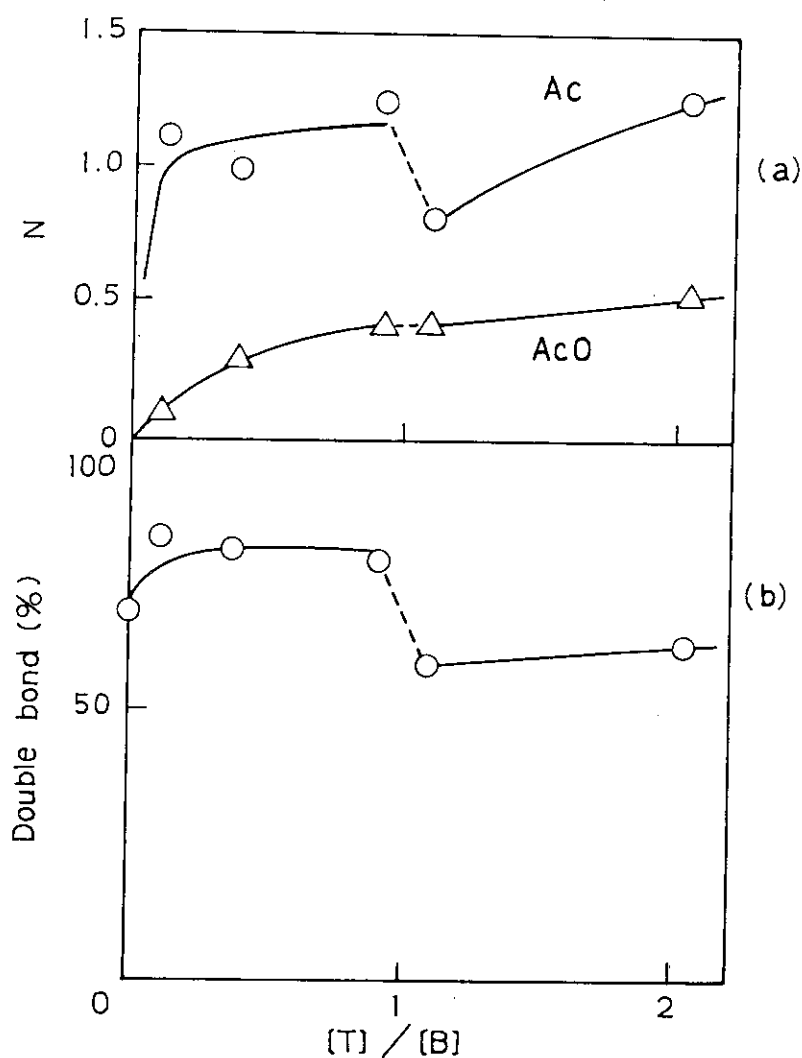


Fig. 2. Number of acetyl and acetate terminal per molecule (a) and fraction of remaining double bond in the oligomer (b) as a function of $[T]/[B]$.

of double bond remained in the oligomer is approximately 80%, a little higher than the value in n-hexane solution⁵⁾ when $[T]/[B]$ is less than 1, suggesting a relatively low cation yield in the system and low reactivity of acetyl cation. The fraction of pendant vinyl group to the total double bond does not change with $[T]/[B]$, and is 34% in average.

In all of the four figures, there seems to be a discontinuity of results at $[T]/[B] = \text{ca. } 1$. Supposedly, this is due to some phase change at this liquid composition, where the average number of associated AA molecules is changed.

It is well known that AA decomposes into acetic acid in the presence of water. In the present system, therefore, it is reasonable to consider that AA contains a small amount of acetic acid which probably behaves as a chain terminator for cationic polymerization. If the rate of chain transfer to AA is exceedingly higher than the termination rate, i.e., the ordinary case of telomerization, there must be no difference between the number of acetyl and acetate terminals, which is not the case. Otherwise, there should be some terminal group other than acetate, which is not detected in NMR measurement so far. If the chain transfer rate is not much different from the termination rate with acetic acid, it is quite reasonable that number of acetyl terminal, which is introduced into an oligomer mainly through the initiation process between acetyl cation and monomer, exceeds the number of acetate terminal which is introduced through the chain transfer reaction to AA. The precise mechanism of the oligomerization is still uncertain at present.

(K. Hayashi and S. Okamura)

- 1) T. Asahara, H. Kise, and K. Abe, *Kogyokagaku-zasshi*, 73, 790 (1970).
- 2) K. Hayashi and S. Okamura, *JAERI-M* 9856, 91 (1981).
- 3) K. Hayashi and S. Okamura, the first article in this issue.
- 4) K. Hayashi and S. Okamura, the second.
- 5) K. Hayashi, K. Kagawa, and S. Okamura, *J. Polym. Sci. Polym. Chem. Ed.*, 19, 1977 (1981).

4. Bulk Polymerization of Methyl Methacrylate

In the studies on high dose rate polymerization of vinyl and diene monomers, a component was found to be relatively high MW, $10^5 \sim 10^6$ in addition to the ordinary products by radical and cationic mechanisms. Such a component of high MW was observed by GPC in the high dose rate products of styrene¹⁾, methyl methacrylate (MMA)^{2,3)}, methyl, ethyl and n-butyl acrylates³⁾, and vinyl acetate⁴⁾. Although some detailed studies on the high MW component were made for styrene⁵⁾ and MMA⁶⁾, the reaction mechanism is still uncertain. In this article, results on the MW and stereoregularity of the high MW component produced from MMA are described.

Bulk polymerization of MMA was carried out by electron beam irradiation at 0.22 Mrad/s at room temperature. Since the fraction of the high MW component decreases with increasing the polymer conversion, the irradiation was made for a short period so that the polymer yield did not exceed 5%. The main part of high MW and radical components were fraction-collected by Toyo Soda Type 827 GPC with CP8-III controller. The chromatogram is shown in Fig. 1. Hereafter, the fractions appeared at shorter

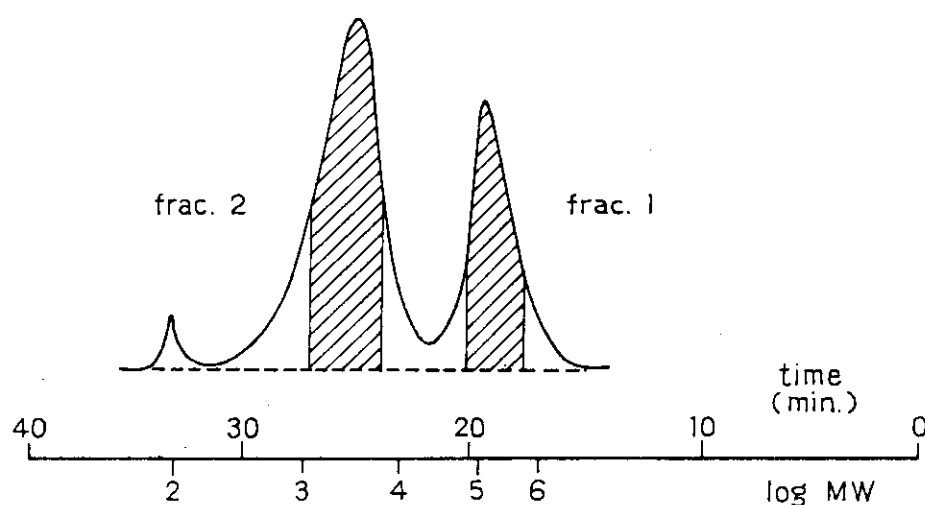


Fig. 1. GPC curves for fraction-collection of PMMA polymerized by high dose rate electron beam irradiation.

and longer elution time are called by fraction 1 and 2, respectively.

A GPC-LALLS measurement was made for fraction 1 to obtain the accurate values of MW. The calculated MW values using a program supplied by Toyo Soda are $\bar{M}_n = 1.08 \times 10^6$, $\bar{M}_w = 1.37 \times 10^6$ and $\bar{M}_w/\bar{M}_n = 1.27$. This proved the existence of the high MW component which had been based only on the result of GPC measurement.

The microtacticity of PMMA was determined by ^{13}C -NMR measurement at 15.0 MHz in CDCl_3 solution at about 60°C. The triad splittings of α -methyl carbon atom are observed at 17.0 (rr) and 19.0 (mr) ppm. The third absorption due to (mm) unit which should appear at ca. 22 ppm was absent in our polymers. As shown in Table 1, there seems a significant difference between the tacticities of the two fractions when an error of $\pm 2\%$ is assumed in the present estimations. The high MW component is more syndiotactic than the radical component.

To study the influence of the polymerization temperature on the tacticity on the radical component, measurements were carried out for the polymer by γ -ray polymerization. It was found that the fraction of (rr) unit changed by 7% between 25 and 50°C. The values for fraction 1 and 2 agree well with those for radical component at 25 and 50°C, respectively.

Table 1. The Triad Tacticities of PMMA's

Sample	Dose rate (rad/s)	Polym. temp. (°C)	Tacticity (%)		
			(rr)	(mr)	(mm)
Fraction 1	2.2×10^5	room temp.	70.6	29.4	0
Fraction 2	2.2×10^5	room temp.	63.4	36.6	0
Sample 1	21.2	0	69.1	30.9	0
Sample 2	21.2	25	70.1	29.9	0
Sample 3	21.2	50	62.5	37.4	0

In the present work, the polymerization by electron beam irradiation was carried out in a stainless steel cell where the sample temperature rose gradually with irradiation. On the other hand, the fraction of the high MW component was not much increased when the irradiation was made in a temperature controlled cell at 25°C. These results lead to a conclusion that the formation of the high MW component is somehow limited to the very early stage of the polymerization, which was also pointed out for styrene⁵⁾.

(J. Takezaki and K. Hayashi)

- 1) J. Takezaki, T. Okada, and I. Sakurada, J. Appl. Polym. Sci., 21, 2684 (1977); *ibid.*, 22, 3311 (1978).
- 2) JAERI-M 6260, 33 (1975).
- 3) JAERI-M 6260, 37 (1975).
- 4) J. Takezaki, T. Okada, and I. Sakurada, JAERI-M 9214, 98 (1980).
- 5) J. Takezaki, T. Okada, and I. Sakurada, JAERI-M 9856, 77 (1981).
- 6) K. Hayashi, unpublished work.

5. Emulsion Polymerization of Styrene in a Batch System

The emulsion polymerization of styrene by high dose rate electron beam irradiation in a flow system was described in the previous issues of this report^{1,2)}. It is notable that an emulsion of fine particles, 50 ~ 70 nm in average diameter was obtained by this process²⁾. In this article, results of the polymerization in a batch system are described. The largest advantage of using a batch system instead of a flow one is to save the time to prepare the experimental setup and to clean up the system after the polymerization. In spite of greater ambiguities in dose rate inhomogeneity and in sample temperature, the batch system was employed to make a number of experimental runs.

The polymerization was carried out in a cylindrical glass

vessel of 66 mm in diameter and 40 mm in depth, which was placed 15 cm below the window of a Van de Graaf accelerator. A 30 ml of styrene (St) emulsion in the vessel covered with a thin aluminum foil was stirred magnetically at 200 rpm. The irradiation was made at room temperature at the beam energy of 1.5 MeV and current of 50 μ A, which gave an average dose rate in the sample of approximately 8×10^4 rad/s. Generally the polymerization was carried out at the monomer fraction of 20 wt% and sodium lauryl sulfate (SLS) was used as an emulsifier.

The variations of R_p and \bar{M}_n at the initial stage of the polymerization are plotted against the relative concentration of SLS to the monomer in Fig. 1. The rate is almost constant at low SLS concentration and it tends to increase greatly when

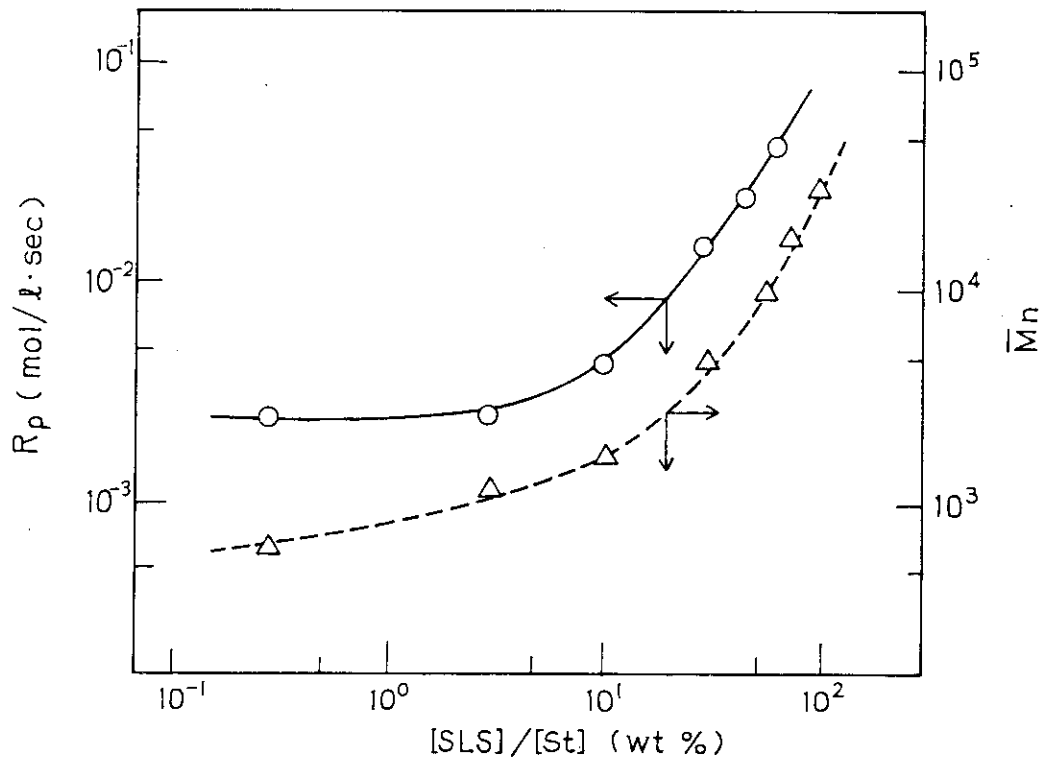


Fig. 1. The variations of R_p and \bar{M}_n as a function of $[SLS]/[St]$ in the emulsion polymerization of 20% styrene by electron beam irradiation: approximate dose rate, 8×10^4 rad/s.

[SLS]/[St] exceeds 10%. In this system, the critical micelle concentration of SLS corresponds to [SLS]/[St] = 1.0% and a full coverage of the emulsion surface with SLS is achieved at 4.1% when average diameter of the particle is 50 nm. Therefore, the acceleration of R_p starts at the SLS concentration higher than ca. 4% to achieve a full coverage of the particle surface. The variation of R_p with [SLS]/[St] obtained in our previous study in a flow system²⁾, is apparently similar to the result in Fig. 1 except that the increase of R_p started at the concentration lower than that corresponding to a full coverage. It is hard to explain at present the close similarity between the variations of R_p and \bar{M}_n as a function of [SLS]/[St].

The average diameter of the particle was determined by time-correlation light scattering method using a "Nanosizer". Although the number of data is quite limited, a few reasonable tendencies are obtained from the data shown in Table 1. Difference in the initial monomer concentration between 20 and 30% does not seem to give a significant change in particle size when the relative concentration of SLS is the same. In the SLS

Table 1. Particle Diameters of Polystyrene Emulsions Prepared by Electron Beam Irradiation: irradiation, 8×10^4 rad/s; 200 sec; at room temperature

[St] (wt%)	[SLS]/[St] (wt%)	Additive	Solid content (%)	Particle diameter (nm)
30	3.0	-	22.4	44
20	1.0	-	15.8	95
20	3.0	-	13.0	46
20	10.0	-	16.3	57
20	10.0	MeOH 1 ml/30 ml emulsion	19.6	39
20	10.0	KOH 92 mg/30 ml emulsion	19.9	39

concentration between 3 and 10%, the increase of the SLS concentration does not contribute to lower the particle size in spite of the increase in R_p , while lowering of SLS concentration from 3 to 1% increased the particle size. Addition of methanol or potassium hydroxide to the system substantially reduced the particle size.

Further studies on this polymerization system are now going on.

(J. Takezaki and K. Hayashi)

- 1) K. Hayashi and S. Okamura, JAERI-M 9214, 113 (1980).
- 2) K. Hayashi and S. Okamura, JAERI-M 9856, 97 (1981).

6. Polymerization of Acetylene in the Plastic Crystalline State by γ -Irradiation

It is well known that polyacetylene shows high electrical conductivity after doping and polyacetylene is obtained by polymerization using Ziegler-Natta catalysts¹⁾. Although it was reported that acetylene polymerized both in the liquid and the solid states by γ -irradiation²⁾ as well, the structure and the electrical property of the polymers obtained are not elucidated. In the present work, the radiation-induced polymerization of acetylene was carried out mainly in the plastic crystalline state where polymerization study was not yet made so far, and the structure of polyacetylene obtained was discussed on the basis of measurement of the infrared spectra.

Solid acetylene melts at -81.8°C and has a phase transition point at -124°C ³⁾. The phase between the melting and the phase transition points is a so-called plastic crystal and the phase below the phase transition point is in ordinary crystalline state⁴⁾. It is known that in a plastic crystal the molecules occupy the regular crystal lattice sites, rotating freely about their centers of gravity, although they undergo translational motion to some extent by self-diffusion.

Table 1. Radiation-Induced Polymerization of Acetylene
at Different Temperatures*

Temp. (°C)	Phase	Dose (R)	Conversion (%)	Color of polymer
-196	S _I	19 x10 ⁶	0.3	reddish brown
-95	S _{II}	7.8x10 ⁶	0.50	dark purple
-72	Liquid	9.0x10 ⁶	0.53	dark yellow

* Dose rate, 2.1×10^5 R/hr at -196 ~ -72°C

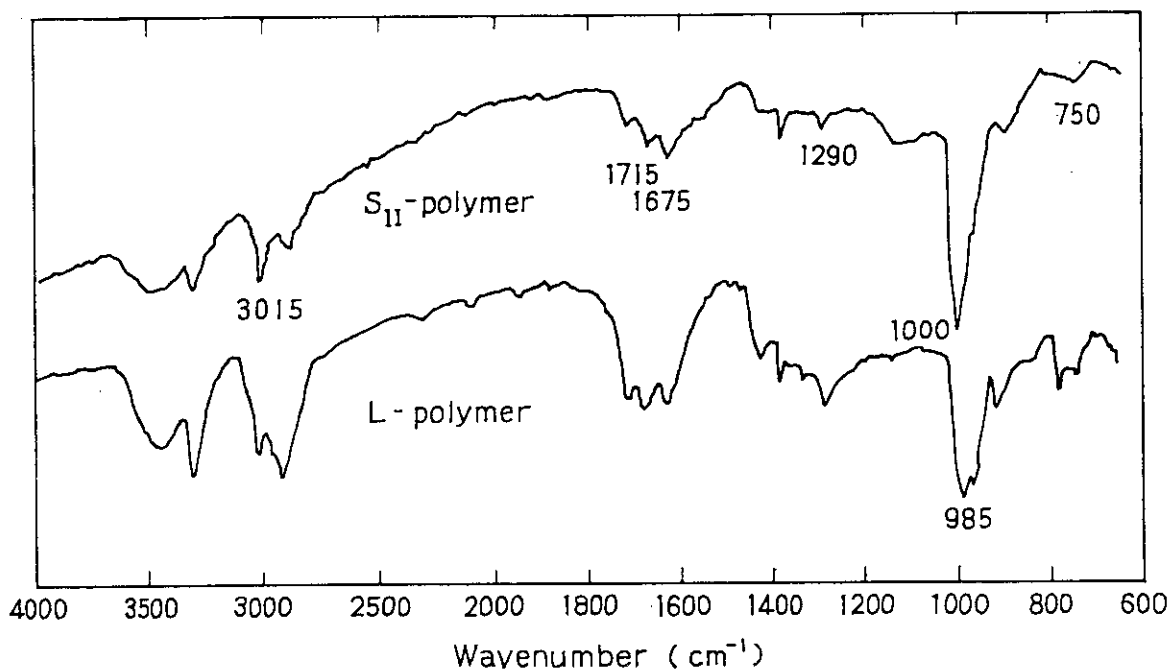


Fig. 1. Infrared spectra of polyacetylene obtained
in the S_{II} and liquid phases.

Therefore, the polymerization in the plastic crystalline state is expected to take place in a similar manner in the liquid state rather than in the crystalline state.

Acetylene was purified by passing through a molecular sieves 5A dehydrated at 350°C in vacuum, prior to use. The purified acetylene, ca. 1 g was condensed in a glass ampoule, flame-sealed and irradiated with γ -rays at a dose rate of 2.1×10^5 R/hr in Dewar vessel using by an appropriate cryostat. The polymerization was carried out in each of the three phases, i.e., the ordinary crystalline (S_I), the plastic (S_{II}), and the liquid states. In all phases, the polymer conversions were low in agreement with the results obtained by Tabata et al.²⁾, as shown in Table 1. The conversion per 1 MR in phase S_{II} was approximately 4 times higher than that in phase S_I and almost equal to that in the liquid phase.

The properties of these polymers were remarkably different depending on the phase of the monomer irradiated. The polymer obtained in the liquid phase was soluble in dimethylformamide, but the polymer obtained in phase S_{II} was insoluble in all of the conventional organic solvents tested. The polymer obtained in phase S_{II} was dark purple in color indicating the presence of highly conjugated double bonds. These properties of the polymer obtained in phase S_{II} are similar to those of the polymer prepared with Ziegler-Natta catalysts.

The polymer obtained in each phase was in very fine powder form. The shape of the polymer powder obtained in phase S_{II} was near to plate like crystal, and no fibril structure was recognized with a scanning electron microscopic observation.

Infrared spectra of the polymers obtained in phase S_{II} and the liquid phase are shown in Fig. 1. These spectra resemble those of polyacetylene prepared with Ziegler-Natta catalysts^{5,6)}, although they are substantially different from those of the polymers prepared with γ -radiation by Tabata et al.²⁾ With the aid of the assignments⁵⁾ of the major absorption bands of polyacetylene prepared with the catalyst, the absorption bands for the polymer obtained in phase S_{II} are assigned as follows. The most noticeable band at 1000 cm^{-1} can be assigned to the out-of

-plane deformation vibration of C-H bond consisting of trans -C=C- structure. The weak bands at 1290 and 3015 cm^{-1} are assigned to the in-plane deformation and to the stretching vibrations of C-H bonds in trans configuration, respectively. The weak band at 750 cm^{-1} is assigned to the out-of-plane deformation vibration of cis C-H bond. The bands at 1675 and 1715 cm^{-1} can be attributed to carbonyl groups formed by auto-oxidation of the polymer during preparation of the KBr disk. Therefore, it is considered that the S_{II} phase polymer has linear chains comprising mainly conjugated double bonds of trans configuration. The spectrum of the polymer obtained in the liquid phase is essentially similar to that of the polymer obtained in phase S_{II} , although the trans C-H out-of-plane deformation band shifts from 1000 to 985 cm^{-1} . Thus it appears that the polymer formed in the liquid phase consists of linear chains of mainly trans configuration as well.

Table 2. C-H Out-of-Plane Deformation Band in trans-Polyacetylene and Its Model Compounds

	Wavenumber (cm^{-1}) and intensity
This work, in S_{II} , γ	1000 vvs
in Liquid, γ	985 vs
Tabata, et al., in S_I , γ	970 w
in Liquid, γ	980 w
Shirakawa and Ikeda, $\text{Ti}(\text{OBu})_4\text{-AlEt}_3$	1015 vvs
Ikeda, et al., $\text{TiCl}_4\text{-AlEt}_3$	1010 vvs
trans-stilbene	960
trans,trans-1,4-diphenylbutadiene-1,3	985
all-trans-1,6-diphenylhexatriene-1,3,5	994
all-trans-1,8-diphenylctatetraene-1,3,5,7	1010

It is known that the trans C-H out-of-plane deformation band in various ethylenic compounds is observed in the vicinity of $980 \sim 960 \text{ cm}^{-1}$, the wavenumber increasing with the increase in the extent of trans conjugation⁵⁾. The wavenumbers for the polymers obtained are listed in Table 2 with those for polyacetylene presented in references and for several ethylenic compounds. The shift of the wavenumbers for ethylenic compounds suggests that the wavenumber observed for polyacetylene depends on the sequence length of trans conjugated double bonds. Accordingly, the polymer formed in phase S_{II} is supposed to be composed of the linear chains containing sequence of three to four trans conjugated double bonds between which a cis configuration interposed as a stereo block copolymer. In the case of the polymer formed in the liquid phase, it is considered that the sequence length of the trans conjugated double bonds should be shorter than that of the polymer formed in phase S_{II}, and its color and solubility suggest that the molecular weight of the polymer is probably lower than in phase S_{II}-polymer.

In conclusion, it is found that, when the polymerization of acetylene is carried out with γ -radiation, the polymerization in phase S_{II} is favorable for preparing polyacetylene with long conjugated double bonds of trans configuration as in the polymerization with Ziegler-Natta catalysts. The arrangement and the mobility of the monomer molecules in phase S_{II} are presumably more appropriate to produce long conjugated chains in the polymer than those in phase S_I or in the liquid phase.

(M. Nishii, K. Hayashi, and S. Okamura)

- 1) C. K. Chiang, M. A. Druy, S. C. Gau, A. J. Heeger, E. J. Louis, A. G. MacDiarmid, Y. W. Park, and H. Shirakawa, J. Amer. Chem. Soc., 100, 1013 (1978).
- 2) Y. Tabata, B. Saito, H. Shibano, H. Sobue, and K. Oshima, Makromol. Chem., 76, 89 (1964).
- 3) H. K. Koski and E. Sándor, Chem. Phys. Letters, 30, 501 (1975).
- 4) T. Sugawara and E. Kanda, Sci. Rept. Res. Inst. Tohoku Univ., 4A, 607 (1952).

- 5) H. Shirakawa and S. Ikeda, *Polymer J.*, 2, 231 (1971).
- 6) S. Ikeda, *Kogyo Kagaku Zasshi*, 70, 1880 (1967).

[3] Modification of Polymers

1. Preparation of Cation-Exchange Resin by Graft Copolymerization

It has been reported that poly(vinyl chloride-83%, vinyl acetate-17%) copolymer grafted by 2-acrylamide-2-methylpropane sulfonic acid (AMPS) showed a good cation-exchange property in a wide pH range including higher ion-exchange rate than the commercial one¹⁾. In order to prepare a cation-exchange resin with higher heat resistance than poly(vinyl chloride-vinyl acetate) copolymer, poly(vinyl chloride) (PVC) resin and poly(vinylidene chloride-80%, vinyl chloride-20%) copolymer (PVD) were used as a trunk polymer.

Radiation-induced graft copolymerization was performed in a heterogeneous water-acetone system. Cupric sulfonate is used as an inhibitor of the homopolymerization of AMPS in a liquid phase. Acetone is a swelling agent for PVC, while for PVD cyclohexanone is added to the water-acetone system to swell the polymer to a suitable extent.

Figure 1 shows adsorption behavior of lithic ions by the grafted polymers of PVC and PVD at room temperature together with that by a commercial resin, Diaion AHPK-16S. Both the grafted polymers adsorb lithic ion much faster than the commercial one, but the equilibrium adsorption value of the grafted PVD seems to be a little lower than that of commercial one. A similar tendency has also been obtained at 50°C. Figure 2 shows the thermogravimetric (TG) curves and also the DTA heating curves of the original PVC, PVD and their grafted polymers. In TG curves, it is clarified that the decomposition of the grafted poly (AMPS) occurs at about 180°C, while the decomposition of trunk polymers occurs at about 220°C for PVD and at about 260°C for PVC, respectively. DTA heating curves indicate the glass transition temperature (T_g) at about 70°C for PVC and about 120°C for PVD in both specimens before and after grafting. Therefore, it is suspected that the grafted resin can be used

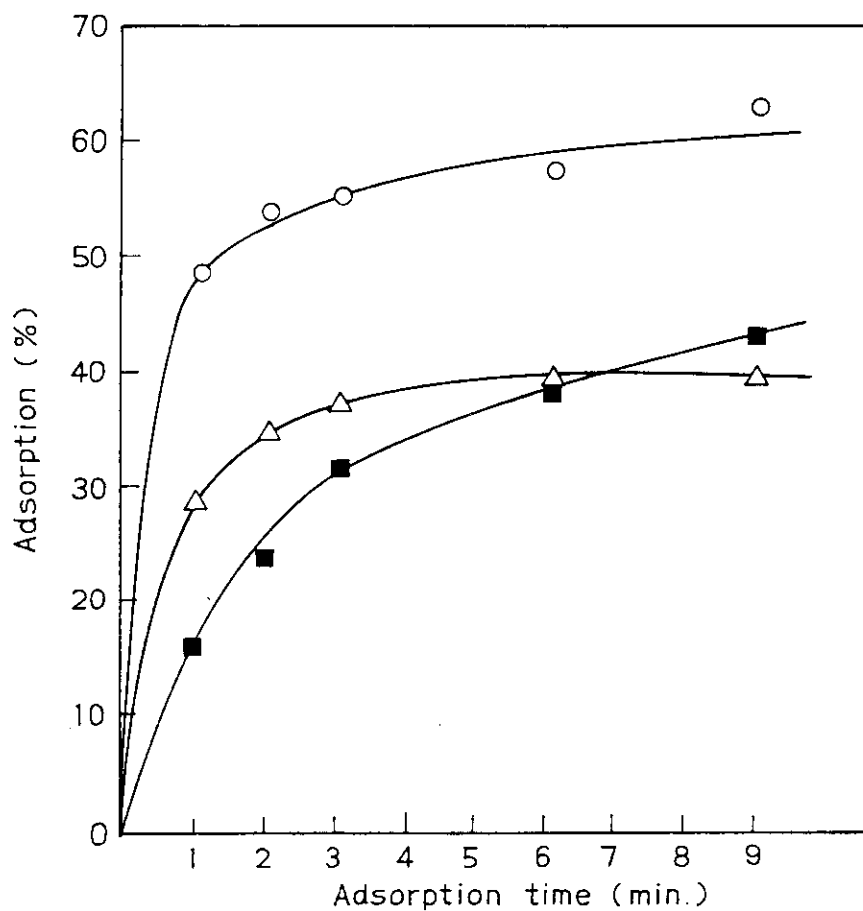


Fig. 1. Comparison of adsorptive activities between grafted polymer and commercial resin.

- : Commercial resin (Diaion AHPK-16S)
- : Grafted PVC (15%, Water/Acetone/AMPS/PVC = 4ml/6ml/5.5g/2g, 520KGy/h for 3h at 35°C)
- △ : Grafted PVD (10%, Water/Acetone/AMPS/PVD = 3ml/7ml/4g/2g, 520 KGy/h for 6h at 35°C)

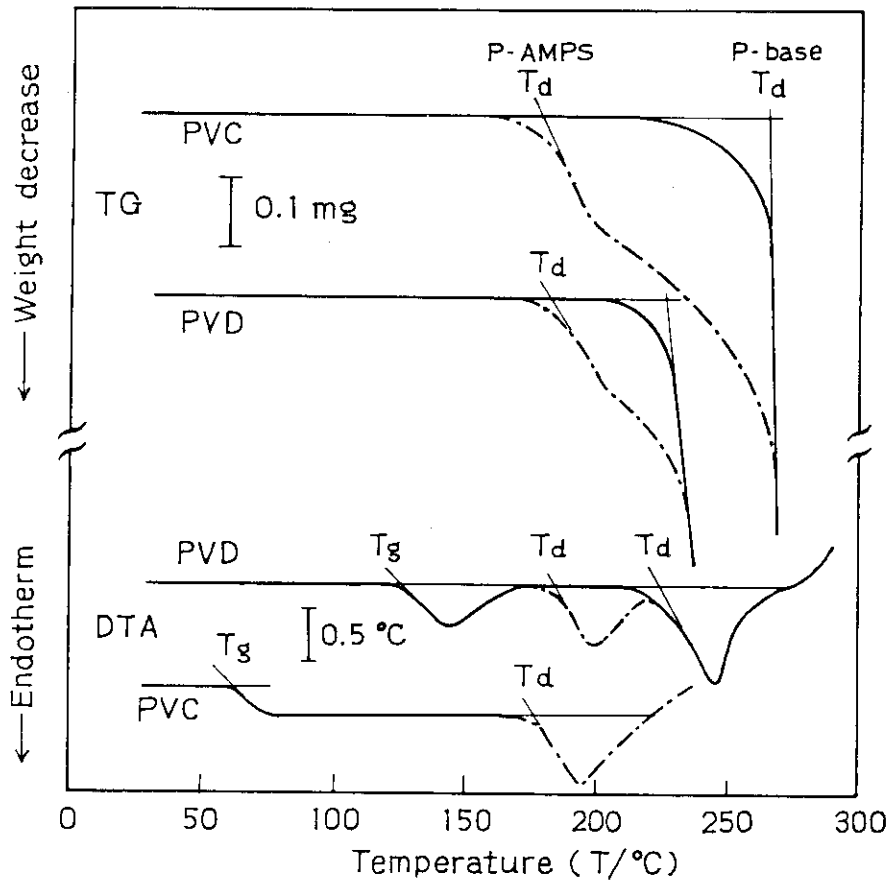


Fig. 2. Thermogravimetric curves and heating curves of differential thermal analysis of sample before and after grafting.

- : Base polymer (Trunk polymer alone)
- - - - : Grafted polymer (PVC: 13.5% grafting,
PVD: 15.0% grafting)

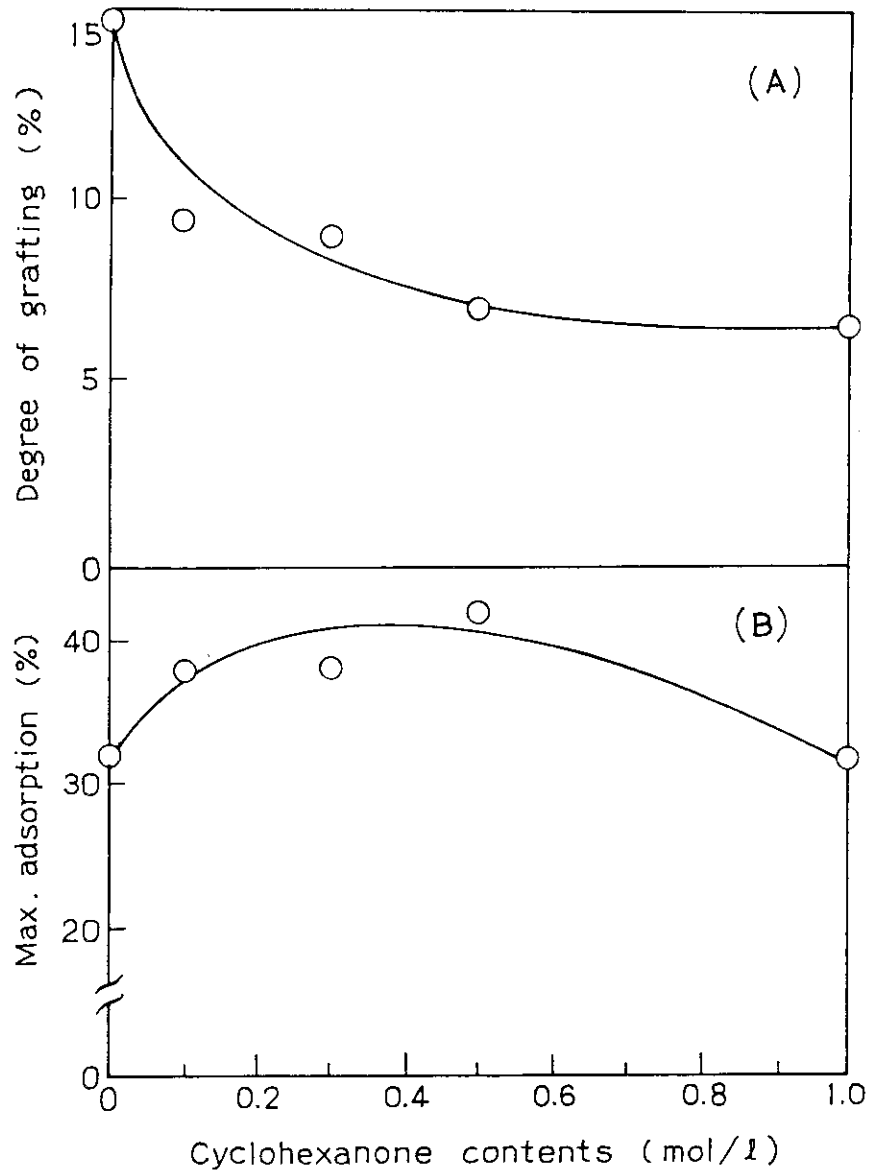


Fig. 3. Effect of cyclohexanone on the degree of grafting of AMPS onto PVD (A) and the adsorptive activity (B) of the grafted polymer: polymerization, 520KGy/h for 6h at 50°C; Water/Acetone/AMPS/PVD = 3ml/7ml/4g/2g; adsorption, lithic ion at 25°C.

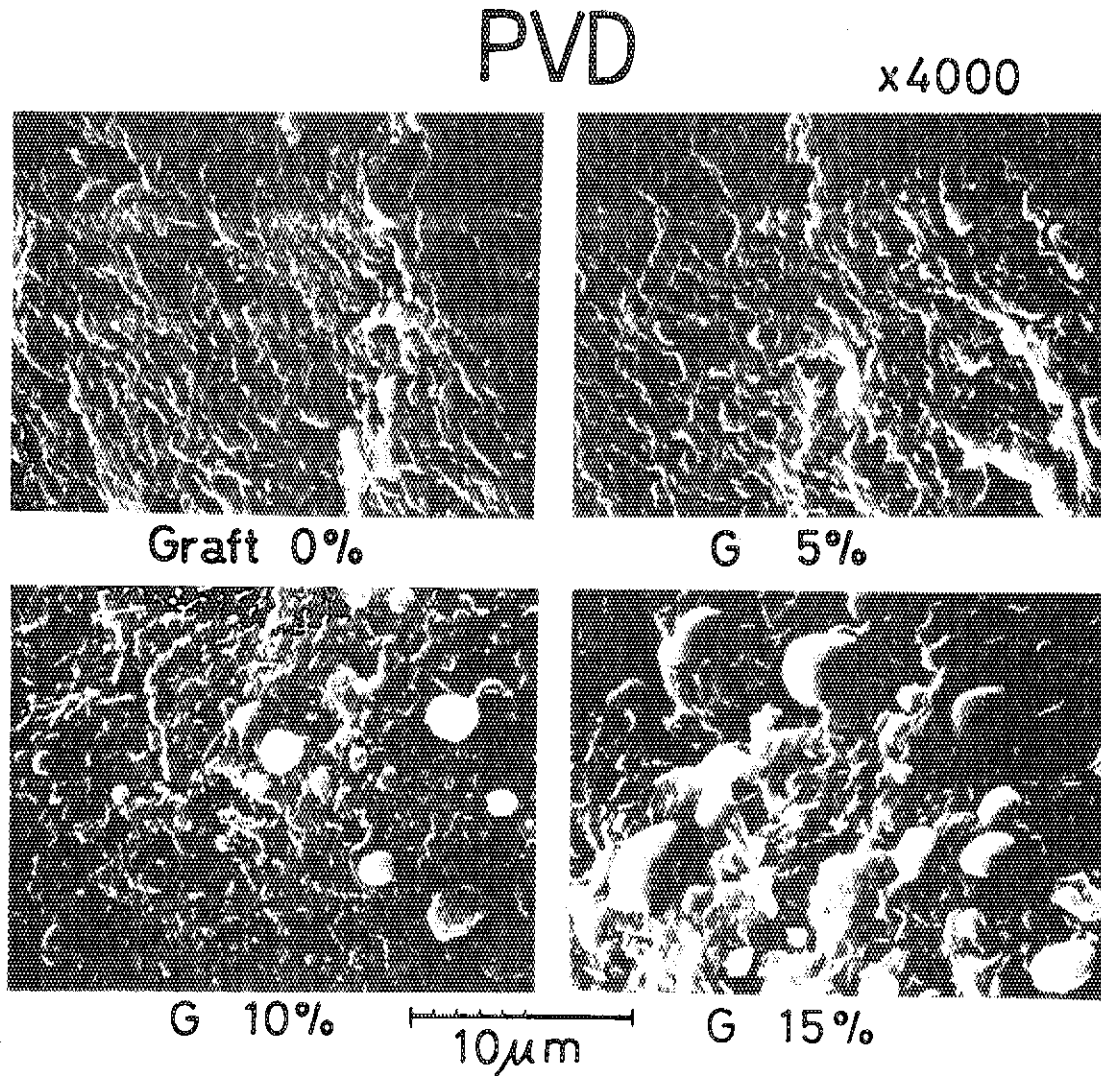


Fig. 4. Scanning electron microscopic observation of PVD powder with different degree of grafting. Polymerization condition: dose rate, 520 KGy/h;

Graft(%)	Water(ml)	Acetone(ml)	AMPS(g)	PVD(g)	Temp.(°C)	Irradn. time(h)
5	4	6	4	2	35	4
10	3	7	4	2	35	6
15	3	7	4	2	50	7

at a temperature below T_g of the trunk polymer.

Figure 3 shows the effect of swelling agent of cyclohexanone on the degrees of grafting onto PVD and their adsorptive activity. Degree of grafting decreases monotonically with the increase of the amount of cyclohexanone due to the easiness of migration of the inhibitor into the sample, while adsorption of lithic ion becomes most effective at a lower range of cyclohexanone concentration. These facts indicate that the grafting sites on the trunk polymer seem to be more effective in the localized surface of the sample powder. This is also supported by scanning electron microscopic observation as shown in Fig. 4. The higher the degree of grafting occurs, the more the amount of grafting on the polymer surface is observed. The details of this work has been described in Ref. 2.

(Y. Nakase)

- 1) T. Yagi, K. Hayashi, and S. Okamura, JAERI-M 9856, 107 (1981).
- 2) Y. Nakase and N. Akasaka, JAERI-M 82-059 (1982)

2. Grafting of Fluorine-Containing Monomer onto Poly(Vinyl Chloride) Composite Disc

Study has been carried out on the surface grafting of fluorine-containing monomers onto a VHD type video disc in an attempt to improve friction properties of the disc.

The video disc employed is made of poly(vinyl chloride) (PVC)-carbon black composite (100 : 20 by weight) and is 1 mm thick and 26 cm in diameter with many small pits on the surface. The disc was cut into small pieces (6 mm x 20 mm) and used for the experiments. Commercially available hard PVC plates were also employed for reference purpose. Fluorine-containing monomers used were 2,2,2-trifluoroethyl methacrylate (F_3C_2MA), 2,2,3,3-tetra fluoropropyl methacrylate (F_4C_3MA), 1H,1H,5H-octafluoropentyl methacrylate (F_8C_5MA) and pentafluoro styrene (F_5St). The thermal graft polymerization was carried out using

a vapour phase grafting technique which is more suitable for the present study than an immersion grafting technique, since by the former technique, the grafting can be performed without unwanted deformation of the fine structure of the small pits on the disc surface and with excellent monomer utilization which is especially important in the study which uses expensive monomers.

The vapour phase thermal grafting of fluorine-containing monomers of the PVC composite disc proceeded smoothly even at low temperatures as $40 \sim 50^{\circ}\text{C}$. The order of the grafting rate of the monomers is not the same as that of the rate of homopolymerization, and is not correlated with the vapour pressures of the monomers. For example, the rate of homopolymerization of F_5St , which gave the highest grafting rate, was the lowest among the four, while the vapour pressure was the second after the highest. Similar results were obtained for the commercially available PVC plates.

The contact angle measurement of aniline by the sessile drop method at room temperature and X-ray photoelectron spectroscopic measurement using a Shimadzu ESCA 750 electron spectrometer (with $\text{Mg K}\alpha$ radiation) were carried out on the F_5St grafted PVC disc. The results indicate that the grafting of F_5St did not take place on the surface, but did take place in the inner part below the surface.

Friction of the F_5St grafted PVC disc was measured using an apparatus which was designed so that a steel ball slides on the surface of the sample. The result of the dynamic friction test shows that the coefficient of friction on the video disc surface was reduced by the grafting to the value which was considerably lower than that of the commercial PVC plates. The volume of material removed by the friction test which was calculated from the average width of the wear grooves of the sample observed by optical microscopy, was not reduced by the grafting when the degree of grafting was less than 10%, although the volume increased for the samples with more than 10% grafting.

All the results obtained in the present study revealed that the graft polymerization of the fluorine-containing monomers

took place not on the surface of the PVC disc but in the bulk. This is possibly resulted by the high diffusibility of the monomers into the bulk polymer. Therefore, for successful surface grafting it is necessary to modify the disc materials so that the monomers do not easily diffuse into inside the disc materials. A result of an experiment on the modified disc materials suggests the possibility of surface grafting as expected, and the study on this line is in progress.

(K. Kaji and K. Hayashi)

III. LIST OF PUBLICATIONS

[1] Published Papers

1. H. Arai, S. Nagai, and M. Hatada, "Radiolysis of Methane Containing Small Amounts of Carbon Monoxide--Formation of Organic Acids", *Radiat. Phys. Chem.*, 17, 211 (1981).
2. H. Arai, S. Nagai, K. Matsuda, and M. Hatada, "Radiolysis of Methane by Electron Beam Irradiation over Wide Range of Dose and Dose Rate", *Radiat. Phys. Chem.*, 17, 217 (1981).
3. S. Nagai, H. Arai, and M. Hatada, "Radiation-Induced Reactions of CO-H₂ Gas Mixtures over Various Solid Catalysts", *Radiat. Phys. Chem.*, 18, 807 (1981).
4. H. Arai, S. Nagai, and M. Hatada, "The Formation of Formic Acid by Electron Irradiation of a CO-H₂ Mixture Containing CO₂", *Z. Phys. Chem., N.F.*, 126, 187 (1981).
5. S. Nagai, "Desorption by Ions and Electrons", *JAERI-M 9775*, 59 (1981).
6. N. Tamura, R. Tanaka, S. Mitomo, K. Matsuda, and S. Nagai, "Properties of Cellulose Triacetate Film Dose Meter", *Radiat. Phys. Chem.*, 18, 947 (1981).
7. K. Hayashi, Y. Tanaka, and S. Okamura, "Radiation-Induced Polymerization at High Dose Rate. V. Butadiene in Bulk", *J. Polym. Sci. Chem. Ed.*, 19, 1435 (1981).
8. K. Hayashi, K. Kagawa, and S. Okamura, "Radiation-Induced Polymerization at High Dose Rate. VI. Butadiene in n-Hexane Solution", *J. Polym. Sci. Chem. Ed.*, 19, 1977 (1981).
9. K. Hayashi, M. Tachibana, Y. Tanaka, and S. Okamura, "Copolymerization of Butadiene with Vinyl Chloride by Radiation", *J. Polym. Sci. Polym. Chem. Ed.*, 19, 1571 (1981).
10. K. Hayashi and S. Okamura, "Copolymerization of Butadiene with Vinyl Chloride by Radiation", *Radiat. Phys. Chem.*, 18, 1133 (1981).
11. J. Takezaki, T. Okada, and I. Sakurada, "Radiation-Induced Polymerization of Styrene in Amines", *Radiat. Phys. Chem.*, 18, 1125 (1981).
12. K. Kaji, T. Okada, and I. Sakurada, "Radiation-Induced Grafting of Acrylic Acid onto Polyethylene Filaments",

Radiat. Phys. Chem., 18, 503 (1981).

13. K. Kaji, "Modification of Synthetic Fibers by Radiation-Induced Grafting", JAERI-M 9481 (1981).
14. Y. Nakase, M. Ito, and I. Kuriyama, "Radiation Resistance of Ethylene-Propylene Rubber Vulcanized by Sulfur. II. Practical Ingradient Compounding Materials", Trans. IEEJ, 101A, 279 (1981).
15. Y. Nakase and M. Ito, "Radiation Resistance of Ethylene-Propylene Terpolymer Vulcanized by Sulfur. I. Basic Ingradient Compounding Material", IEEE Trans. Electr. Insul., EI-16, 528 (1981).
16. Y. Nakase, "Light Water Reactor and Polymeric Materials", JAERI-M 9584 (1981).

Reviews and Patent Applications

17. S. Okamura, "Advances in Applied Radiation Chemistry", Radiat. Phys. Chem., 18, 1125 (1981).
18. I. Sakurada, T. Okada, and K. Kaji, "Preparation of Synthetic Fibers of Excellent Heat Resistance", Japan Kokai, 56-63074, May 29, 1981.
19. I. Sakurada, K. Kaji, and T. Okada, "Synthesis of Heat Resistive and Non-Flammable Fiber", French Pat., No. 7731658, Apr. 6, 1981.
20. I. Sakurada, T. Okada, and K. Kaji, "Non-Flammable Polyethylene Fiber", Japan Kokai, 56-107071, Aug. 25, 1981.
21. K. Hayashi and S. Okamura, "Copolymer of Butadiene and Vinyl Chloride", Japan Kokai, 56-59817, May 23, 1981.

[2] Oral Presentations

1. S. Nagai, H. Arai, and M. Hatada, "Hydrocarbon Formation by Irradiation of CO-H₂ Gas Mixture in the Presence of Silica Gel", The 34th Discussion Meeting on Colloid and Interface Science, Oct. 8, 1981.
2. Y. Shimizu, S. Nagai, and M. Hatada, "Selective Formation of Low Molecular Weight Hydrocarbons by Radiation-Induced Reaction of Methane", The 34th Discussion Meeting on Colloid and Interface Science, Oct. 8, 1981.
3. S. Nagai and Y. Shimizu, "Radiation-Induced Reaction of Adsorbed Water with Carbon Monoxide", The 24th Discussion Meeting on Radiation Chemistry, Oct. 21, 1981.
4. K. Hayashi, H. Okuno, and S. Okamura, "Cationic Telomerization of Butadiene by Electron Beam Irradiation", The 29th Annual Meeting of the Polymer Society, Japan, May 28, 1981.
5. K. Hayashi, H. Okuno, and S. Okamura, "Cationic Telomerization of Butadiene by Electron Beams in the Presence of Chlorine Containing Hydrocarbons", The 29th Discussion Meeting of the Society of Polymer Science, Japan, Oct. 9, 1981.
6. K. Hayashi, T. Kijima, and S. Okamura, "Emulsion Polymerization of Styrene by High Dose Rate Electron Beams", The 24th Discussion Meeting on Radiation Chemistry, Oct. 21, 1981.
7. I. Kuriyama, "Radiation-Resistance for Polymeric Materials", The 5th Annual Meeting of Radiation Laboratory, The Scientific and Industrial Research Institute, Osaka University, Mar. 23, 1982.

IV. EXTERNAL RELATIONS

On June 5, Professor Sun Shu-Qi, Deputy Director of Changchng Institute of Applied Chemistry, Chinese Academy of Sciences, delivered a lecture on "Recent Progress in the Studies of the Stereoregular Polymerization by the Transition Metal Catalysts". Dr. Koji Matsuda, a senior engineer of the Nissin High Voltage Engineering Co., gave a lecture on "Ion Accelerators and Their Applications" on Nov. 14.

The laboratory welcomed the visits by Mrs. Begum on Apr. 1, and Mr. Hegazy on May 29, both IAEA trainees from Bangladesh and from Egypt, respectively, to Takasaki Research Establishment.

We also welcomed trainees from industrial companies for two week training course on pure and applied radiation chemistry from Oct. 1 through Oct. 14.

Prof. Y. Tabata of the University of Tokyo visited the Laboratory with 18 members of Japan Atomic Energy Forum on Jan. 19, 1982.

Dr. Kuriyama was invited to deliver a lecture on "Radiation-Resistance for Polymeric Materials" at the 5th Annual Meeting of Radiation Laboratory, the Institute of Scientific and Industrial Research, Osaka University on Mar. 23.

V. LIST OF SCIENTISTS

(Mar. 31, 1982)

[1] Staff Members

Isamu KURIYAMA	Dr., polymer physicist, Head
Seizo OKAMURA	Professor emeritus, Kyoto University
Motoyoshi HATADA	Dr., physical chemist
Kanae HAYASHI	Dr., polymer chemist
Yoshiaki NAKASE	Dr., polymer chemist
Siro NAGAI	Dr., physical chemist
Shun'ichi SUGIMOTO	Physical chemist
Koji MATSUDA	Radiation physicist
Jun'ichi TAKEZAKI	Physical chemist
Masanobu NISHII	Dr., polymer chemist
Torao TAKAGAKI	Radiation physicist
Kanako KAJI	Dr., polymer chemist
Yuichi SHIMIZU	Physical chemist
Toshiaki YAGI*	Engineering chemist

[2] Advisors

Yoshito IKADA	Assoc. Professor, Kyoto University, Advisor
---------------	--

*) Takasaki Radiation Chemistry Research Establishment